Aus dem Walter-Brendel-Zentrum für Experimentelle Medizin

Institut der Ludwig-Maximilians-Universität München

Direktor: Prof. Dr. med. Ulrich Pohl

Platelets in the pathogenesis of obesity

DISSERTATION

zum Erwerb des Doctor of Philosophy (Ph.D.) an der Medizinischen Fakultät der Ludwig-Maximilians-Universität München

Vorgelegt von

Henrik H. Herbert

aus Fulda

16.09.2016

Mit Genehmigung der Medizinischen Fakultät

der Ludwig-Maximilians-Universität München

Berichterstatter:	Prof. Dr. med. Steffen Massberg
	Prof. Dr. med. Markus Sperandio
Mitberichterstatter:	Prof. Dr. rer. nat. Jürgen Bernhagen
	Priv. Doz. Dr. med. Christoph Reichel
Dekan:	Prof. Dr. med. dent. Reinhard Hickel

Tag der mündlichen Prüfung: 04.04.2017

Meiner Familie

TABLE OF CONTENTS

I. **Introduction** **1**

II. Literature Review **2**

1. Platelets **2**

1.1. Definition 2

1.2. Anatomy and function 2

1.2.1. Structure and activation 3

1.2.1.1. Peripheral Zone 3

1.2.1.2. Sol-gel Zone 4

1.2.1.3. Organelle Zone 4

1.2.1.4. Membranous Zone 5

1.3. Receptors 5

2. Leukocytes **7**

2.1. Definition 7

2.2. Neutrophil Granulocytes 8

2.2.1. Definition 8

2.2.2. Anatomy and function 8

2.2.3. Signal transduction 9

2.2.4. The neutrophil adhesion cascade 9

3. Transmembrane Receptors **11**

3.1. Definition 11

3.2. Integrins 11

3.2.1. GPIIb/IIIa-Integrin 13

3.3. Selectins 15

3.4. Interactions between neutrophils and platelets 16

4. Cytokines **17**

4.1. Definition 17

4.2. TNFα 18

4.2.1. Blockage of TNF-α 18

4.2.1.1. Infliximab 19

5. Adipose tissue **20**

5.1. Definition 20

5.2. Adipogenesis 20

5.2.1. Phases of Adipogenesis 21

5.3. Adipocyte biology 22

5.3.1. White adipose tissue 22

5.3.2. Brown adipose tissue 23
5.3.3. Fat depots 23
5.4. Obesity 23
5.4.1. Obesity and inflammation 24

III. Aim of the Study 26

IV. Materials & Methods 27

1. Research animals 27
1.1. Wild type strain C57BL/6 27
1.2. Genetically modified animals 27
1.3. Animal Breeding 28
1.4. Animal Husbandry 28

2. Operation Methods 30
2.1. Anesthesia 30
2.2. Tail vein injection 31
2.3. Cardiac blood withdrawal 31
2.4. Platelet isolation and labeling 32
2.5. Neutrophil labeling 33
2.6. Mouse preparation for intravital fluorescence-microscopy 33
2.7. Surgical operation 34
2.8. Fat pad removal 35
2.9. Chimera Creation 37
2.9.1. Isolation of bone marrow cells 37
2.9.2. Irradiation process 37
2.10. High Fat Diet Regime 39

3. Intravital epifluorescence video microscopy 40
3.1. Structure of the epifluorescent microscopy 40
3.2. The epifluorescence microscope 41
3.3. Procedure of the epifluorescence microscopy 42
3.4. Data evaluation with Microsoft Excel 43
3.5. Documentation 43

4. *In vitro* culture of adipocytes 44
4.1. Maturation of preadipocytes 44
4.2. Differentiation of preadipocytes into adipocytes 45
4.3. Sudan III staining 45
4.4. Adipocyte growth evaluation 46
4.5. Neutrophil Isolation 47

4.5.1. Preparation of the Percoll gradient 47
4.5.2. Preparation of the bone marrow 48
4.5.3. Isolation of the PMNs 48
4.6. Co-Incubation of Adipocytes with diverse substances 48
4.6.1. Co-incubation with stimulated platelets 49
4.6.2. Co-incubation with stimulated platelet supernatant 50
4.6.3. Co-incubation with stimulated neutrophils 51
4.6.4. Co-incubation with unstimulated neutrophils 52
4.6.5. Co-incubation with unstimulated neutrophils and stimulated platelets 52
4.6.6. Co-incubation with TNF-α 53
4.6.7. Co-incubation with ADP 55
4.6.8. Co-incubation with PMA 55
4.6.9. Co-incubation with Tyrodes 55
4.7. Adipocyte preparation for ELISA quantification 55
5. Infliximab Setting 56
5.1. ELISA quantification 56
5.1.1. Performance of the ELISA 57
5.1.2. ELISA data evaluation 58
6. Analysis of Fat pad vascularization 59
6.1. Principle of the two-photon microscopy 59
6.2. Structure of the two-photon microscope 60
6.3. Whole mount staining 61
6.3.1. Injection of the primary antibody 61
6.3.2. Secondary antibody staining 61
6.3.3. Fat pad imaging using 2-photon microscopy 62
6.3.4. Data evaluation with IMARIS 62
7. Statistical Analysis 63
V. Results 65
1. Platelet and leukocyte adhesion in visceral WAT 65
2. Effect of High Fat Diet on platelet and leukocyte adhesion 70
3. Fat pad and body weight measurement 77
3.1. GPIIb deficient and wild type mice 78
3.2. GPIIb deficient and wild type bone marrow chimera mice 79
4. Analysis of fat pad vascularization 81
5. *In vitro* culture of adipocytes 84
5.1. TNF-α ELISA after adipocyte treatment 85
5.2. Adipocyte proliferation evaluation 86
6. TNF-α blockade via Infliximab 89

VI. Discussion 93
1. Experimental procedure 93
1.1. Choice of mouse strain 93
2. Discussion of results 94
2.1. Platelet and leukocyte adhesion in visceral fat 94
2.2. Effect of High Fat Diet on platelet and leukocyte adhesion 97
2.3. Fat pad and body weight measurement 100
2.3.1. Transgenic GPIIb deficient and wild type mice 100
2.3.2. GPIIb deficient and wild type bone marrow chimera mice 102
2.4. Analysis of fat pad vascularization 102
2.5. *In vitro* culture of adipocytes 103
2.5.1. TNF-α ELISA after adipocyte treatment 103
2.5.2. Adipocyte proliferation evaluation 105
2.6. TNF-α blockage via Infliximab 107
3. Summary 109
VII. Table of Figures 113
VIII. Abbreviation List 116
IX. Acknowledgement 120
X. Literature 122
XI. Appendix 138
Affidavit 138

I. INTRODUCTION

Chronic inflammatory processes occur during onset and development of obesity in white adipose tissue (WAT). Activation of endothelial cells was recently shown to occur early during initiation of weight gain. This thesis shows regulation of inflammatory processes in WAT by platelets. Chronic platelet adhesion was detected using intravital microscopy at the endothelium of adipose tissue. This platelet adhesion seems to promote recruitment of white blood cells (leukocytes) to adipose tissue. Platelet-leukocyte interactions are a well-established phenomenon in various inflammatory settings of vascular inflammation.

In the here described scientific project transgenic mice models with deficient platelet adhesion due to altered adhesion receptor expression and impaired platelet biogenesis show decrease of white blood cell accumulation in WAT. Reduced platelet and leukocyte adhesion provokes a significant increase in body fat. Therefore, the results described in this thesis indicate a potential and probably crucial role of platelets in chronic inflammatory processes during obesity.

II. LITERATURE REVIEW

1. Platelets

1.1. Definition

The first characterization of platelets dated in the 19th century as small, curious beads or grains which accumulate to each other to irregular clusters (*19*). Today it is widely established that platelets play a crucial role in inflammatory reactions, immune response (*232*), atherosclerosis (*158*) and thrombus formation upon plaque rupture (*160*). Platelets function to stop hemorrhage after tissue trauma or vascular injury. Activation and aggregation of platelets are induced after the interaction of platelet receptors with matrix proteins. The most important component for this interaction is collagen (*136*), a protein in the various connective tissues, but also the serine protease thrombin plays a crucial role. Other components reacting with platelets are the von Willebrand factor (vWF) and fibronectin; they are both localized especially in the extracellular matrix (ECM).

1.2. Anatomy and function

In their resting form platelets show a diameter of 2-4 µm, circulating in a range of 150.000 - 400.000 / µl in the bloodstream (*207*). The anuclear cells derive from megakaryocytes in the bone marrow and lack genomic DNA (*109*), however they contain megakaryocyte-derived mRNA for the synthesis of proteins (*182*). With a multitude of functions, in some aspects platelets resemble leukocytes when it comes to change of shape or formation of oxygen radicals (*156*). Platelets have an average lifetime of 8-9 days with a daily renewal rate (*96*) and can emit chemotactic factors for monocytes and neutrophil granulocytes (*63*), moreover they show cytotoxic activity against blood parasites (*25*) and tumor cells (*107*).

1.2.1. Structure and activation

Inactivated platelets show a lens-shaped form (*112*) with an average surface area of 8 μm^2, however within activation they undergo a shape change with formation of pseudopods that represent protrusions of the plasma (echinospherocytes) and the surface area increases up to 13 μm^2 (Fig. 1) (*86*).

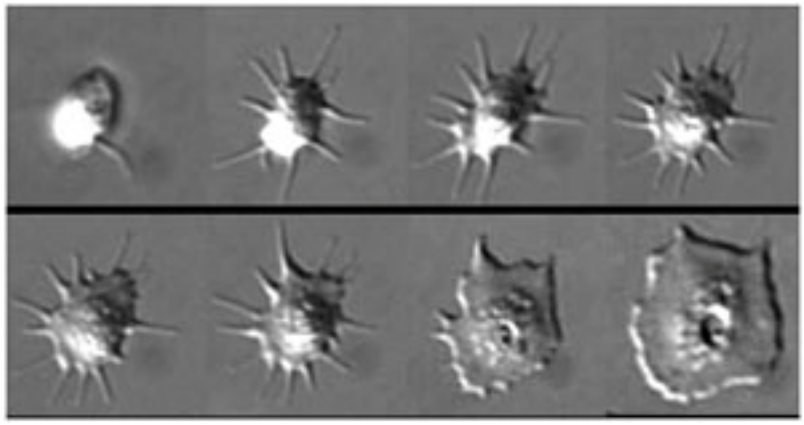

Figure 1: Human platelet spreading

A human platelet undergoes a conformational change after activation on surface of fibrinogen (*193*)

The platelet can be divided into four zones, from peripheral to innermost:

1.2.1.1. Peripheral Zone

The platelet plasma membrane is smooth, however high resolution electron microscopy revealed a rugose appearance somehow resembling the surface of the brain (*105*). These folds may provide additional membrane when platelets need to stretch on surfaces. Thin sections revealed that the platelet plasma membrane has a thicker glycocalyx than other blood cells (*187*). The lipid bilayer on which the glycocalyx rests, is a unit membrane and serves an extremely important role in the acceleration of clotting, a process solely found in platelets.

The glycocalyx is covered with glycoprotein receptors which are necessary for facilitation of platelet adhesion to a damaged surface, to promote platelet aggregation and interaction with other cells, to accelerate the process of clotting and to trigger full activation of the platelet (*59, 111, 118, 213*).

The main glycoprotein receptors involved in hemostasis are the glycoprotein Ib-IX-V complex (GPIb-IX) and the integrin $\alpha_{IIb}\beta_3$ (GPIIbIIIa). The outside surface of the platelet is covered with about 25.000 GPIb-IX receptors and 80.000 GPIIb-IIIa receptors (*254*).

In the submembrane area a regular system of thin filaments resembling actin filaments can be found. These filaments have an important role in the shape change and also in the translocation of particles and receptors over the cell surface (*277*).

1.2.1.2. Sol-gel Zone

In addition to the contractile filament system of the peripheral zone the sol-gel zone shows two other filament systems in the platelet cytoplasm. One is the microtubules, a cytoskeletal support system. The other is the actomyosin filament system, which is involved in internal transformation, shape change and contraction of the hemostatic plug and clot-retraction (*138*). The cytoplasmic actin filament cytoskeleton serves as a matrix on which all organelles are maintained separate from each other in the resting cell. After activation the cytoplasmic actomyosin cytoskeleton has a unique role in the platelet contraction and the spatial reorganization of the organelles (*86*).

1.2.1.3. Organelle Zone

Within the organelle zone, three major types of organelles can be distinguished, α-granules, dense bodies (δ-granules) and lysosomes. There are also multivesicular bodies, which develop in the megakaryocyte and may serve as some kind of sorting station (*200*).

Some small mitochondria in the platelet cytoplasm serve an important role in energy metabolism.

The most numerous of the platelet organelles are the α-granules, with a number depending of the size of the platelet as well as the presence of other large structures (e.g. glycogen) (*97*). α-granules contain several growth factors like insulin-like growth factor 1, platelet-derived growth factors, platelet factor 4 and other clotting proteins: thrombospondin, fibronectin, factor V (*263*), and von Willebrand factor (*186*).

Dense bodies are smaller than the α-granule and fewer in number. They contain adenosine diphosphate (ADP), adenosine triphosphate (ATP), calcium, histamine and serotonin (*178*).

1.2.1.4. Membranous Zone

The membranous zone contains surface-connected, open-canalicular systems (OCS) as well as the dense tubular system (DTS). The OCS can be seen as an extension and invagination of the platelet cell membrane and contains tubules building up a canal structure to the cell center (*8*).

In this way substances can be transported from the plasma to the cell center or from the cell organelles outward. Moreover the tubules contain large amounts of free calcium-ions that can be secreted into the cytoplasm to activate the platelet (*243*).

1.3. Receptors

Platelet receptors trigger the reactivity of platelets with a range of agonists and adhesive proteins. Due to the fact that platelets lack a nucleus and therefore cannot cope with different situations by protein synthesis (*de novo*), they need to be equipped with a wide range of molecules that are presynthesized with an amount of physiological functions and the ability to adapt to new pathological situations.

One possibility to do this is by altering their phenotype via receptors present in the membrane that get expressed on the platelet surface after activation. This fact causes platelets to have the highest molecular mass compared to their relatively small size. The major platelet receptors have an important role in hemostasis, which is the most import function of platelets, either after platelet activation or after an interaction with damaged cell walls. The first platelet receptor involved in a disorder has been described nearly 100 years ago (*91*), in the late 1970s and early 1980s a more detailed analysis of platelet receptors was published (*11, 52, 188*). Breakthroughs in the known platelet receptors were the description of collagen in 1999 (*51*) and ADP as well as ATP in 2001 (*101*).

2. Leukocytes

2.1. Definition

Leukocytes or White Blood Cells (WBC) are nucleated cells involved in the innate as well as the adaptive immune system to protect the organism against infection and invaders. WBCs can be found in the blood, bone marrow, lymphatic organ and other tissues of mammals (*116*). All WBCs develop from a hematopoietic stem cell in the bone marrow via hematopoiesis and can be differentiated either by structure (granulocytes and agranulocytes) or cell division lineage (myeloid cells or lymphoid cells). This follows a further classification into the five main types: Neutrophils, eosinophils, basophils, lymphocytes and monocytes (Fig. 2). The human blood contains about 4.000 to 10.000 leukocytes / mL.

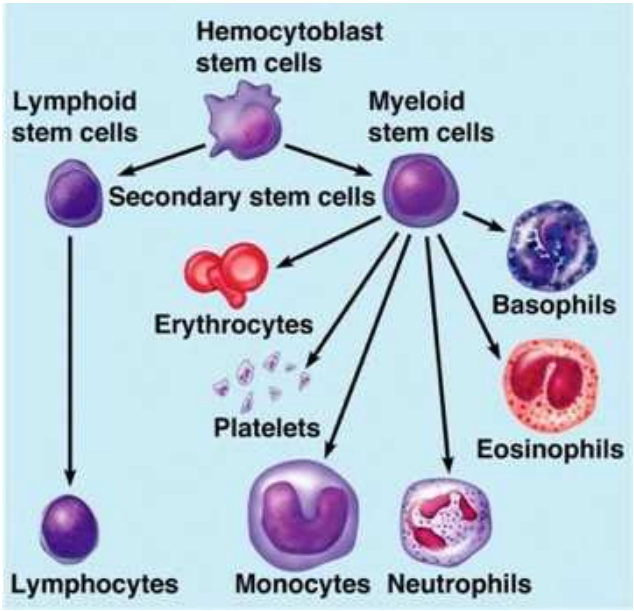

Figure 2: Hematopoiesis

Lymphoid and myeloid stem cells derive from hematopoietic stem cell. Lymphocytes develop from lymphoid stem cells; myeloid stem cells develop into neutrophils, basophils, eosinophils, as well as monocytes, platelets and erythrocytes (61)

2.2. Neutrophil Granulocytes

2.2.1. Definition

Neutrophil granulocytes (neutrophils) are the most abundant immune cells and belong to the innate immune system. They are rapidly recruited to sites of inflammation and infection via chemotaxis where they show defensive attributes as well as the expression and release of cytokines (*117, 242*) that can amplify inflammatory reactions by other cell-types. Pathogen defense is performed via direct ingestion (phagocytosis) (*24, 184*), release of soluble anti-microbials (degranulation) (*40*) and the generation of neutrophil extracellular traps (NETs) (*31*).

2.2.2. Anatomy and function

The term “neutrophil” originated from its staining characteristics on hematoxylin and eosin. In contrast to eosinophils that stained bright red and basophils that stained dark blue, neutrophils stained a neutral pink color. They show a diameter of about 8 µm in the blood stream and 12-15 µm in peripheral blood smears (*181*). The nucleus of a neutrophil is multilobed, with the single lobes connected via chromatin. The cytoplasm contains spars mitochondria and ribosomes, a small Golgi apparatus, but about 200 granules. The rough endoplasmic reticulum is completely absent (*276*).

Neutrophils can accumulate rapidly at a site of infection and provide a host-defense against invading pathogens. When an invader gets ingested the neutrophil is removed via apoptosis, this helps to prevent damage from healthy tissues (*99, 133, 214*). Life span of a neutrophil is about 8-12 hours, however the life span can be prolonged in cytokine respond. The circulating neutrophils are constantly renewed from the bone marrow.

2.2.3. Signal transduction

Patrolling neutrophils in the post-capillary venules get information about foreign invasion by changes on the surface of the endothelium or by soluble agents that were released from the infected tissue. Neutrophils are the first leukocytes to arrive at the site of infection or tissue injury. The released factors are able to promote the migration of the neutrophil towards the site of inflammation. Factors can be cytokines like Tumor necrosis factor α (TNF-α) (*229*) or Interleukin-6 (IL-6) (*23*) but also various products like *N*-Formylmethionine-leucyl-phenylalanine (fMLP) derived from tissue macrophages (*192*) or endothelial cells like C-X-C motif chemokine ligand 5 and ligand 1 (CXCL5, CXCL1) (*173, 196, 217*). The initial response is adherence of the neutrophil to the endothelium of the vasculature followed by transmigration and crawling towards a chemotactic gradient (see section 2.2.4). The process of migration requires the activation of signaling pathways, cytoskeletal rearrangement as well as changes in the cell surface molecules.

2.2.4. The neutrophil adhesion cascade

The recruitment of neutrophils to sites of inflammation is initiated by the release of pathogen-associated molecular patterns from invading pathogens (PAMPs) or damage-associated molecular patterns released from damaged endothelial cells (DAMPs) (*16*). These signals are recognized by surface and also by intracellular receptors, that once activated, can secrete cytokines and chemokines that promote the leukocyte migration and trigger the inflammatory response (*98*) (Fig. 3).

The first adhesion molecules that get expressed on the surface of the stimulated endothelial cells are P- and E-Selectin, expression occurs already after minutes or few hours. They can bind to P-Selectin glycoprotein ligand-1 (PSGL-1) and E-selectin ligand-1 (ESGL-1) present on the neutrophil surface (*249*). This selectin signaling initiates a slow rolling process of the neutrophil, followed by strong adhesive contacts.

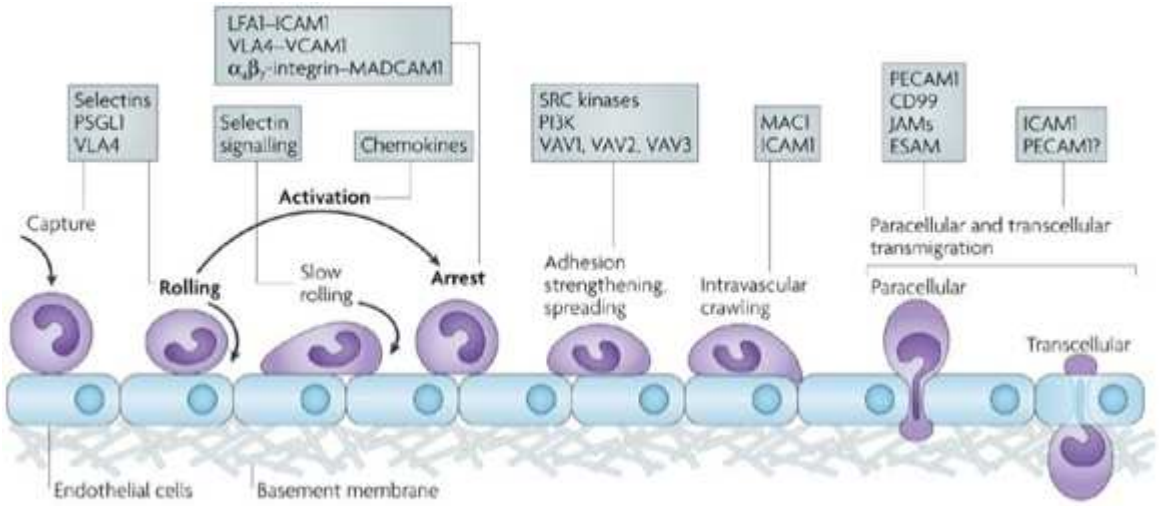

Figure 3: The neutrophil adhesion cascade

Three steps of the neutrophil adhesion cascade can be differentiated: Rolling, activation and arrest. Rolling is mediated by selectins, activation is mediated by integrins and arrest is mediated by integrins. Over the years, the adhesion cascade has been enhanced with the steps of capture, slow rolling, adhesion strengthening and spreading, intravascular crawling, as well as paracellular and transcellular transmigration (*145*).

The adhesion is mainly triggered by the activation of neutrophil integrins (LFA-1) by chemokines like intracellular adhesion molecule 1 and 2 (ICAM-1, ICAM-2) and vascular cell adhesion molecule 1 (VCAM-1) (*2, 103*). These interactions lead to transformational changes of the neutrophil via cytoskeletal rearrangement causing luminal crawling of the neutrophil along the endothelium until they reach the site of transendothelial cell migration.

The neutrophil then crosses the endothelium transcellular via ICAM-1 or paracellular via platelet endothelial cell adhesion molecule 1 (PECAM-1) (*47*). The current evidence from *in vivo* and *in vitro* studies indicates that the paracellular migration is more prominent than the transcellullar (90% vs. 10%) (*265*). After transmigration the neutrophils can initiate their movement towards the site of inflammation through detecting tracks created by chemokine gradients (*84*).

3. Transmembrane Receptors

3.1. Definition

Transmembrane receptors are important proteins for communication between the cell and the environment. Extracellular ligands like hormones, cytokines, growth factors or neurotransmitters bind to the receptor and mostly trigger a change in the conformation of the cell receptor. This conformational change then initiates intracellular signal transduction. Many biological pathways are regulated by cell surface receptors, for example cell growth, differentiation and proliferation (*66, 119, 231, 261*).

Due to the high importance of these signal transduction pathways, a lot of diseases like cancer, neurodegeneration and atherosclerosis are caused by mutations in cell surface receptors (*46, 208*).

Cell surface receptors can be divided into three classes: G protein-coupled receptors, enzyme-linked receptors and ion channel-linked receptors (*57*).

3.2. Integrins

Integrins are present on most cell types and consist of a heterodimer α- and non-covalent binded β-subunit (Fig. 4) (*26*). These subunits are mostly involved in linking adhesive molecules to the cytoskeleton and can exist in two affinity states, low and high, altered by a cytoplasmic signal. It can be differentiated between three major integrin families β1, β2 and β3, which are also important for integrin classification, and five different Integrins, α2β1 (collagen receptor), α5β1 (fibronectin), α6β1 (laminins), $\alpha_{IIb}\beta_3$ (fibrinogen and von Willebrand factor) and αvβ3 (vitronectin). Required for the integrin binding on ligands is the presence of cations (like Mg^{2+}, Ca^{2+} and Mn^{2+}), increased receptor expression on the cell surface and affinity-modulation of the extracellular domain (*74, 128*).

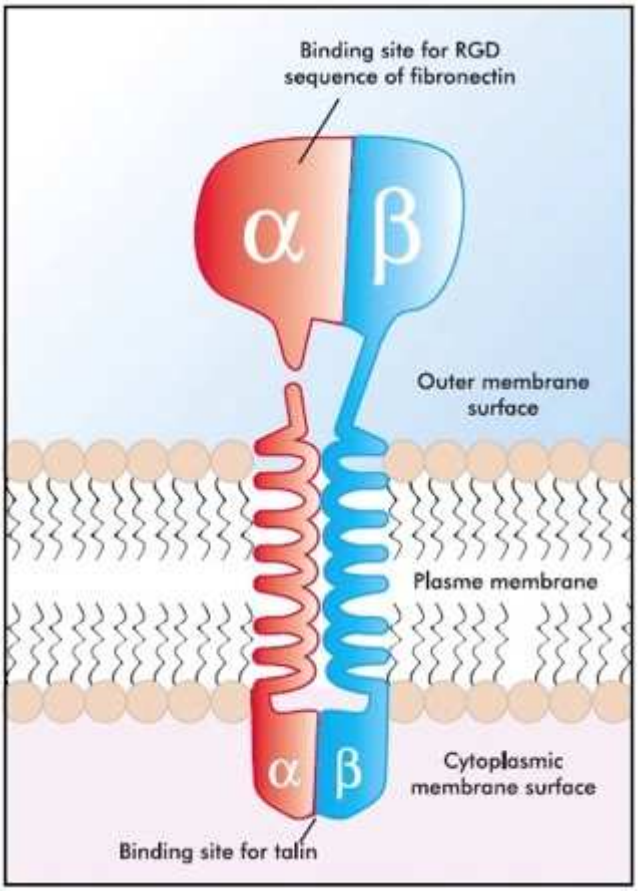

Figure 4: Integrin structure.

Diagram of Integrin α- and β- subunits. In the outer membrane surface the subunits have an adhesive glycoprotein that can interact with proteins (RGD) to form a binding site. On the inner cell site the Integrin can bind to the cytoskeleton (*177*).

A fast presentation of Integrins on the platelet surface can be achieved via interaction and fusion of integrin-rich granules with the cell membrane (*87*). Activation of the integrin receptors is managed through a conformational change, induced by binding of agonists, like thrombin and ADP, with the membrane receptors. This process is called “inside-out-signaling” (*174*), whereas direct binding of ligands on the integrin and the related conformational change is called “outside-in-signaling” (Fig. 5) (*223*).

3.2.1. GPIIb/IIIa-Integrin

Platelet aggregation is mediated by a specific receptor, $\alpha_{IIb}\beta_3$, found on the surface. It is a member of the Integrin family, with a capacity to undergo activation and thereby transition from a low-affinity to a high-affinity state for the extracellular ligands (*38, 219*). This transformation allows binding to fibrinogen (*251*) or von Willebrand factor, which act as bridging molecules between platelets to form aggregates. Also other ligands are recognized, such a vitronectin (*169*), fibronectin (*198*) thrombospondin (*4*) and CD40 (*3*), which help to initiate platelet adhesion to the endothelial matrix and platelet aggregation (*197*).

The key role of platelet aggregation for the GPIIb/IIIa-Integrin was demonstrated many years ago, in particular antibody blockage of GPIIb/IIIa led to absence of platelet aggregation (*54*), defined this integrin as a potential target for antithrombotic therapy (*95*). $\alpha_{IIb}\beta_3$ is of the β3-subfamily of integrins together with αVβ3. The Integrin $\alpha_{IIb}\beta_3$ is found on the surface of platelets, basophils, mast cells, megakaryocytes and tumor cells (*20*), αVβ3 can be found on a lot of cell types where it influences cell adhesion, migration, angiogenesis and atherosclerosis (*33, 37*). All these ligands have the presence of arginine-glycine-asparatic acid sequence (RGD) in common, RGD contains peptides that bind to both of the β3 Integrins.

When platelets are circulating in the blood, $\alpha_{IIb}\beta_3$ exists in a resting and low-affinity conformation. After the stimulation with an agonist, $\alpha_{IIb}\beta_3$ gets transformed to its higher affinity state (*157*). The most prominent agonist is fibrinogen. These conformational changes get transmitted across the transmembrane domain and change the conformation of the extracellular domain ligand-binding site. This leads to a shift from the bent conformation to an extended conformation of the extracellular domain that is competent to bind soluble ligands (Fig. 5). This ligand binding transmits signals from the receptor into the platelet (outside-in-signaling), which are important for platelet responses (*147*).

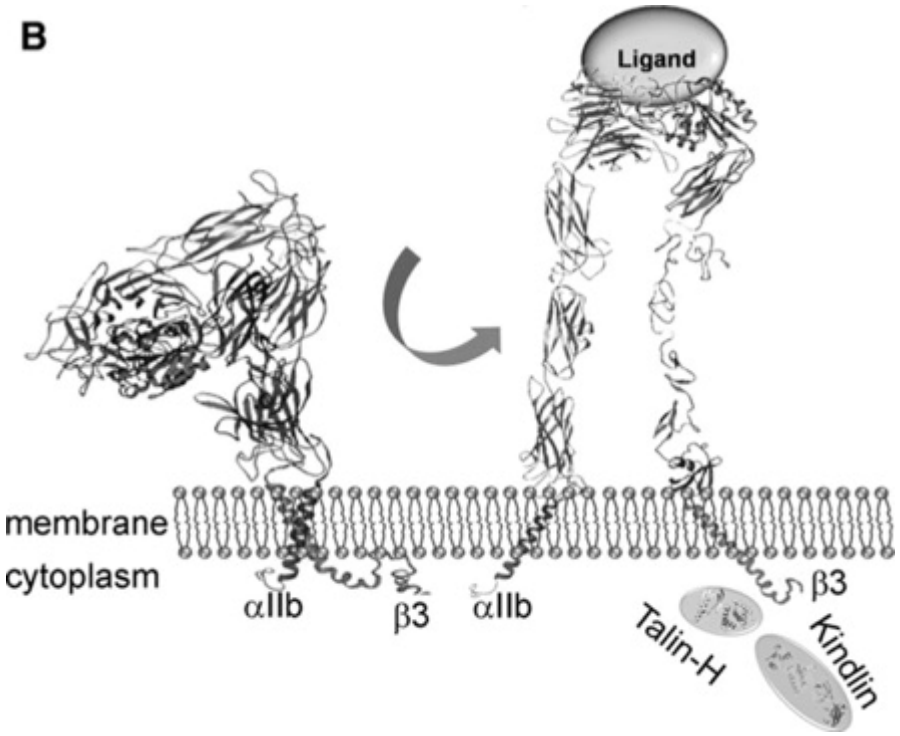

Figure 5: Pathway for activation of $\alpha_{IIb}\beta_3$.

Inside-out-signaling can be induced by binding to a G-protein-coupled receptor. This initiates signaling pathways that lead to cytoplasmic tails of $\alpha_{IIb}\beta_3$. Talin and kindling cooperate in this activation process by triggering the dissociation of the subunits from the transmembrane complex. This leads to a conformational change in the extracellular domain, resulting in a conversion from a resting state to an extended conformation that is competent to bind soluble ligands (*20, 202*).

The GPIIb/IIIa-Integrin mediates the adhesion of activated platelets on the intact endothelium (*45, 50, 146, 203*); in this way the GPIIb/IIIa-Integrin of platelets binds to the endothelial receptor “intracellular adhesion molecule-1” (ICAM-1) via adhesive bridging proteins like fibrinogen (*22*). This adhesion leads to an inflammatory reaction *in vitro*, triggering more adhesive characteristics of the endothelial cells (*165*). Also the von Willebrand factor plays an important role in platelet binding to GPIIb/IIIa via the GPIba-receptor (*30, 36*).

3.3. Selectins

Neutrophils are rolling along the endothelial cell surface to migrate from the blood vessel into the tissue. This process is mediated by selectins, a family of cell adhesion molecules (CAM). There are three known members of the selectin family (L-, E- and P-Selectin, the prefixes were chosen according to the cell type where the molecules were first identified. L-Selectin is expressed on most types of leukocytes; P-selectin in storage granules of platelets and the endothelium and E-selectin is expressed on the activated endothelium. They are distributed along the leukocyte-vascular system and can bind carbohydrate ligands.

The first selectin described to be important for the entry of neutrophils into inflamed tissue was L-selectin based on monoclonal antibody (MAb) inhibition (*143*). It was also shown, that activation and migration of neutrophils accompanied with the down regulation of L-selectin and an upregulation of Mac-1, suggesting that L-selectin acts before the integrins in the adhesion process (*132*). It was also shown *in vivo* that L-selectin mediates the leukocyte rolling; using a recombinant fusion protein blocked the rolling of the leukocyte (*144*). Over the years many studies have confirmed the role of all three selectins in leukocyte rolling and the initiation of leukocyte-endothelium interactions (*70, 190*). And also the entry of neutrophils into the tissue showed to be mediated by all three selectins (*120, 176*).

E-Selectin and P-Selectin are absent from the surface of non-activated endothelial cells and are expressed first after an exposure of the endothelial cells to an inflammatory stimulus. L-selectin however is constitutively expresses on leukocytes; the function is controlled by regulation of the ligand.

E-Selectin expression is triggered by cytokines, like TNF-α or Interleukin-1β (IL-1β), reaching maximum levels of expression on the cell surface 3-4h after the stimulation (*14*).

P-Selectin expression is inducible by two different mechanisms. After stimulation with histamine or thrombin it can rapidly be mobilized to the cell surface of endothelial cells within minutes or even faster within seconds on platelets. It is stored in α-granules in platelets as well as Weibel-Palade bodies (WPB) in endothelial cells (*88, 100*). The expression occurs within 5 to 10 minutes after stimulation; 30-60 minutes later the protein gets already cleared from the cell surface by exocytosis.

L-Selectin is constitutively expressed on neutrophils as well as most myeloid cells and a large subset of lymphocytes (*143*). In lymphocytes it can be downregulated during differentiation, however cell activation of neutrophils and lymphocytes causes rapid downregulation of L-Selectin. On neutrophils it gets shedded within 1-5 minutes after activation by a variety of activating factors like fMLP or TNF-α (*93*).

3.4. Interactions between neutrophils and platelets

Like described before, platelets adhere firmly to the inflamed endothelium by the GPIIb/IIIa Integrin complex via fibrinogen or von Willebrand factor anchoring. Activated platelets release more P-selectin from α-granules than the endothelium, causing likely a recruitment of leukocytes to the activated platelets and in this context a transmigration of the leukocyte through the endothelium (*65, 273*). P-Selectin mediated platelet-leukocyte complexes can be seen rolling along the endothelium after platelet activation and this induces an activation of platelet integrins (*75, 83, 171*). Infusion of activated platelets into mice leads to a secretion of WPB and an increase in the number of rolling leukocytes (*68*).

Other molecular mechanisms responsible of platelet-leukocyte interactions include a central role of platelet P-selectin and P-selectin glycoprotein ligand-1 (PSGL-1), its counter receptor found on leukocytes. In a signaling cascade, this interaction leads to activation of the beta-2 integrin Mac-1 and in a firm adhesion between the two cell types. The interaction of P-selectin with PSGL-1 also induces upregulation of leukocyte tissue factor and biosynthesis of several cytokines (*43*).

4. Cytokines

4.1. Definition

The term ‘cytokine’ comes from the Greek and essentially means to put cells in motion. Cytokines are peptides involved in intracellular signaling and can act in autocrine, paracrine and endocrine way. They are produced by a wide range of cells including macrophages, T- and B- lymphocytes, mast cells, fibroblasts, endothelial cells and stromal cells and include chemokines, interleukins, interferons and Tumor necrosis factor (*79*). The primary definition of cytokines is peptides released from stimulated leukocytes that target other leukocytes; eighteen cytokines have been described according to this pattern (‘interleukin-1’ to ‘interleukin-18’) (*32*).

However, the term ‘cytokine’ may be misleading, because in the meantime also interleukins were described who are produced by non-leukocytes and target non-leukocytes.

In contrast to hormones that circulate in nanomolecular concentrations in the blood, cytokines circulate only in picomolecular concentrations but can increase up to 1.000 fold during inflammation or trauma. Every nucleated cell and especially endothelial cells and macrophages can secrete cytokines in principle (*27*).

Many cytokines play key roles in inflammatory reactions, in particular Interleukin-1 (IL-1), TNF-α, IL-6, IL-11 and Interleukin-8 (IL-8). IL-1 and TNF-α are extremely potent inflammatory molecules and can mediate acute inflammation (*67, 194*).

4.2. TNFα

Tumor necrosis factor α (TNF-α) is an inflammatory cytokine involved in the acute-phase reaction with the definition to increase or decrease its own plasma concentration in response to inflammation. It exists as a trimer (*230*) and is a product of activated macrophages and monocytes, neutrophils, fibroblasts, mast cells, as well as T and natural killer cells (*1, 13, 89*). The role of TNF-α is to regulate immune cells via induction of fever, apoptotic cell death and inflammation. In the central nervous system TNF-α has regulatory functions on crucial physiological processes such as the plasticity of synapses (*6*), learning and memory, as well as sleep functions (*5, 12, 135*). TNF-α is first synthetized as a transmembrane protein, cleaved into a soluble form (sTNF-α).

The soluble form of TNF-α can bind to two surface receptors, TNF receptor 1 and 2 (TNFR1, TNFR2). TNFR1 signaling results in the activation of different signal transduction pathways like nuclear factor-kappa B (NF-κB) and the extracellular signal-regulated kinase (ERK). These pathways regulate the expression of genes that have anti-apoptotic effects, especially the genes regulated by NF-κB (*256*).

4.2.1. Blockage of TNF-α

Inhibition of TNF-α can be achieved in two different ways. One possibility is to bind directly to TNF-α via monoclonal antibodies. Common drugs are Infliximab (Remicade®) (*94*), adalimumab (Humira®) (*28*) and certolizumab pegol (Cimzia®) (*211*).

Another way to inhibit the function of TNF-α is to bind directly to the receptor. A circulating receptor fusion protein that functions as a TNF-α ligand is etanercept (Enbrel®) (*80*).

4.2.1.1. Infliximab

Infliximab binds directly with a high affinity to the soluble and transmembrane form of TNF-α thus neutralizing the biological activity and inhibiting binding of TNF-α with its receptors. Infliximab is capable of neutralizing all forms of TNF-α (extracellular-, transmembrane- and receptor-bound) (*48*).

With a high specificity of TNF- α, Infliximab does not bind to TNF-β, a cytokine produced by lymphocytes, mediating a high variety of inflammatory responses (*180*).

The medical use of Infliximab demonstrated efficiency in autoimmune diseases, including Crohn's disease (*72*), ulcerative colitis (*209*), psoriatic arthritis (*125*) as well as Behçet's disease (*218*).

In a mouse model Infliximab showed an anti-inflammatory effect on allergen-induced lung inflammation of acute asthma (*64*) and was able to prevent colitis-associated carcinogenesis (*131*). It is also known that the immunoreactivity of infliximab stored at 4° C over a period of 6 weeks remains stable, implying Infliximab to be suitable for long-time animal experiments (*7*).

5. Adipose tissue

5.1. Definition

Already in 1987 adipose tissue (AT) was described as a 'major site for metabolism of hormones' (*228*) with production of endocrine factors. The characterization of leptin in 1994 established the theory of adipose tissue as an endocrine organ (*274*). In fact adipose tissue is a complex and essential endocrine organ with a high metabolic rate, to be more specific, AT produces hormones such as leptin, resistin, estrogen, TNF-α (*127*) and the adipocyte-specific hormone adiponectin (*215*). AT contains adipocytes, connective tissue matrix, nerve tissue, immune cells and the so called stromal vascular fraction (SVF), a rich source of preadipocytes, endothelial progenitor cells, T cells, B cells, mast cells, mesenchymal stem cells as well as adipose tissue macrophages (ATM) (*204*). All of these components are able to respond to afferent signals from the traditional hormone system as well as the central nervous system. The main function of adipose tissue is the storage of energy in form of lipids as well as the energy release. But also the expression and secretion of bioactive peptides, called adipokines, plays a crucial role. These adipokines can act in the autocrine and paracrine as well as the endocrine way. These interactive network functions determine AT to coordinate a variety of biological processes, such as energy metabolism, immune function and neuroendocrine function.

5.2. Adipogenesis

The precursor cells of adipocytes are called preadipocytes, a form of undifferentiated fibroblasts that can form adipocytes after stimulation. The process of cell differentiation by which preadipocytes become mature adipocytes is called adipogenesis (*58*). Key features of adipogenesis are morphological change, expression of lipogenic genes, production of hormones like leptin, resistin, TNF-α, as well as growth arrest.

The development of mature adipocytes from preadipocytes is a progression of the activation of many transcription factors. This sequence is initiated with the activation of transcription factors of the activating protein-1 (AP-1) family, continuing with the induction and expression of peroxisome proliferator-activated proteins (PPAR), a proadipogenic transcription factor. Other transcription factors facilitating the maturation of adipocytes are Signal Transducer and Activator of Transcription (STATs), sterol response element-binding protein-1 (SREBP-1) and members of the CCAAT-enhancer-binding proteins (C/EBPs) (*153, 212*).

Mature adipocytes start to expand when the energy intake is higher than the expenditure. This process is highly regulated by counter regulator hormones like insulin, epinephrine, adrenocorticotropic hormone (ACTH) and glucagon. It is also known that mature adipocytes retain the ability to dedifferentiate *in vitro* into fibroblast-like cells, known as dedifferentiated fat cells (DFAT). These cells retain proliferative abilities and are able to differentiate into mature adipocytes again (*163*).

5.2.1. Phases of Adipogenesis

Two phases of adipogenesis can be distinguished (See Review: Rosen, 2006 (*206*)): The determination phase is characterized as a stage resulting in the conversion of the stem cell to the preadipocytes. The preadipocytes is morphologically identical to its precursor cell but has completely lost its ability to differentiate into other cell types.

The terminal differentiation phase describes the stage of the preadipocytes adopting the characteristics of a mature adipocyte. The preadipocytes acquire the machinery necessary for the transport and synthesis of lipids, insulin action as well as the secretion of adipocyte-specific proteins.

Thus *in vitro* cell lines are mostly based on preadipocytes that are unable to transform into other cell types, the terminal differentiation phase is quite better

described and investigated than the determination phase.

5.3. Adipocyte biology

Adipocytes, also known as fat cells or lipocytes are the main components of adipose tissue with a specialization of fat storage as energy (*18*). It can be distinguished between two typed of adipose tissue. White adipose tissue (WAT) and brown adipose tissue (BAT). WAT and BAT comprise two types of fat cells. Morphological differences between brown and white fat cells can already be observed via electron and light microscopy.

5.3.1. White adipose tissue

White adipose tissue consists of spherical cells with an average diameter of 10 mm. The size can increase as much as 10-fold, especially in the epididymal fat pads (*49*).

The increase in size requires a confined arrangement of the adipocyte cell organelles, since they are situated next to a unilocular lipid droplet that occupies a lot of the cytosolic space. Also the nucleus is compressed between the plasma membrane and the fat lipids most of the time. There is a sparse mitochondria distribution in white adipocytes and other cell organelles, like the smooth and rough endoplasmic reticulum and the Golgi apparatus. Adipocytes store energy in form of nutrient-derived triacylglycerol lipids being the main energy reservoir in mammals with the highest energy density of up to 85% of the adipocyte weight consisting of lipids. During periods of fasting the triglycerides are released by lipolysis and enter the mitochondria of metabolizing cells as free fatty acids to produce ATP (*234*). In addition to fuel storage, white adipose tissue also acts as a thermal isolator, protecting other organs from mechanical damage.

The role of white adipose tissue in obesity has become more important over the last years. WAT is now recognized as the main source of hormones involved in energy balance regulation, like leptin (*154, 195*). Also the role of adipokines being involved in overall metabolic regulation and the pathologies associated with obesity got more

significant (*152*).

5.3.2. Brown adipose tissue

Brown adipose tissue consists of brown ellipsoid adipocytes with sizes from 15 to 50 µm that contain multilocular lipid droplets. All classical cell organelles are present; the nucleus has a central position. The most important component of brown adipocytes is an abundant distribution of mitochondria and the expression of the proton transporter uncoupling protein 1 (UCP1) (*39*). UCP1 generates heat by non-shivering thermogenesis, activated by fatty acids, and increases the permeability of the inner mitochondrial membrane to allow for a return of protons from the inter-membrane space back into the mitochondria.

5.3.3. Fat depots

For this work four major fat depots in the mouse are defined. The epididymal fat pads are paired gonadal, attached to the epididymis/testes in males and the uterus/ovaries in females. The retroperitoneal fat pads are located along the dorsal wall of the abdomen and surround the kidney. The inguinal fat pads are found anterior to the limbs, directly underneath the skin. The brown fat pads are found under the skin between the dorsal crests of the scapulae (*155*).

5.4. Obesity

Obesity and overweight are defined as abnormal fat accumulation that may impair health. The body mass index (BMI) is commonly used to classify obesity and overweight in adults and is an index of weight-for-height. It is calculated as the weight divided by the square of the height in meters (kg/m^2). Overweight is defined with a BMI greater than 25, obese is defined with a BMI greater than 30 kg/m^2. With a dramatic worldwide increase of obesity over the past decades, it has become one of the most serious public health problems of our time.

In fact the worldwide obesity rate has doubled since 1980 with more than 1.9 billion adults (over 18 years old) being overweight in 2014 (39%), 13 % being obese (*264*).

Obesity and overweight are furthermore part of the so-called 'metabolic syndrome', a group of risk factors for heart disease, diabetes mellitus and stroke. Other risk factors being classified within the metabolic syndrome next to obesity are insulin resistance, impaired glucose tolerance, hypertension and hyperinsulinemia (*124*).

5.4.1. Obesity and inflammation

In 1993 Hotamisligil reported the first evidence that TNF-α disrupts the insulin-signaling cascade in adipose tissue (*104*). In addition, animals lacking macrophage chemotactic protein-1 (MCP-1), the receptor for macrophage trafficking, were characterized by a decrease in macrophage infiltration into adipose tissue that resulted in an insulin resistance (*122*).

Nowadays it has become fully accepted that the inflammation associated with obesity contributes to insulin resistance. There are many inflammatory mediators described including Interleukin-1-β (IL1-β), IL-6, IL-8, Interleukin-10 (IL-10), TNF-α and MCP-1. The stromal vascular fraction may also play an important role in the development of obesity-associated inflammation as well as insulin resistance; cells of the SVF have showed to secrete levels of inflammatory mediators exceeding the levels secreted by adipocytes (*76*).

There are a number of immune cells present in lean adipose tissue. These cells inhibit immune cell activation, characterized by expression of anti-inflammatory cytokines IL-4, IL-10 and IL-13 that trigger a T-helper cell 2 (Th2)–type response (*275*). Macrophages in lean adipose tissue are a dominant immune cell population, represented by macrophages with an M2-like phenotype. M2 macrophages are mostly characterized by their ability to metabolize the repair molecule arginine to ornithine, which inhibits the activity of nitric oxide synthase (*150*), a main player in the regulation of inflammation. Macrophages have shown to play a key role in the inhibition of immune cell activation in murine fat. A failure of ATM responses results

in the production of pro-inflammatory cytokines like TNF-α (*164, 267*).

Early phases of obesity are characterized by an increase in lipid accumulation per adipocyte but also by an increase in the accumulation of pro-inflammatory immune cells. Mice are the most common used animal models to study obesity via an induction of obesity by feeding the animals a high fat diet (HFD). This diet-induced obesity (DIO) triggers an accumulation of neutrophils, macrophages and NK cells already within the first weeks of HFD, measured as the production of the proteolytic enzyme elastase from neutrophils. Inhibition of neutrophil elastase results in enhanced insulin sensitivity, *in vivo* administration of exogenous elastase reduced insulin sensitivity (*238*).

One of the key events in the onset of DIO inflammation and insulin resistance seems to be the polarization of anti-inflammatory M2-macrophages to inflammatory M1-macrophages (*150*). A depletion of macrophages causes an improvement of insulin resistance (*134*). In addition macrophages seem to be the main source of pro-inflammatory cytokines in diabetic patients (*235*), suggesting that macrophages are one of the crucial factors in the development of AT inflammation.

Later stages of AT inflammation are characterized by necrotic cell death of adipocytes as a result of hypoxia (*272*). This necrosis results in the release of DAMPs that drive macrophages to produce even more pro-inflammatory cytokines. As a result, adipocytes are surrounded by rings of pro-inflammatory macrophages building “crown-like structures” (*260*) activating the NF-κB signaling cascade in macrophages and converting anti-inflammatory cytokines into pro-inflammatory cytokines (*140*) and producing even more pro-inflammatory cytokines like TNF-α (*42*). TNF-α impairs glucose uptake into adipocytes and inhibits the uptake of free fatty acids (FFA) (*166*), hallmarks of lipid metabolism. In addition TNF-α impairs the lipid storage capacity by suppressing the differentiation of new adipocytes from precursor cells by preventing the induction of PPARγ and C/EBPα, resulting in an inhibition of adipogenesis (*41*). In addition, production of TNF-α also triggers the NF-κB pathway resulting in an inhibition of adipose tissue growth (*241*).

III. AIM OF THE STUDY

Chronic inflammatory processes occur during the onset and development of obesity in WAT. With nearly 2 billion people being overweight worldwide (in 2014), obesity has become one of the most serious public health problems of our time (*264*). Furthermore, obesity and overweight are part of the so-called 'metabolic syndrome', a group of risk factors for heart disease, diabetes mellitus and stroke. Other risk factors are insulin resistance, impaired glucose tolerance, hypertension and hyperinsulinemia. Therefore, understanding the cellular mechanisms behind the onset and development of obesity is an important factor for a potential future treatment.

With leukocytes being well-established players during obesity development, this thesis focuses rather on a potential role for platelets and their potential interaction with leukocytes in the pathogenesis of obesity.

Specific aims are:

- Analyze WAT development in wild type animals as well as animals with malfunctioned platelets *in vivo*
- Document the adhesion of platelets and leukocytes in lean animals, as well as animals receiving high fat diet using intravital microscopy
- Check for specific chemokine and cytokine expression levels in diverse fat tissues
- Analyze the role of potential cytokines on adipocyte proliferation and differentiation *in vitro*
- Design a scheme of how the interaction of leukocytes and platelets could influence the development of WAT

IV. MATERIALS & METHODS

1. Research animals

All experiments in this thesis have been done using mice as research animals. Mice are easy available, cost-efficient and have a high reproduction rate. There are several genetically strains available which are highly congenic and can easily be compared with human biological characteristics. Due to their low size, they are easy to handle and therefore ideal when it comes to in-vivo experiments.

1.1. Wild type strain C57BL/6

The inbred mouse strain C57BL/6 was created in 1921 by C.C. Little from a mating of Miss Abbie Lathrop at the Bussey Institute for Research in Applied Biology. It is the most popular mouse inbreeding strain for animal experiments, also presenting the genetically background for many other mouse strains.

In this thesis the C57BL/6 mice were used for the infliximab treatment as well as the genetical background strain for the genetically manipulated GPIIb mice.

1.2. Genetically modified animals

The strain GPIIb$^{-/-}$ is characterized by a genetical defect on the GPIIb-locus. The defect suppresses the expression of the platelet-specific GPIIb-IIIa-receptor that plays a crucial role in the platelet-adhesion on the endothelium. GPIIb deficient mice show Glanzmann's thrombasthenia, an extremely rare coagulopathy. Due to the defective levels of the glycoprotein IIb/IIIa, a receptor for fibrinogen, platelet-fibrinogen-bridging is impaired, thus bleeding time is significantly prolonged.

GPIIb$^{-/-}$ mice have been created by Prof. J. Frampton (University of Oxford, Department of Pharmacology, United Kingdom)(*73*).

1.3. Animal Breeding

Animal breeding took place as a bigamy mating in our own animal facility. One buck was put together with two female animals. The animals were separated after a certain time, or at the latest when the female animals got pregnant. Pubs were separated from their mother animals after an upbringing phase of 4 weeks, male and female animals were then kept separately.

1.4. Animal Husbandry

Animal husbandry happened at the Medizinische Klinik und Poliklinik I, Ludwig-Maximilians-Universität München under SPF conditions (“Specific Pathogen Free”). SPF includes closed barrier system with personnel lock, material lock, pass-through autoclave and overpressure-ventilation. Cages were renewed every week, after washing by 80°C and autoclaving by 120°C.

Animals were held in IVC-system (individual ventilated cages) polysulfone-cages type M III (TECNIPLAST, Germany) with a maximum of 3 female animals per cage, male animals were held in individual cages. The cages were opened under appropriate transfer-stations. The mice got standard chow (Haltungsfutter V 1536, Altromin, Germany) and sterile tap water *ad libitum*. Food, water and litter were autoclaved in the animal husbandry only. The temperature measured 20-23°C with a stable air humidity of approximately 60%. The sleep-wake-cycle was set to 12h light and 12h dark, controlled by a time switch.

As an appropriate enrichment the cages were equipped with red plastic-houses (TECNIPLAST, Germany), sterile pulp paper and coarsely litter to enhance nest-building and animal welfare.

The SPF-status of the animals was controlled regularly testing Sentinel-animals for specific pathogens.

The entire animal experiments were approved by the government of Upper-Bavaria (Regierung von Oberbayern) pursuant to §8 of the German Protection of Animals Act (Deutsches Tierschutzgesetz, TierSchG, May 2006)

2. Operation Methods

2.1. Anesthesia

Surgeries were initiated using inhalation narcosis with Isoflurane (cp-pharma, Germany) and oxygen. Isoflurane was given using an evaporator (3% Isoflurane mixture). The usage of Isoflurane helps to reduce stress and the injury risk for the animals; therefore the entire surgeries were initiated in this way. Animals were set into a narcotic-chamber consisting of plexiglas®, which is easy to clean and sterilize, connected to the evaporator. After the inhalation of Isoflurane and the extinct of the startle reflexes, animals were taken carefully out of the chamber and then injected intraperitoneally (i.p.) with a triple-narcosis to bring them into the surgical tolerance-stadium. After injection the animals were layed into a shaded paper-box to reduce noises and optical stimuli. Operation was started after the interdigital reflex extinguished as well. The triple-narcosis consisted of Medetomidin (Dorbene vet 1 mg/mL, Pfizer GmbH, Germany), Fentanyl (Fentanyl 0.5 mg Rotexmedica GmbH, Germany) und Midazolam (Midazolam-hameln 5 mg/mL, Hameln Pharmaceuticals GmbH, Germany).

Medetomidin, a α2-agonist, functions as a sedative-hypnotical analgesic with muscle-relaxing and analgesic effects. As side effects it has depressing impact on the cardiovascular and the respiratory system.

Fentanyl is a synthetic generated opioid with a highly efficient pain inhibition. Side effects can be psycho-motoric symptoms and depression of the respiratory system.

Midazolam, a benzodiazepine, has sedative and muscle-relaxing effects.

For a proper usage of general anesthesia, the three narcotics should always be injected together.

The animals got a mixture of 0.5 mg/kg Medetomidin, 0.05 mg/kg Fentanyl and 5.0 mg/kg Midazolam, diluted with sterile NaCl (isotonic saline solution, Fresenius, Germany) as a total capacity of 0.35 mL. The triple narcosis was injected i.p., 10-20 min after the injection the animals should reach the surgical tolerance-stadium III2.

Pulse and respiratory frequency, as well as the continuous extinction of the interdigital reflex were checked in regular intervals. The animals lay on a heating mat (Dehner, Germany) to guarantee a homothermic state, oxygen was given via a respiratory mask.

2.2. Tail vein injection

The administration of fluorescently labeled dye was done via tail vein injection using an appropriate restrainer (Broome HAR- 52-04, Föhr Medical Instruments GmbH, Germany), which was cleaned properly after usage to avoid pheromonally-induced stress.

To stimulate dilation of the tail veins it was helpful to warm them via putting a glove filled with warm tap water directly on top of the tail for a few seconds. The tail was taken on its upper end between middle finger and trigger finger to pond the venous blood after disinfection of the puncture with Octeniderm (Schülke & Mayr GmbH, Germany).

The stain was injected over a catheter intravenously (i.v.), consisting of a 10 cm long polyethylene tube (Portex, 0,28 mm ID 0,61 mm OD, Smiths Medical International, USA) equipped with a cannula (30 G, BD Microlance, Becton Dickinson Labware, USA) combined with a 1 mL syringe (B. Braun, Germany). The cannula was inserted into the dilated Vena coccygea laterals and afterwards the substance was injected evenly.

2.3. Cardiac blood withdrawal

To obtain large amounts of blood for platelet isolation and labeling the mouse was anesthetized as described above. After reaching the narcotic state the mouse was put on a heating mat in dorsal position and disinfected in the thorax area. The skin was severed using a sterile operation-scissor.

A 2 mL syringe (B.Braun, Germany) combined with a 30 G cannula was injected vertical, diagonal to the hind leg, between the first and the second ridge. Blood was taken slowly to prevent pre-activation, 100 µL sodium citrate was provided in the syringe to prevent coagulation.

2.4. Platelet isolation and labeling

For platelet labeling approximately 1.5 to 2 mL whole blood was needed, furthermore it was crucial that the donor mouse had the same genotype as the recipient mouse. Mice should also be age and sex-matched. Whole blood was filled with Tyrodes (pH 6.5) up to 2 mL total capacity.

After first centrifugation (20 min, 66 G, brake off, RT) platelet rich plasma (PRP) was slowly taken off using a transfer-pipette, transferred into a new FACS-tube, filled up with Tyrodes (pH 6.5) up to 4 mL total capacity and labeled using Rhodamine B (2 mg/mL). After incubation at room temperature (RT) in the dark for 3 min, the blood was centrifuged again (10min, 1230 G, brake on). Supernatant was discarded, the pellet was resuspended in 4 mL Tyrodes (pH 6.5) and in the next step centrifuged (10min, 1230 G, brake on) again. The pellet was resuspended in 250 µL Tyrodes pH 6.5 and 250 µl Tyrodes pH 7.4. All of the steps were performed carefully to prevent platelets form being activated during the isolation process. 100 µL of the Tyrodes-platelets-mixture were measured using a hematology-analysis-device (ABX Micros ES 60, Axonlab, Germany) to obtain the exact platelets count. Afterwards it was calculated how much Tyrodes-platelet-mixture was needed to produce a platelet-suspension with a concentration of 120.000 platelets / µL using an Excel-Sheet (Microsoft, USA). The isolated and stained platelets mostly lasted for up to two recipient mice.

2.5. Neutrophil labeling

The neutrophils were labeled using CD45 antibody (Anti-Mouse, Alexa Fluor ® 488, Clone: 30-F11, 0,5 mL@1,0 mg/mL, eBioscience, USA). Alexa Fluor ® 488 has a maximum emission of 519 nm after excitation at 488 nm (Fig. 6). 20 µL antibody were drawed into a syringe submitted with 180 µL NaCl. To prevent fading of the dye, the injection should be done directly before imaging. The antibody was injected via tail vein (see 2.2.).

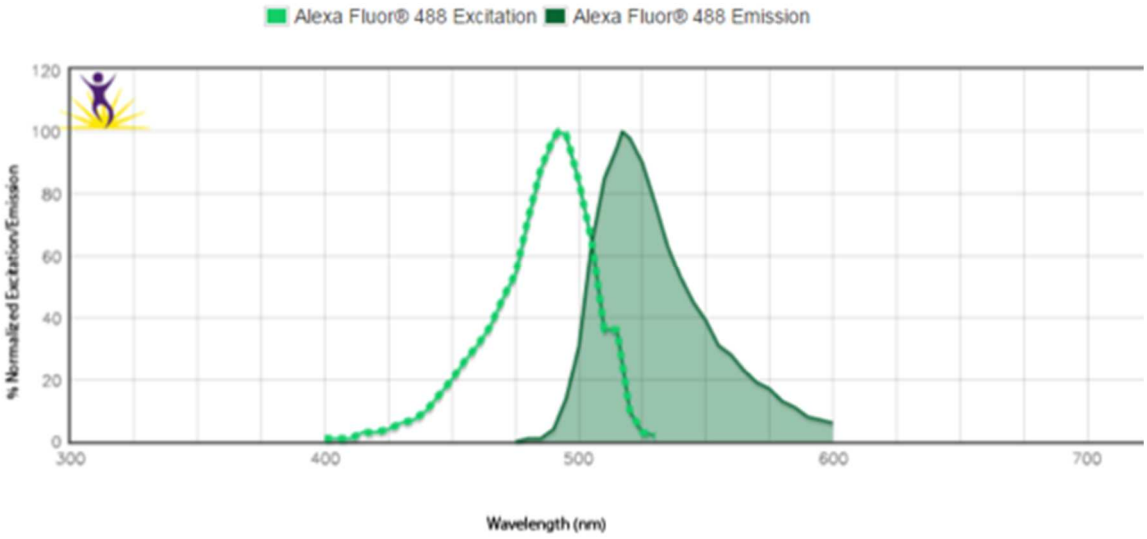

Figure 6: Excitation and emission spectrum of Alexa Fluor ® 488

Alexa Fluor ® 488 is best excited at 488 nm and emits light with a maximum of 519 nm (BioLegend spectral data (*17*)

2.6. Mouse preparation for intravital fluorescence-microscopy

Preparation of the anesthetized mouse started after reaching the surgical tolerance-stadium III2. The mice were weighed at first and then laid dorsal on a heating mat (IOW-3704, Föhr Medical Instruments GmbH, Germany), the snout was put into an oxygen mask, connected to an Isoflurane and oxygen evaporator. The abdominal region was shaved (Ermila Magnum Handy, Wahl, Germany), unhaired using depilatory cream (Veet, Germany), cleaned and disinfected.

Operation was done under a stereo-microscope (Zeiss, Germany); a swan-neck-light (Zeiss, Germany) illuminated the operation field in an optimal way.

Right before the intervention the Rhodamine B labeled platelets from the donor mice as well as the CD45 antibody (Anti-Mouse, Alexa Fluor ® 488, Clone: 30-F11, eBioscience, USA) were given via tail vein injection.

2.7. Surgical operation

Operation of the visceral fat pad started after the mouse reached the surgical tolerance stadium III2. After disinfection of the skin the mouse was fixed using adhesive tapes (Transpore, Germany). The abdominal skin was carefully grabbed using a fine forceps (FST, USA) and a lateral incision was performed cranial with a surgical scissor (FST, USA), afterwards the upper skin layer was carefully removed from the peritoneum. The skin was then fixed laterally on a foam rubber stage using a cannula (30 G, Braun, Germany). To ensure isothermal conditions, the whole incision area was kept warm and wet using 37°C warm sodium chloride (Braun, Germany), which was retained in a tube-like stage made of foam rubber. A small incision was made lateral in the peritoneum to get access to the visceral fat pad. The fat pad was grabbed using a wet cotton swap and carefully shifted onto the laterally pinned skin. A coverslip placed on the fat pad served as a lens in combination with a drop of sodium chloride (Fig. 7).

Figure 7: Surgical preparation of the visceral fat pad

After performing a lateral incision of the abdominal skin the visceral fat pad is slowly shifted outside. All of the surgical operation steps are performed under wet and warm conditions to feature a natural environment.

2.8. Fat pad removal

To get a detailed overview about the weight gain in different fat pads, it was important to do a proper fat pad removal. Also the size and weight of the organs were measured in this way. The fat pad removal started with the perfusion of the mouse with 0.9% NaCl. Therefor the mouse got an inhalation narcosis with Isoflurane in the narcotic chamber. After the extinct of the startle reflexes, the mouse was slowly taken out of the narcotic chamber and terminated via neck fracture. Afterwards the body weight was measured. The mouse was laid dorsal onto a polystyrene mat and fixed with adhesive tape. The body was wetted and disinfected with Ethanol (70%); a couple of tissues were put underneath for an optimal liquid absorption.

After an abdominal incision the sternum was opened cranially. The right heart ventricle was punctured and the left ventricle was perfused with 20mL sterile saline (0.9% NaCl). The skin was incised caudally and the uppermost skin layer was dissected carefully from the peritoneum. Afterwards the skin was pinned laterally onto the polystyrene mat. The subcutan located lymph nodes were removed carefully and discarded. Next the subcutan fat pad was removed; left and right side were weighed separately from each other.

All of the removed fat pads were stored, one part for histologic analysis in paraformaldehyde and the other part at -80°C in liquid nitrogen for real-time PCR analysis.

The peritoneum was opened caudally and the peritoneal skin was likewise pinned laterally onto the polystyrene mat. The epididymal fat pads were removed; also the intraperitoneal located fat at the digestive tract was removed and added to the epididymal fat depot.

The retroperitoneal fat pad was be found directly next to the kidneys and was removed equally.

The mouse was then put ventral onto the mat, the fur was wetted and disinfected with Ethanol (70%) again, and the skin located cranially above the scapula was sliced. The brown fat pads were found directly subcutaneous between the dorsal crests of the scapulae and were removed as well.

After the fat pad removal it was important to weigh solely the carcass. This meant to remove all of the organs out of the peritoneum and the thorax, as well as the removal of the skin. The extremities were cut off likewise. The tail was removed and the animal was decapitated. Afterwards the pure carcass was weighed.

The elevated fat pad and animal weights were documented properly (according to chapter 3.5.) and then inserted into an Excel sheet. The data of the body weight, the individual fat pads as well as the carcass weight were furthermore transferred to SigmaPlot (Chapter 3.4.) for graphical and statistical analysis.

2.9. Chimera Creation

2.9.1. Isolation of bone marrow cells

For the bone marrow isolation two GPIIb$^{-/-}$ as well as two GPIIb$^{+/+}$ respectively were used. The animals got an inhalation narcosis with Isoflurane in the narcotic chamber. After the extinct of the startle reflexes, the mice were taken out of the narcotic chamber and terminated via cervicale dislocation. After the mice were terminated the extremities were cut off, femur and tibia were dissected and freed from surplus tissue using a scalpel. Epiphyses were severed in the area of the metaphysis. The bone marrow cavity was rinsed with a brown cannula (26G) using sort buffer, that consisted of 1-fold PBS, 2 mM Ethylenediaminetetraacetic acid (EDTA) and 2% fetal bovine serum (FBS) through a 70 µm mesh into a new 50 mL Falcon tube. The solution was centrifuged for 5 min at 300G, 4°C, acceleration 5, brake 9. The supernatant was carefully discarded and the pellet was resuspended in 1 mL ammoniumchloride (NH_4CL) and afterwards incubated for 5-7 min at 4°C. The solution was then filled up with 10-20 mL sort buffer and centrifuged for 5 min at 300 G, 4°C, acceleration 5, brake 9 again. The cells were resuspended in 1 mL sort buffer, diluted 1:10 and the cell count was determined using the counting chamber. At least 5 million bone marrow cells should be used per recipient animal. The cells were resuspended and later on injected in a maximum of 300 µL NaCl per mouse.

2.9.2. Irradiation process

Two C57BL/6 mice were put into an autoclaved box at a time. Mice were not situated in boxes longer than 3 hours due to animal welfare conditions. The recipient animals being irradiated had the same genotype and sex as donor mice and were of similar age.

Irradiation was performed using a radiation-unit Mueller RT-250 (200 kV, 10 mA, Thoraeus filter, 1 Gray in 1 min 52 s) with a dosage of 6 Gray per mouse, resulting in duration of 11 min 20 sec (Fig. 8). Irradiation was repeated once 12-14 hours later. The irradiation process resulted in elimination of bone marrow cells.

4 h after the second irradiation animals received previously isolated bone marrow cells from donor animals via tail vein injection as described above. 5 million bone marrow cells per recipient animal, diluted in a maximum of 300 µL NaCl were applied. After injection the animals were brought into a specialized chimera husbandry room. The animals received acid, autoclaved drinking water (pH 3.1) with an addition of an antibiotic for 2 weeks (Cotrimoxazol, 5 mL / L).

About 12 weeks after the irradiation the animals were ready to be used for the fat pad removal (described in chapter 2.8.) and the evaluation of the animal and fat pad weights.

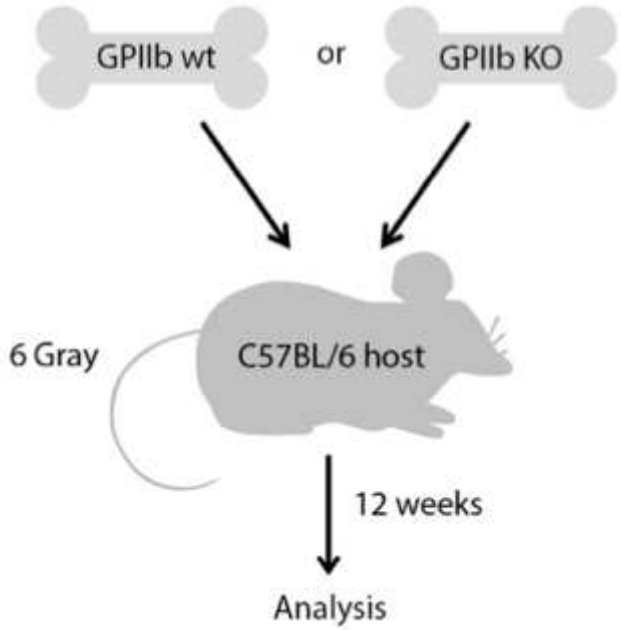

Figure 8: Schematic overview of the chimera creation process

C57BL/6 mice receive GPIIb wt or GPIIb KO bone marrow cells respectively. After a radiation of 6 Gray the animals are ready for further experiments after 12 weeks. Figure modified (*259*)

2.10. High Fat Diet Regime

The animal groups were set to seven per genotype. Mice were age and sex-matched. Animals who were planned to serve as platelet donors in experimental set-ups with high fat diet regime underwent an identical feeding regime as recipient mice.

For adaption of the gastro-intestinal flora animals received a control diet for one week before the experiment. This control diet contained 10% metabolizable energy from fat (C1090-10, 4% raw fat content, Altromin, Germany).

After this one-week initial phase the animals were split into two groups. One group received normal chow (Haltungsfutter V 1536, Altromin, Germany) for two more weeks, the other group received a high fat diet with 60& of the metabolizable energy from fat (C1090-60, 34% rat fat content, Altromin, Germany), also for two more weeks.

Food and water was available *ad libitum* over the whole experiment duration.

The animals were weighed twice a week, at the same time of day, to observe the weight development as well as the state of health.

After two weeks mice were prepared for intravital microscopy analysis as described in chapter 2.7. and imaged using an epifluorescence microscope. Again the number of rolling and adherent WBCs and also the number of transient adherent and firm adherent platelets were counted and further evaluated as described in chapter 3.3. and the following.

3. Intravital epifluorescence video microscopy

Epifluorescence microscopy enabled analysis of cells that were labeled with specific fluorescent dyes in *in vivo* models. The technique was based on the fact that fluorophores absorb short-wave stimulation light and emit it as long-wave light. Platelets were isolated and stained as described above using Rhodamine B. Rhodamine B, a dye from the group of Rhodamine, a Xanthen derivative, had already been described in the early 20th century (*179*). Rhodamine B (Fig. 9) reached it maximum absorption between 542 and 554 nm and its emission at a maximum of 600 nm in a neutral and aqueous solution (*226*).

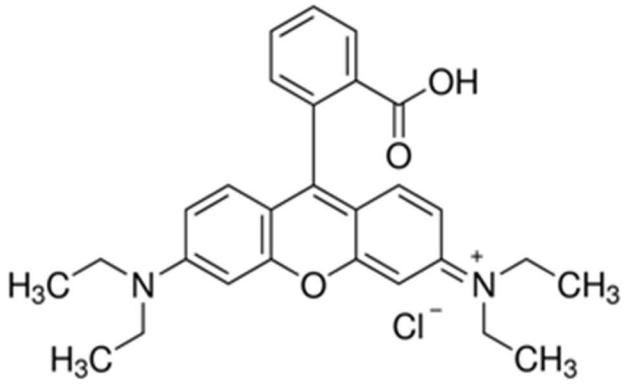

Figure 9: Structural formula of Rhodamine B

By choosing specific filters the epifluorescence microscope could be set to different spectral-light-areas, as a result only short-wave light reached the dyed cells. Filter in front of a camera let pass solely long-wave light around 600 nm to exclude remaining excitation-light.

3.1. Structure of the epifluorescent microscopy

The working area consisted of different parts. One part was the surgery space, which guarantees optimal oxygen care of the mice together with a heating mat, the surgical instruments and a swan-neck light. The other part was the epifluorescence microscope (Olympus BX54WI, Japan) with the illumination system MT20-E 150 W xenon arc burner (Olympus, Japan) and a charge-coupled device (CCD) camera (ORCA-ER, Hamamatsu Photonics, Japan).

The third part was a computer (Fujitsu, Japan) with an analysis software Cell-R (Olympus, Japan) and a monitor (Samsung, South Korea). Data was directly stored on the computer, a copy was burned onto a DVD for backup.

3.2. The epifluorescence microscope

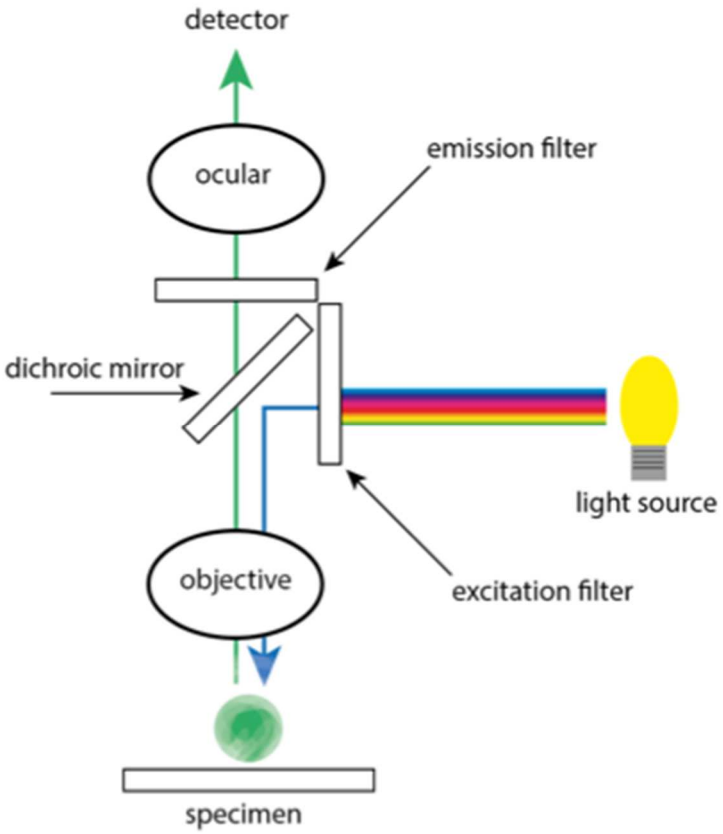

Figure 10: Optical path of the epifluorescence microscope

The epifluorescence microscope requires a near-monochromatic illumination from the light-source only xenon-arc lamps can provide. Light with a special excitation wavelength is focused through the objective lens and encounters the specimen. The specimen emits a fluorescence light that gets focused to the detector (*175*)

The term “fluorescent” referred to a microscope that uses fluorescence light to generate an image. Fluorescent dyes got excited with light of a specified wavelength, right before emitting light in another wavelength. Optical filters removed scattered light (Fig. 10). The structures that wanted to be analyzed could be stained with specific fluorochromes. In this study, neutrophils and platelets (Chapter 2.4. and 2.5.) were stained as mentioned above and injected directly via tail vein right before the imaging process.

Only light able to excite the fluorescence dye passed the excitation filter. It was important that the excitation filter prevents light of the same wavelength in which the fluorescence dye glows from getting through. A dichroic mirror mirrored the excitation light to the objective, resulting in a fluorescing specimen. This emitted light had a higher wavelength than the excitation light and passed the dichroic mirror towards the ocular and the CCD camera. The emission filter was an additional barrier to prevent reflected excitation light coming from the specimen from reaching the ocular.

3.3. Procedure of the epifluorescence microscopy

After clicking “database” → “administration” → “new database” the database is named after the experimental date in the format YYMMDD. The camera was set up: “Binning” 2x2 (672x512 pixel), “exposure time”: 30 ms, “brightness adjustment” was set to automatic. The laser was set depending on the used fluorochromes: “NIBA” for Fluor ® 488 stained neutrophils, “Rhod B” for Rhodamine B stained platelets, “Acri/Rho” for the dual view of neutrophils and platelets.

The epifluorescence microscopy started with a first orientation within the fat pad area and the search for large and small vessels through the ocular. After the objective was adjusted to an adequate area the software was configured in the same way. The fat pad was visualized in a 200x magnification. The camera was set into the live mode via and a video could be recorded.

3.4. Data evaluation with Microsoft Excel

Neutrophils and platelets per video were counted. The file “IVM-Excel” was opened and the mouse and the video were named.

The following values were inserted into the excel sheet: vessel diameter in µm, vessel length in µm, WBC adherent, WBC rolling, platelets adherent and platelets transient adherent.

Excel now calculated the factor to norm the vessel length to 500 µm (500 / vessel length) and the vessel radius (0.5 * vessel diameter). Also the half cylinder barrel was calculated via (vessel length * π * vessel radius) and this value was also normed to 150.000 qm² (150.000 / half cylinder barrel).

This normed value was used to calculate the number of adherent WBC corrected to 150.000 µm², rolling WBC corrected to 150.000 µm², adherent platelets corrected to 150.000 µm², as well as transient adherent platelets corrected to 150.000 µm², via multiplying the values of the manually counted cell with this normed half cylinder barrel value. These values could be quantified and plotted using SigmaPlot® (Systat, Germany).

3.5. Documentation

Whenever an animal was used for an experiment, a proper experimental protocol had to be made. This protocol provided information about the genetical background of the mouse, the genotype, the date of birth, the sex as well as the weight. Every operation step had to be logged. The most important thing was also to mention the reference number of the animal experiment proposal (Tierversuchsantrag) over which the experiment was reported. It was also of high importance to log the amount and time point of narcosis given to the animal during the duration of the procedure.

In experiments about the fat pad and organ removal it had further be logged which organs and fat pads were removed as well as the specific weight of the different fat pads.

4. *In vitro* culture of adipocytes

To study the effect of different substances on the development and proliferation of adipocytes, it was necessary to switch into an in vitro model additionally to the intravital experiments.

4.1. Maturation of preadipocytes

The murine 3T3-L1 preadipocytes were bought from ZenBio, Inc, USA (SP-L1-F, 3T3-L1 Preadipocytes Cryopreserved, 500.000 cells / vial) and stored in liquid nitrogen until usage.

The 3T3-L1 cell line derived from mouse 3T3 cells is a well-established cell line for the research on adipose tissue. The cells show a fibroblast like morphology and can differentiate into an adipocyte like phenotype (*92*).

For beginning the PM-1-L1 preadipocyte medium was warmed up to 37°C in the water bath for around 30 min. The frozen 3T3-L1 cells were heated up for 2 min in the water bath as well. 10 mL of the PM-1-L1 medium were put into a 15 mL Falcon tube and the 3T3-L1 cells were added. After a centrifugation for 5 min, 265G, brake on, the cell pellet was resuspended in 10 mL PM-1-L1 medium and added into a cell culture flask. Afterwards, the cell culture flask was put into a humified incubator, 37 °C, with 5-10% CO_2. The medium was changed every 2-3 days until cells reached confluency of approximately 70-80%.

After reaching 70-80% confluency the medium was completely removed from the cell culture flask and the flask was washed with 10 mL Ca^{2+} and Mg^{2+} free phosphate buffered saline (PBS). 2 mL Trypsin heated to 37°C were added into the flask and together incubated for 3 min at 37°C. Cells were detached carefully from the base by tapping the flask. To stop the Trypsin activity at least the twice the amount of PM-1-

L1 medium was added.

The cell culture flask was rinsed and the medium was transferred into another 50 mL Falcon tube. After centrifugation at 265 G for 5 min at RT, with brake, cells were resuspended in 2 mL PM-1-L1 medium. In the next step cells were transferred into a 12-well-plate. Cells were counted with a “Neubauer-Zählkammer” counting chamber, 20.000 cells were transferred per well.

1.2 mL PM-1-L1 medium were submitted into the wells. The plate was put into the incubator for 6-8 days, until the cells reached 100% confluency. Medium was changed every 2 days. According to different experiment setups the cells were co-incubated with different substances during their maturation phase (for details see below)

After the cells were confluent there was an additional incubation time of 48 hours without medium change before the initiation of the differentiation phase.

4.2. Differentiation of preadipocytes into adipocytes

The PM-1-L1 medium was first completely removed and 1.2 mL of DM-2-L1 differentiation medium added per well. After an incubation of 72h the DM-2-L1 medium was removed and 1.6 mL of the adipocyte maintenance medium (AM-1-L1) added. Medium was changed every 2 to 3 days. After 14 days cells were suitable for experiments.

4.3. Sudan III staining

The Sudan III staining is a fat-soluble dye that is used to stain nonpolar substances

(Fig. 11), in this case lipids for a better visualization and the possibility to quantify the cell sizes *in vitro* (*106*).

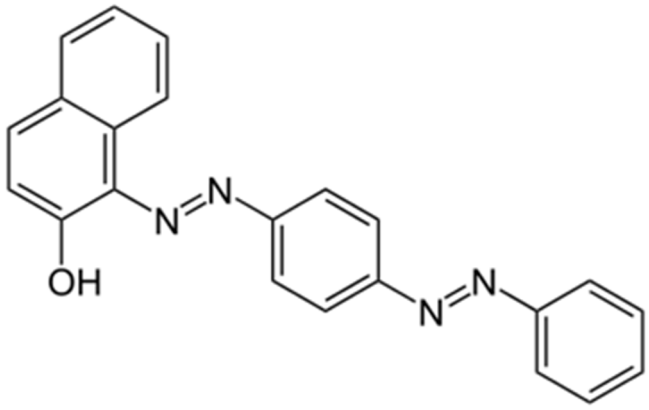

Figure 11. Structural formula of Sudan III

The Sudan III dye has a reddish brown appearance and is used to stain triglycerides, lipids and lipoproteins (*227*)

The Sudan III solution was prepared by weighing in 300 mg Sudan III powder with 100 mL Isopropanol (99%). 15 mL of the Sudan III solution were mixed with 10 mL of deionized (DI) H2O and then incubated for 10 min at RT. This solution was stable for about 2 hours and was supposed to be filtered directly before usage.

The adipocyte maintenance medium AM-1-L1 was removed from wells and wells were washed with PBS. After the removal of PBS the cells were first fixed with Paraformaldehyde (4%) for 60 min at RT. The Paraformaldehyde was then removed and the wells were washed with PBS again. Afterwards 1.5 mL Isopropanol (60%) were added and incubated for 5 min at RT. Isopropanol was removed, 1.5 mL Sudan III solution were added in each well and after incubation for 5 min at RT and removal of Sudan III solution cells were washed with 1.5 mL tap water. The cell nuclei were stained using 1.5 mL of hematoxylin, incubation for 1 min at RT and rinsed. For storage the wells should also be covered with tap water to prevent drying.

4.4. Adipocyte growth evaluation

The evaluation was made using a phase contrast microscope (Axiovert, Zeiss, Germany). The microscope was set to 20-fold magnification (Objective 1x), phase contrast 1, 7.4 V illumination. The software was set to mono, 1300x1030 pixel, standard, illumination 20 ms.

Wells were centered and photographed without magnification. One photo was taken per well, saved as JPEG and transferred to a computer for further evaluation with ImageJ (National Institutes of Health, USA).

Data was evaluated and quantified using SigmaPlot.

4.5. Neutrophil Isolation

Within the *in vitro* experiments adipocytes were co-incubated with polymorphonucelar neutrophils (PMN)

4.5.1. Preparation of the Percoll gradient

An isotonic Percoll solution was mixed with 90% Percoll (45 mL) and 10% 10-fold PBS (5 mL). This worked best if all the substances were brought to 4 °C before. Three different Percoll concentrations were prepared.

- 72% Percoll (10 mL): 7.2 mL isotonic Percoll + 2.8 mL 1x PBS
- 64% Percoll (10 mL): 6.4 mL isotonic Percoll + 3.6 mL 1x PBS
- 52% Percoll (10 mL): 5.2 mL isotonic Percoll + 4.8 mL 1x PBS

Afterwards 3 mL of each Percoll concentration were pipetted into a 15 mL Falcon tube. The 72% concentration was first, then came the 64% and the 52% concentration was added last. The gradient was set on ice afterwards.

4.5.2. Preparation of the bone marrow

After neck-dissection on anaesthetized mouse extremities were cut off, femur and tibia were dissected and freed from surplus tissue using a scalpel. Epiphyses were severed in the area of the metaphysis. The bone marrow cavity was rinsed with a brown cannula (26G) using 1-fold PBS through a 40 µm mesh into a new 50 mL Falcon tube. The solution was centrifuged for 5 min at 300G, 4°C. The supernatant was discarded and the pellet resuspended in 1 mL 1-fold PBS and afterwards pipetted onto the previously prepared Percoll gradient.

4.5.3. Isolation of the PMNs

The gradient was centrifuged at 1000G, 30 min, 4°C. After centrifugation two red and one white layer within the gradient were visible. The white layer, containing PMNs was pipetted into another 50 mL Falcon tube together with 50 mL 1-fold PBS and centrifuged again at 300G, 5 min, 4°C. The supernatant was discarded and the pellet resuspended in 3 mL 1-fold PBS again. After diluting the solution 1:10 with 1-fold PBS, 20 µL were transferred into the “Neubauer Zählkammer” counting chamber and evaluated as described in chapter 4.1.

4.6. Co-Incubation of Adipocytes with diverse substances

To examine the effect of diverse substances on the adipocyte proliferation, the cells were co-incubated on different days during their maturation and differentiation phase for 24 h each as described below.

4.6.1. Co-incubation with stimulated platelets

Platelets were isolated from donor mice as described in chapter 2.4. and counted. The platelet solution was diluted 1:10 using Tyrodes buffer and activated with ADP (5 µM stock solution, 9 µL / mL platelet solution) for 5 min at RT. Per well a total count of 2 * 10^6 / mL platelets was added, resulting in a concentration of 1.2 mL (2.4 * 10^6), platelets diluted in 200 µL tyrodes buffer. The adipocytes were co-incubated with platelets for 24 h and the medium was renewed afterwards. The following protocol was used for the co-incubation studies:

Differentiation day 1:

- Addition of 1 mL DM-2-L1 medium
- Incubation for 24h

Differentiation day 2:

- Addition of the calculated platelet amount
- Incubation for 24h
- Removal of platelets and medium
- Renewal of DM-2-L1 medium

Differentiation day 3:

- Incubation for 24h

Maturation day 8:

- Addition of the calculated platelet amount
- Incubation for 24h
- Removal of platelets and medium
- Renewal of AM-1-L1 medium

Maturation day 14:

- Addition of the calculated platelet amount

- Incubation for 24h
- Removal of platelets and medium
- Renewal of AM-1-L1

4.6.2. Co-incubation with stimulated platelet supernatant

The platelets were isolated from donor mice as described in chapter 2.4. and counted. The platelet solution was set to 100.000 platelets / mL and resuspended in 1 mL tyrodes buffer pH 6.5 and 1 mL tyrodes buffer pH 7.4. The solution was activated with ADP (5 µM stock solution, 9 µL / mL platelet solution) for 5 min at RT and centrifuged at 1230G for 10 min. The supernatant was then added to the adipocytes according to the following protocol:

Differentiation day 1:

- Addition of 1 mL DM-2-L1 medium
- Incubation for 24h

Differentiation day 2:

- Addition of the calculated supernatant amount
- Incubation for 24h
- Removal of supernatant and medium
- Renewal of DM-2-L1 medium

Differentiation day 3:

- Incubation for 24h

Maturation day 8:

- Addition of the calculated supernatant amount
- Incubation for 24h
- Removal of supernatant and medium
- Renewal of AM-1-L1 medium

Maturation day 14:

- Addition of the calculated supernatant amount
- Incubation for 24h
- Removal of supernatant and medium
- Renewal of AM-1-L1

4.6.3. Co-incubation with stimulated neutrophils

PMNs were isolated from donor mice as described in chapter 4.5.3. and counted using the counting chamber. The neutrophil solution was diluted 1:10 using PBS and activated with phorbol myristate acetate (PMA) (Calbiochem, Merck Millipore, Germany, 20 ng/ mL neutrophils) for 5 min at RT. Per well a total count of $2 * 10^5$ / mL neutrophils was added, resulting in an end concentration of 1.2 mL ($2.4 * 10^5$), neutrophils diluted in 200 µL PBS. The adipocytes were co-incubated with the neutrophils for 24 h and the medium was renewed afterwards. The following protocol was used for the co-incubation studies:

Differentiation day 1:

- Addition of 1 mL DM-2-L1 medium
- Incubation for 24h

Differentiation day 2:

- Addition of the calculated neutrophil amount
- Incubation for 24h
- Removal of neutrophils and medium
- Renewal of DM-2-L1 medium

Differentiation day 3:

- Incubation for 24h

Maturation day 8:

- Addition of the calculated neutrophil amount
- Incubation for 24h
- Removal of neutrophils and medium

- Renewal of AM-1-L1 medium

Maturation day 14:

- Addition of the calculated neutrophil amount
- Incubation for 24h
- Removal of neutrophils and medium
- Renewal of AM-1-L1

4.6.4. Co-incubation with unstimulated neutrophils

The neutrophils were isolated from donor mice as described in chapter 4.5.3. and counted using the counting chamber. The neutrophil solution was diluted 1:10 using PBS. Per well a total count of $2 * 10^5$ / mL neutrophils was added, resulting in an end concentration of 1.2 mL ($2.4 * 10^5$), neutrophils diluted in 200 µL PBS. The adipocytes were co-incubated with the neutrophils for 24 h and the medium was renewed afterwards. The time protocol was identical to chapter 4.6.3..

4.6.5. Co-incubation with unstimulated neutrophils and stimulated platelets

The neutrophils were isolated from donor mice as described in chapter 4.5.3., platelet isolation followed the protocol in chapter 2.4., platelets were counted using the counting chamber. The neutrophil solution was diluted 1:10 using PBS and added to the activated platelets diluted in tyrodes. Per well a total count of $2 * 10^5$ / mL neutrophils and $2* 10^6$ / mL platelets were added. The adipocytes were co-incubated with the neutrophils and platelets for 24 h and the medium was renewed

afterwards. To improve the cellular environment for the combination of platelets and neutrophils Ca^{2+} (100 mM) and MG^{2+} (100 mM) were added to the tyrodes buffer beforehand.

Differentiation day 1:

- Addition of 1 mL DM-2-L1 medium
- Incubation for 24h

Differentiation day 2:

- Addition of neutrophils and platelets
- Incubation for 24h
- Removal of neutrophils, platelets and medium
- Renewal of DM-2-L1 medium

Differentiation day 3:

- Incubation for 24h

Maturation day 8:

- Addition of neutrophils and platelets
- Incubation for 24h
- Removal of neutrophils, platelets and medium
- Renewal of AM-1-L1 medium

Maturation day 14:

- Addition of neutrophils and platelets
- Incubation for 24h
- Removal of neutrophils, platelets and medium

4.6.6. Co-incubation with TNF-α

Another group of adipocytes was co-incubated with recombinant murine TNF-α (ImmunoTools, Germany), 10 ng / mL as well as 1 ng / mL respectively. The TNF-α stock solution was 100 µg dissolved in 1 mL sterile H_2O, diluted 1:100 to produce 72 ng as well as 7.2 ng in 200 µL sterile H_2O, resulting in an end concentration of 10 ng as well as 1 ng dissolved in 1200 µL.

Differentiation day 1:

- Addition of 1 mL DM-2-L1 medium
- Incubation for 24h

Differentiation day 2:

- Addition of TNF-α
- Incubation for 24h
- Removal of TNF-α and medium
- Renewal of DM-2-L1 medium

Differentiation day 3:

- Incubation for 24h

Maturation day 8:

- Addition of TNF-α
- Incubation for 24h
- Removal of TNF-α and medium
- Renewal of AM-1-L1 medium

Maturation day 14:

- Addition of TNF-α
- Incubation for 24h
- Removal of TNF-α and medium
- Renewal of AM-1-L1

4.6.7. Co-incubation with ADP

Adipocytes were also co-incubated with ADP to examine if this stimulus alone already has an effect on the adipocyte proliferation. The ADP was added in the same concentration as described in chapter 4.6.1., dissolved in tyrodes, also the co-incubation protocol was identical to chapter 4.6.1..

4.6.8. Co-incubation with PMA

Adipocytes were also co-incubated with PMA to examine if this stimulus alone already has an effect on the adipocyte proliferation. PMA was added in the same concentration as described in chapter 4.6.3., dissolved in PBS, also the co-incubation protocol was identical to chapter 4.6.3..

4.6.9. Co-incubation with Tyrodes

The cells were co-incubated solely with tyrodes as a control group to check whether the cell cultural work steps influence the adipocyte proliferation. 200 µL tyrodes pH 7.0 were added per well. The time-protocol was identical to chapter 4.6.1..

4.7. Adipocyte preparation for ELISA quantification

To check for the expression of the cytokine TNF-α, the adipocytes were co-incubated comparatively to chapter 4.6., but in this setting, co-incubation took place after adipocytes were completely maturated at day 18 and incubation time was reduced to a time of 3 hours. The ELISA process can be looked up more precisely in chapter 5.1.

5. Infliximab Setting

The mice were treated with Infliximab® (MSD, Germany), a monoclonal antibody against tumor necrosis factor alpha for 6 weeks. Afterwards the TNF-α expression was measured using a suitable ELISA Kit.

60-70 day old C57BL/6 mice received an intraperitoneal administration of 6.25mg/kg Infliximab® or vehicle (aqua ad iniectabilia) intraperitoneally. Animals were treated once a week over 6 weeks. Body weight was measured once a week, directly before the treatment. After 6 weeks, mice were anesthetized and fat pads were removed as described above.

Blood serum was collected and TNF-α serum concentrations were determined using ELISA according to manufacturers' instructions (R&D Systems, USA).

5.1. ELISA quantification

For the quantification of the TNF- α concentrations in the blood serum and the *in vitro* supernatant enzyme linked immunosorbent assays (ELISA) were used. The ELISA Kit was used according to manufacturer's instruction (R&D Systems).

After Infliximab treatment blood was collected via cardiac blood withdrawal and serum was centrifuged at 300G, 15 min, 4°C.

In case of cell culture experiments supernatant was taken, centrifuged (300G, 15

min, 4°C) and subjected to ELISA analysis.

5.1.1. Performance of the ELISA

The samples were stored at -80°C at brought to RT before usage. The samples and the standard series were used as a dual approach.

For the standard series the Mouse TNF-α Standard was first reconstituted with deionized water to produce a stock solution of 7000 pg/mL. After adding 900 µL of the calibrator diluent (RD5K for cell culture supernatant, RD6-12 for serum samples) to a 700 pg/mL tube, 200 µL of the appropriate Calibrator diluent were added into the remaining tubes. The stock solution was used to produce a dilution series (Fig. 12).

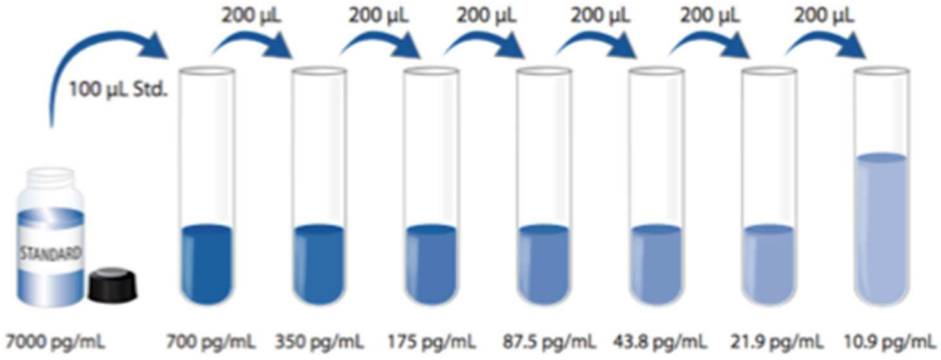

Figure 12: Production of the standard series

The TNF-α Standard was reconstituted with deionized water and was then used to produce the standard series. At first 100 µL were added into the 700 pg/mL tube. Afterwards 200 µL were transferred into the next tube and so on.

The appropriate Calibrator diluent served as the zero standard and the 700 pg/mL as the high standard. From each sample as well as the standard series 50 µL were pipetted into the 96 well ELISA plate. The plate was covered and incubated at RT for 2h on an ELISA plate shaker (Heidolph Duomax 1030, Heidolph Instruments, Germany). After the incubation the wells were emptied completely and washed using 250 µL wash buffer (20 mL wash buffer concentrate were mixed with 500 mL

deionized water before). The wash procedure was performed 5 times. Afterwards 100 µL Mouse TNF-α Conjugate were added to each well and incubated at RT for 2h again. The wash steps were repeated as described above. 100 µL of the Substrate solution were added to each well and the plate was incubated dark at RT for 30 min. Afterwards 100 µL of the Stop solution was added directly into each well.

5.1.2. ELISA data evaluation

Directly after the stop solution was added the chemical reaction was measured using an ELISA plate reader (Infinite F200, Tecan Deutschland GmbH, Germany). The software icontrol 1.9 (Tecan Austria GmbH, Austria) then measured the absorption of the colored wells. The data was prepared as an Excel sheet and further evaluated using an online software tool (myassays.com). The tool calculated the concentration of TNF-α per well in ng/mL. The different groups were then compared and statistically evaluated using SigmaPlot.

6. Analysis of Fat pad vascularization

6.1. Principle of the two-photon microscopy

Two-photon microscopy was used to determine the vascularization level in fat pads of whole mount specimen of GPIIb-KO mice and controls. It was an imaging technique that was able to perform fluorescent imaging in the living tissue up to 100 µm in depth. In this way it was possible to perform a three-dimensional *in vivo* analysis in different kinds of tissues over a certain time period (*62*). Maria Göppert-Mayer established the theoretical basis of the excitation of two photons in 1931 and this photo-physical effect was further verified experimentally in 1963 by Kaiser and Garret (*121*).

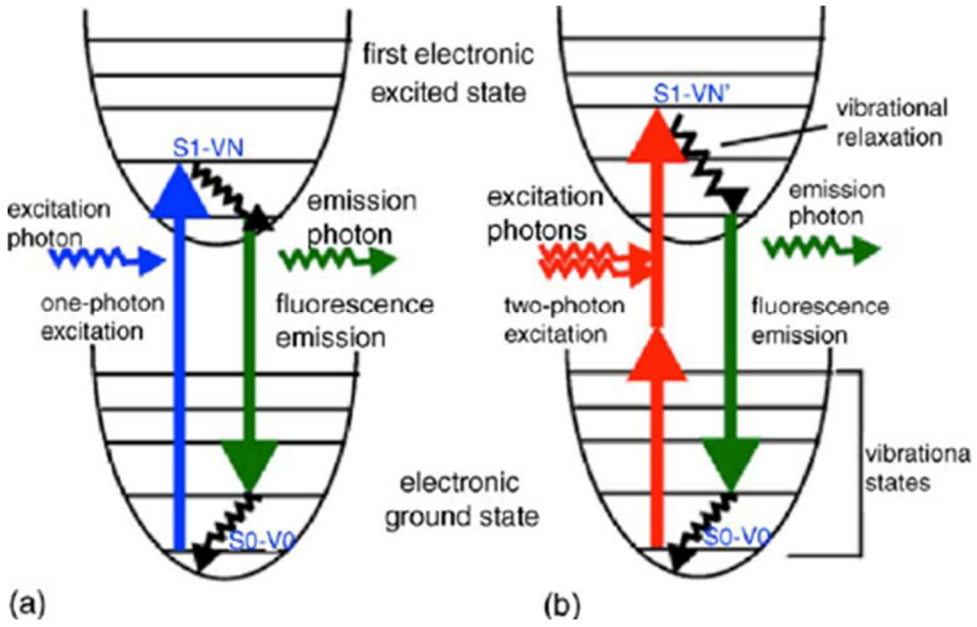

Figure 13: Jablonski diagram for one-photon (a) and two-photon (b) excitation.

Two photons arrive simultaneously within a few femto-seconds and excite the electrons of the fluorochromes. The femto-second laser source provides sufficient intensity for two-photon absorption within a single pulse but is still low enough to avoid damage of the specimen (*137, 233*).

In the excitation process a fluorophore was excited by a simultaneous absorption of two infrared photons (Fig. 13).

The one-photon microscope involved the excitation of a fluorophore by a single photon, typically in the ultraviolet spectra range. The simultaneous absorption of two less energetic photons could generate the same excitation process if the sum of the energies of two photons was greater than the energy gap between ground state and excited state of the molecule.

6.2. Structure of the two-photon microscope

The two-photon microscope (TrimScope, LaVision BioTec, USA) was composed of a titanium-sapphire laser (MaiTai, Spectra Physics, Germany) with a wavelength range from 700-1000 nm. An optical-parametric oscillator (OPO) enhanced the excitation

wavelength to 1100-1600 nm and increased the imaging depth with a higher resolution. The dichroic mirror reflected the excitation light to the objective and towards the specimen. Fluorescence was created and raster scanning in three dimensions (x-y-z) constructed an image. Afterwards the same objective collected the emission signal and transmitted it through the dichroic mirror along the emission path.

6.3. Whole mount staining

6.3.1. Injection of the primary antibody

To evaluate the vessel structure of fat pads in GPIIb $^{+/+}$ and GPIIb $^{-/-}$ mice a CD144 primary antibody was injected via tail vein to stain the vascular endothelial Cadherin (20 µL, Anti-Mouse, Clone: eBioBV13, 20 µg, eBioscience, USA), diluted in 180 µL NaCl 0.9%. After 1h incubation transcardial perfusion was performed to reach bloodlessness. The method of tail vein injection and transcardial perfusion were described in more detail in chapter 2.2. and 2.8.

6.3.2. Secondary antibody staining

For whole mount staining subcutaneous fat pads were removed as described in chapter 2.8. and transferred into a 1.5 mL Eppendorf tube and fixated with paraformaldehyde (4%) for 30 min in the dark at RT. After washing with PBS the secondary antibody was added. The secondary antibody was diluted 1:100 in a 1.5 mL Eppendorf tube. Therefor 500 µL PBS were mixed with 5 µL Alexa Fluor ® 594 (donkey anti Rat IgG, 2 mg/mL, Thermo Fisher Scientific, USA). The fat pad was added and incubated for 1 hour in the dark at RT and afterwards washed with PBS.

6.3.3. Fat pad imaging using 2-photon microscopy

Right before the imaging process fat pads were washed with PBS again to remove possible unbound antibodies. Fat pads were fixed onto a histology-case filled with modeling clay using cannulas and immediately covered with 0.9% NaCl to prevent it from drying. The whole mount was put under the 2-photon microscope (LaVision, Biotech, Germany) and Imspector software (LaVision, Germany) set to:

- 3D-Scan
- Laser: Wavelength 820 µm
- Size: 558x558
- Pixel: 837x837
- Step Size: 2 µm
- Frequency: 800
- Line Average: 2 µm
- Channel: Red, green, blue

The range was set to 100 µm using the Cell-R software. Per fat pad a total of 6-8 videos in different areas were recorded.

6.3.4. Data evaluation with IMARIS

The two-photon scans were analyzed using IMARIS imaging software (Bitplane, Switzerland).

After analysis a spreadsheet was opened showing different parameters (Area, Volume, X-Position). This spreadsheet was “saved as” an Excel file and opened in a separate Excel window. The ratio between total fat pad volume and the vessel volume (Surface) per fat pad was evaluated as percentage. The ratio values of all videos taken from one fat pad were averaged and statistically and graphically evaluated using SigmaPlot.

7. Statistical Analysis

Statistical analysis was performed using SigmaPlot 12.5 ® (Systat Software Inc., Germany). Results with a p-value smaller than 0.05 were considered as statistically significant. Before testing for statistical significance SigmaPlot ® proofed the data for being normally distributed using the Shapiro-Wilk-test. After passing the normal distribution test data was compared between the wild type group and the Knockout animals in the *in vivo* settings, the untreated with the treated cells for the *in vitro* setting, as well as the untreated with the treated group in the infliximab setting. In each case the Student's t-test was used. If the data did not pass the test for normal distribution the Mann-Whitney *U* test was used.

For using the statistical tests mean values of each groups were counted and compared. Also the standard error of the mean was calculated using SigmaPlot ®.

Mean values and standard errors were presented using bar charts. For some experiments dot-plots were used for better overview. Here the mean value and the standard error of the mean were indicated in the text.

V. RESULTS

The thesis addresses the role of platelets and leukocytes in adipose tissue vasculature. Therefore, it was analyzed whether platelets interact with activated endothelium of adipose tissue vessels. *In vivo* microscopy was performed in wild type versus GPIIb deficient mice. It was further tested, whether platelet adhesion assisted leukocyte recruitment and status of adipose tissue mice.

1. Platelet and leukocyte adhesion in visceral WAT

In the here described scientific project the role of platelet adhesion and the recruitment of WBC during the initiation of adipose tissue inflammation is evaluated. In the first part of the project, performed by PhD-Student Tristan Konrad, platelet dynamics in subcutaneous fat depot microcirculation were evaluated. Therefore 8-10-week old lean α_{IIb}-deficient mice, which lack $\alpha_{IIb}\beta_3$-surface expression, as well as wild type control animals were used. Using *in vivo* microscopy, T. Konrad found constant low grade platelet adhesion in the microcirculation of subcutaneous tissue, which was abolished in the $\alpha_{IIb}\beta_3$-deficient mice. Lack of platelet adhesion culminated in increased body fat in $\alpha_{IIb}\beta_3$-deficient mice. Additionally, Alexa Fluor ® 488 labeled CD45 antibody was infused to visualize leukocyte dynamics in subcutaneous adipose tissue vessels of lean, wild type or $\alpha_{IIb}\beta_3$-deficient 8-10 week old mice. T. Konrad found only rare firm leukocyte adhesion. No significant differences between leukocyte adhesion in animal groups was found, though data show a tendency in reduced leukocyte adhesion in $\alpha_{IIb}\beta_3$-deficient mice compared to controls (unpublished data). In the pathogenesis of obesity current data described more prominent inflammatory processes and WBC actions in visceral compared to subcutaneous WAT (*35, 77*). In a consecutive part of the project I thus analyzed platelet and leukocyte dynamics in the visceral WAT of lean 8-10 week old $\alpha_{IIb}\beta_3$-deficient mice and controls.

In the first part of the project epifluorescent *in vivo* microscopy was performed to study platelet and CD45+ WBC dynamics in the microcirculation of visceral white adipose tissue of lean wild type and $\alpha_{IIb}\beta_3$-deficient mice. Fluorescently labeled platelets and Alexa Fluor ® 488 labeled CD45 antibody were administered to wild type or α_{IIb}-deficient 8-10 week old mice and platelet and WBC adhesion analyzed. Transient and firm adherent platelets were mitigated in α_{IIb}-deficient mice (transient adherent platelets: p-value 0.013, n = 6, 57.62 ± 11.62 vs. 16.88 ± 7.01, firm adherent platelets: p-value 0.009, n = 6, 28.19 ± 7.59 vs. 3.08 ± 1.97) (Fig. 14).

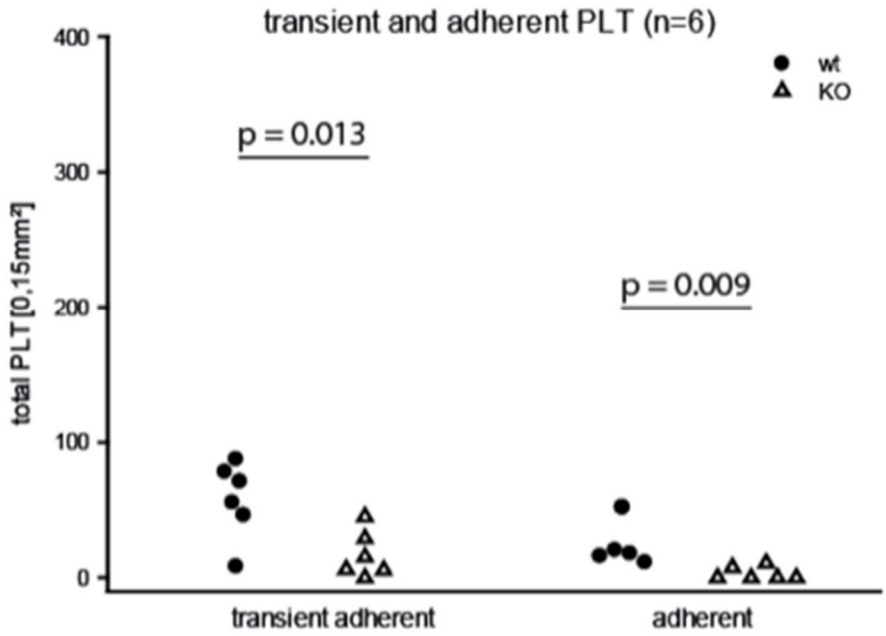

Figure 14: Number of transient and firm adherent platelets

Platelet adhesion in visceral WAT vasculature was evaluated in GPIIb deficient mice versus wild type control. The number of transient adherent as well as firm adherent platelets is reduced in the GPIIb deficient mice versus controls (p-value 0.01 and 0.009)

Platelets adhered to visceral fat pad endothelium in lean GPIIb wild type mice (Fig. 15). This effect was almost abolished in the GPIIb Knockout mice, platelets passed through the vasculature without firm or transient adhering to the endothelium.

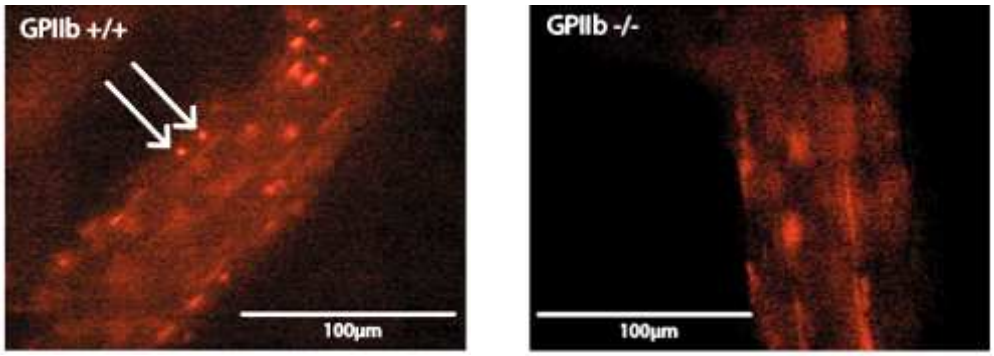

Figure 15: Rhodamine B labeled platelets in GPIIb wild type and Knockout mice

Representative freeze images of *in vivo* microscopy of visceral fat pad vasculature shows firm frequent platelet adhesion in GPIIb $^{+/+}$ animals (white arrows) that is virtually abolished in GPIIb $^{-/-}$ mice.

Unlike in platelet adhesion dynamics number of rolling WBC remained stable in GPIIb deficient mice (p-value 0.562, n = 6, 151.701 ± 19.62 vs. 133.47 ± 23.18) and reduced firm leukocyte adhesion in α_{IIb}-deficient mice was found though this effect did not reach statistical significance (p-value 0.180, n = 6, 56.98 ± 14.19 vs. 24.02 ± 5.52) (Fig. 16). The intravital microscopy revealed rolling and adherent WBC in GPIIb wt as indicated by arrows. Rolling and adherent WBCs were also detected in GPIIb deficient mice in comparable numbers (Fig. 17).

Chronic platelet and leukocyte adhesion was detected already in lean 8 to 10 week old mice. Moderate leukocyte recruitment occurred in both, GPIIb wild type and Knockout mice. Visualization of platelet and leukocyte dynamics was restricted when using epifluorescent microscopy because of insufficient optical penetration depth in more obese adipose tissue. Also, visualization time was restricted due to insertion of tissue damage upon prolonged imaging processes. Although leukocyte adhesion events occur already in early stages of fat pad metabolism the analysis using this imaging technique was not satisfactory to address consecutively arising questions. Thus multiple experimental settings like multi-photon microscopy in WAT were tested allowing for prolonged visualization of leukocyte dynamics but in our hands it was impossible to reach satisfactory fat tissue stabilization without induction of mechanical injury to the visualized adipose tissue.

We hence used the following set of experiments to address how platelet and WBC recruitment reacted in a more advanced stage of obesity.

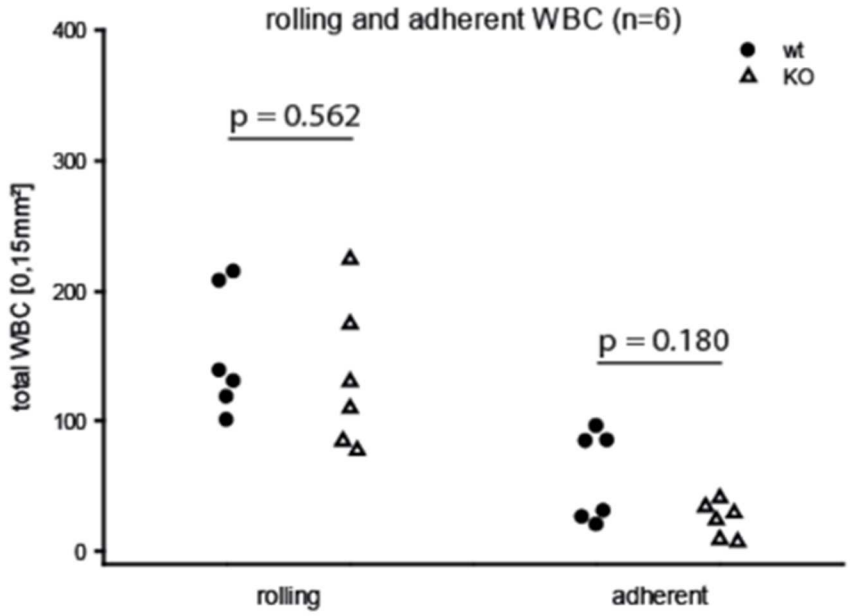

Figure 16: Number of rolling and adherent leukocytes

WBC adhesion in visceral WAT vasculature was evaluated in GPIIb deficient mice versus wild type control. The number of rolling WBC was not reduced in Knockout animals (p.value 0.56) compared to wild type mice. WBC adhesion is decreased in GPIIb deficient mice compared to controls (p.value 0.18).

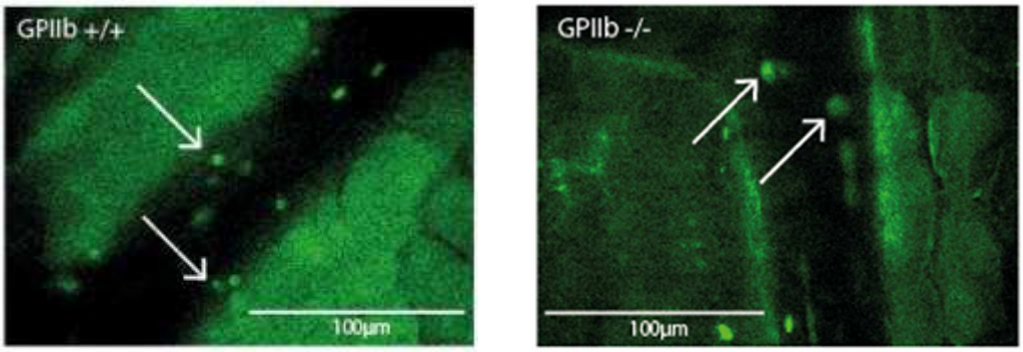

Figure 17: Alexa Fluor ® 488 labeled leukocytes in GPIIb wild type and Knockout mice

Representative freeze images of in vivo microscopy of visceral fat pad vasculature shows firm frequent leukocyte adhesion in GPIIb +/+ animals (white arrows) and GPIIb -/- mice. Adherent WBC were reduced in GPIIb deficient animals compared to controls. No differences were detected in rolling leukocytes between GPIIb deficient and wild type animals.

In a next step immunohistological quantification and FACS analysis were used to analyze whether chronic inhibition of platelet adhesion culminated in decreased leukocyte recruitment to WAT in more advanced stages of WAT expansion. Subcutaneous and visceral WAT were harvested of body weight matched 16-17-week old sex-matched α_{IIb}-deficient and wild type mice and prepared for immunohistological and FACS analysis. For the immunohistological analysis of leukocyte recruitment WAT was paraffin-embedded, sectioned and stained using a monoclonal rat anti-CD45 antibody. The CD45 positive cells were quantified and related to the analyzed area (Fig. 18).

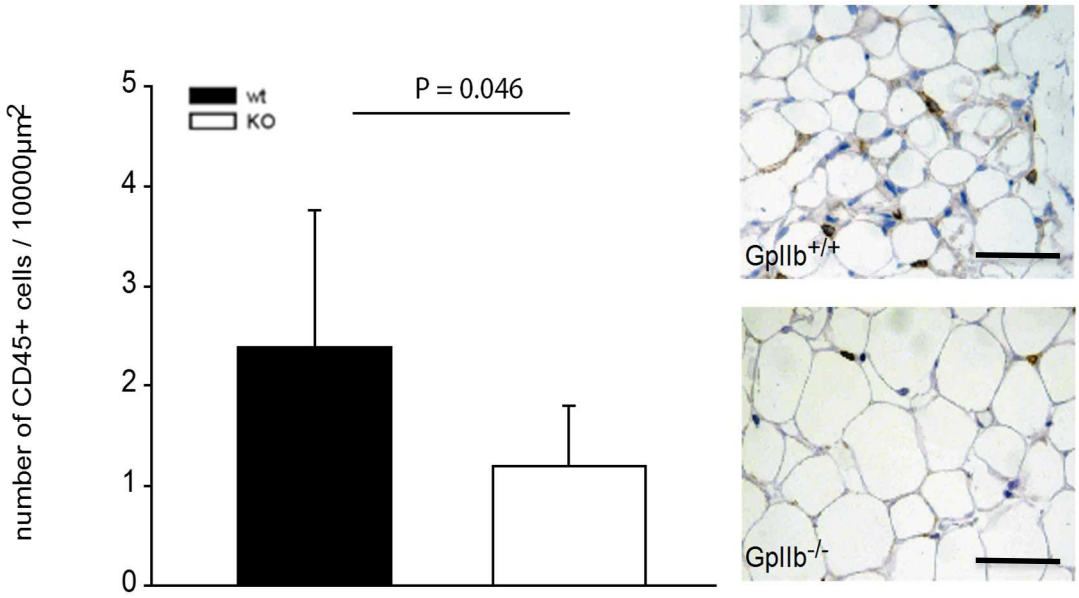

Figure 18: CD45+ cell count in WAT of wild type and GPIIb deficient mice

Left side: Number of CD45+ cells in WAT was evaluated in GPIIb deficient mice versus wild type control. The number of CD45+ cells was reduced in Knockout animals (p-value 0.046) compared to wild type mice.
Right side: Representative freeze images of immunohistochemical microscopy of WAT shows reduced number of CD45+ cells in GPIIb deficient animals compared to wild type mice (Scale = 20 µm).

Number of CD45+ cells was reduced in GPIIb deficient mice (p-value 0.046, n = 6, 2.34 ± 1.59 vs. 1.22 ± 0.62) compared to wild type mice.

Immunohistological analysis revealed that leukocyte recruitment to WAT was impaired in α_{IIb}-deficient mice compared to wild type controls.

2. Effect of High Fat Diet on platelet and leukocyte adhesion

The next question was whether platelet adhesion was relevant to assist leukocyte adhesion even upon provocation of high-grade inflammatory response in WAT. Talukdar et al. showed an aggravation of WAT inflammatory reaction and leukocyte recruitment upon high fat or high caloric diet.

The experiment was set up with 7-week-old α_{IIb}-deficient mice or controls that were subjected to high fat diet or control chow. After a control diet for 1 week the animals were held on a high fat diet or continuous control diet for 2 weeks respectively. Fluorescently labeled platelets and Alexa Fluor ® 488 labeled CD45 antibody were administered. At the age of 10 weeks *in vivo* microscopy of visceral fat depots was performed and platelet as well WBC dynamics were evaluated.

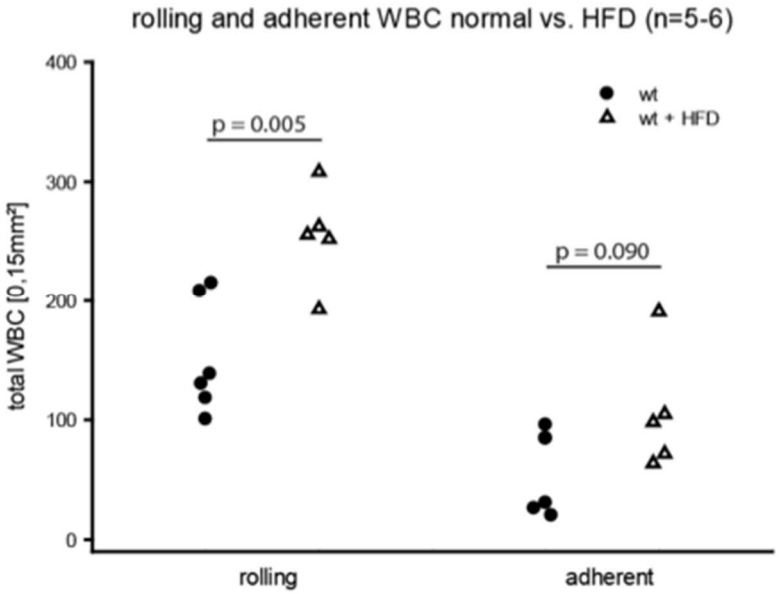

Figure 19: Number of rolling and adherent leukocytes normal chow vs. HFD

WBC adhesion in visceral WAT vasculature was evaluated in wild type mice receiving normal chow versus wild type animals that received HFD for 2 weeks respectively. The number of rolling as wells as the number of adherent WBC was increased in HFD group compared to animals that received a normal diet (p-value 0.005 and 0.09).

The number of rolling WBC increased in the HFD group (p-value 0.005, n = 5-6, 151.70 ± 19.62 vs. 254.08 ± 18.43). There was a tendency to an increase in the number of adherent WBC in mice on a HFD (p-value 0.09, n = 5-6, 56.98 ± 14.19 vs. 105.83 ± 22.58) compared to animals that received normal chow (Fig 19).

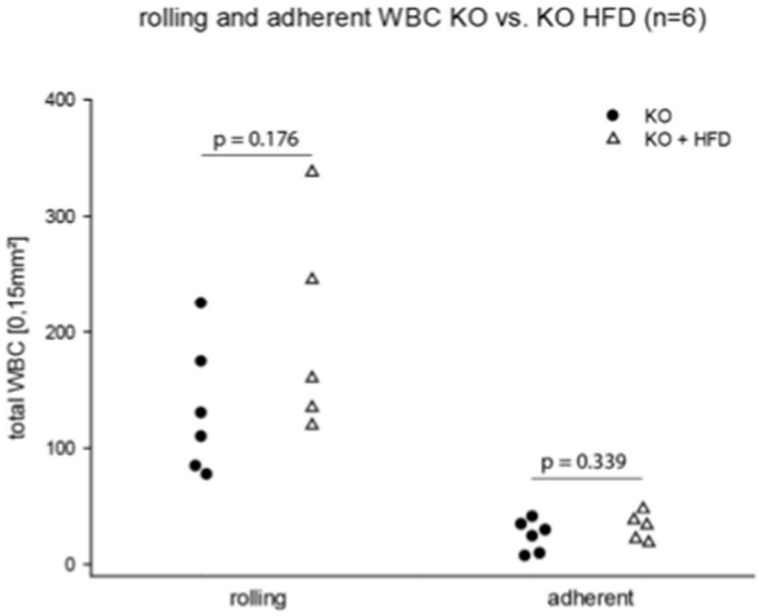

Figure 20: Number of rolling and adherent leukocytes normal chow vs. HFD

WBC adhesion in visceral WAT vasculature was evaluated in Knockout mice receiving normal chow versus Knockout animals that received HFD for 2 weeks respectively. The number of rolling leukocytes increased slightly in the Knockout animals that were fed a HFD compared to Knockout animals that received normal chow (p-value 0.18). No differences were detected in the number of adherent WBC in Knockout animals that received a HFD compared to Knockout animals that were fed normal chow (p-value 0.34).

The number of rolling WBC increased slightly in the HFD group (p-value 0.18, n = 6, 133.47 ± 23.18 vs. 199.48 ± 40.84) compared to the normal diet group. There was nearly no difference in the number of adherent WBC in knockout mice on a HFD (p-value 0.34, n = 6, 24.03 ± 5.52 vs. 31.85 ± 5.26) compared to Knockout animals that received normal chow (Fig. 20, Fig. 21).

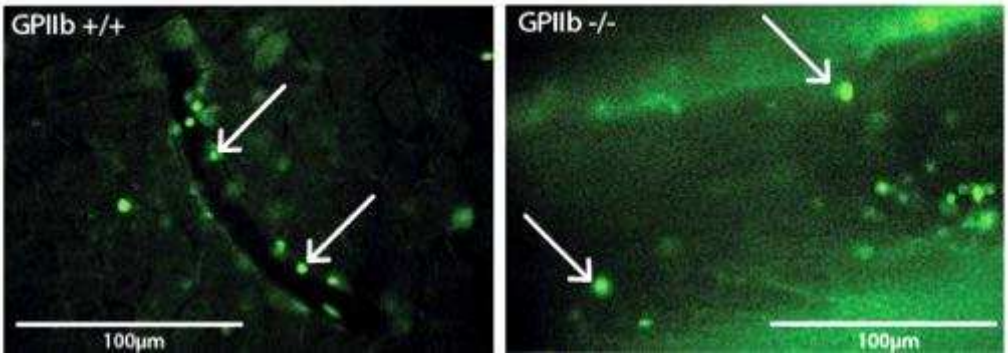

Figure 21: Alexa Fluor ® 488 labeled leukocytes in GPIIb wild type and Knockout mice after high fat diet for 2 weeks

Representative freeze images of *in vivo* microscopy of visceral fat pad vasculature shows firm frequent leukocyte adhesion in GPIIb $^{+/+}$ animals after HFD for 2 weeks (white arrows) and GPIIb $^{-/-}$ mice after HFD for 2 weeks. WBC adhered firmly to the endothelium in wild type animals after HFD as well as Knockout animals after HFD for 2 weeks respectively.

There was no effect of the HFD on the number of transient adherent platelets (p-value 0.88, n = 5-6, 57.62 ± 11.63 vs. 60.24 ± 11.33) and the number of adherent platelets respectively (p-value 0.29, n = 5-6, 28.19 ± 7.59 vs. 17.62 ± 4.90) (Fig. 22, Fig. 23).

There were similar results in the GPIIb deficient mice concerning the platelets. No effect of the HFD on the number of transient adherent platelets was detected (p-value 0.204, n = 6, 16.88 ± 7.01 vs. 5.06 ± 4.21) and there was no effect on the number of adherent platelets respectively (p-value 0.43, n = 6, 3.047 ± 1.97 vs. 0 ± 0) (Fig. 24).

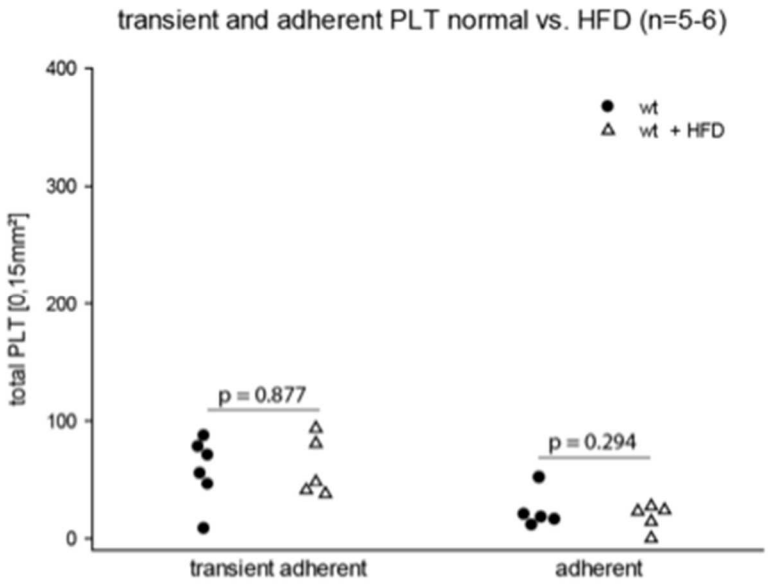

Figure 22: Number of transient adherent and firm adherent platelets normal chow vs. HFD

Platelet adhesion in visceral WAT vasculature was evaluated in wild type mice receiving normal chow versus wild type animals that received HFD for 2 weeks respectively. No differences were detected in the number of transient adherent platelets and firm adherent platelets between the wild type animals that received normal chow for 2 weeks and the animals that received HFD for 2 weeks (p-value 0.88 and 0.29).

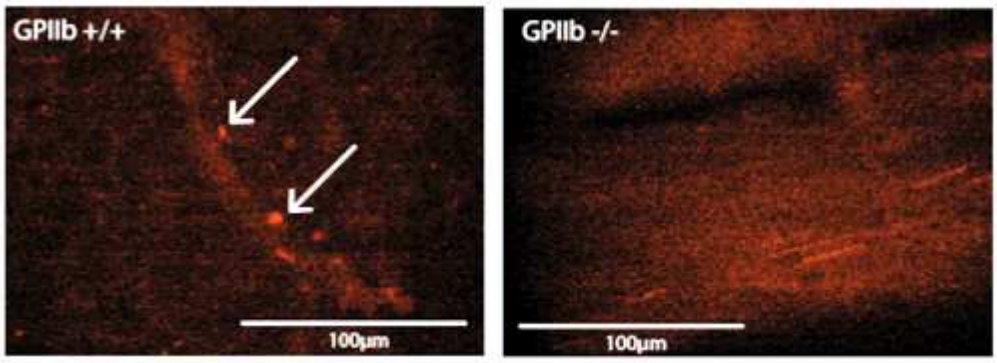

Figure 23: Rhodamine B labeled platelets in GPIIb wild type and Knockout mice after high fat diet for 2 weeks

Representative freeze images of *in vivo* microscopy of visceral fat pad vasculature shows firm frequent platelet adhesion in GPIIb $^{+/+}$ animals (white arrows) that received HFD for 2 weeks that is virtually abolished in GPIIb $^{-/-}$ mice after high fat diet for 2 weeks.

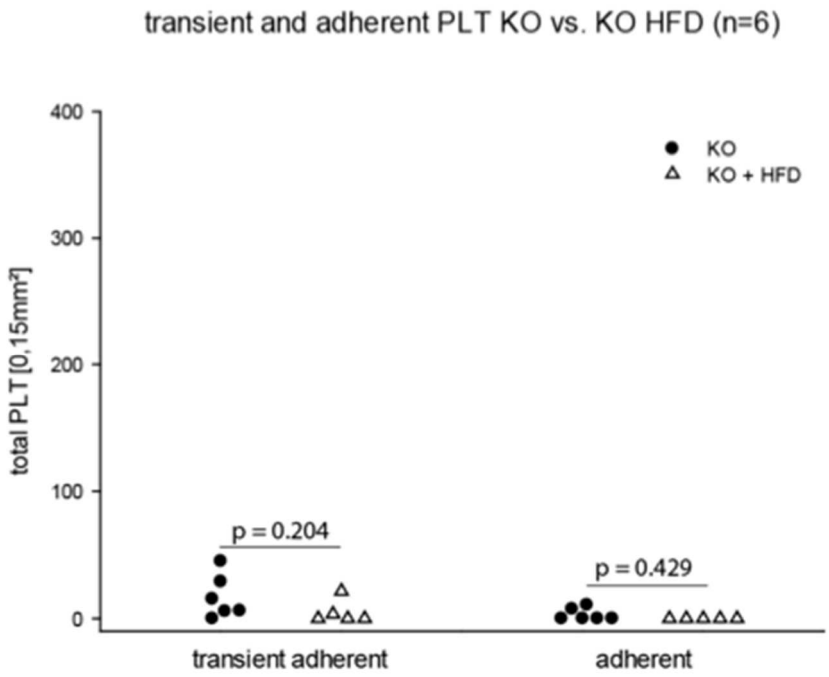

Figure 24: Number of transient adherent and firm adherent platelets normal chow vs. HFD

Platelet adhesion in visceral WAT vasculature was evaluated in Knockout mice receiving normal chow versus Knockout animals that received HFD for 2 weeks respectively. No differences were detected in the number of transient adherent platelets and firm adherent platelets between the wild type animals that received normal chow for 2 weeks and the animals that received HFD for 2 weeks (p-value 0.204 and 0.43).

Comparing the number of rolling WBCs between the wild type and the Knockout animals both fed a HFD for 2 weeks showed no differences (p-value 0.26, n = 5, 254.08 ± 18.43 vs. 199.48 ± 40.84). Importantly, WBC adhesion was significantly impaired in α_{IIb}-deficient mice compared to wild type siblings after consuming high fat diet for 2 weeks respectively (p-value 0.008, n = 5, 100.65 ± 25.42 vs. 31.85 ± 5.26) (Fig. 25).

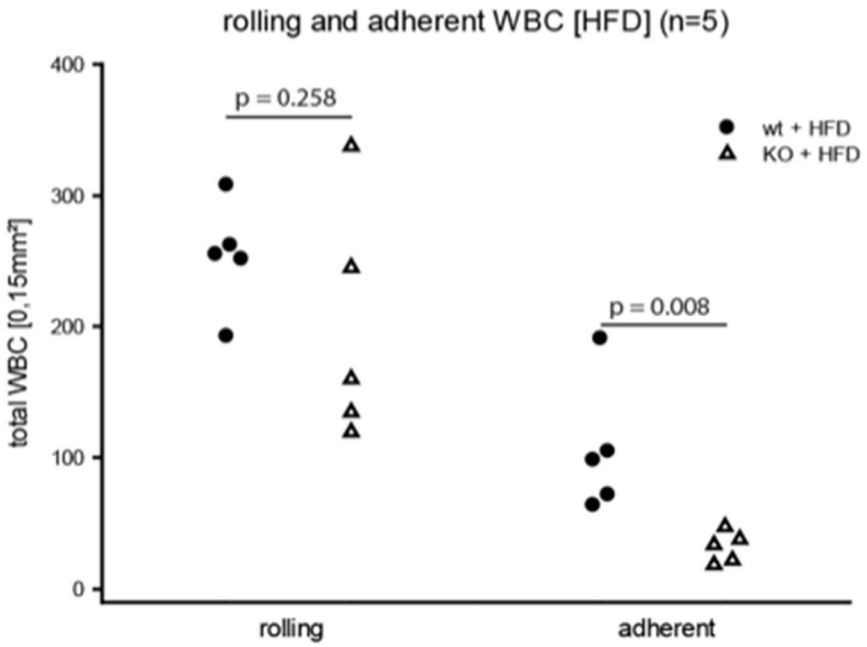

Figure 25: Number of rolling and adherent leukocytes wild type vs. KO fed a HFD

WBC adhesion in visceral WAT vasculature was evaluated in wild type mice receiving high fat diet for 2 weeks versus Knockout animals that received high fat diet for 2 weeks. No differences were detected in the number of rolling leukocytes in wild type animals that received HFD compared to Knockout animals that received HFD for 2 weeks respectively (p-value 0.26). The number of adherent WBC was significantly reduced in Knockout animals that were fed a HFD for 2 weeks compared to wild type animals fed a HFD for 2 weeks (p-value 0.008).

Comparing the number of transient adherent platelets between the HFD groups, similar results to the normal diet groups were confirmed. There was a decrease in the number of transient adherent platelets in GPIIb deficient mice fed a HFD for 2 weeks (p-value 0.002, n = 5, 60.244 ± 11.33 vs. 5.06 ± 4.21) compared to wild type mice that received a HFD for 2 weeks. There was also a decrease detected in the number of adherent platelets in the GPIIb deficient mice fed a HFD for 2 weeks (p-value 0.03, n = 5, 17.61 ± 4.90 vs. 0 ± 0) compared to wild type animals that received a HFD for 2 weeks (Fig. 26).

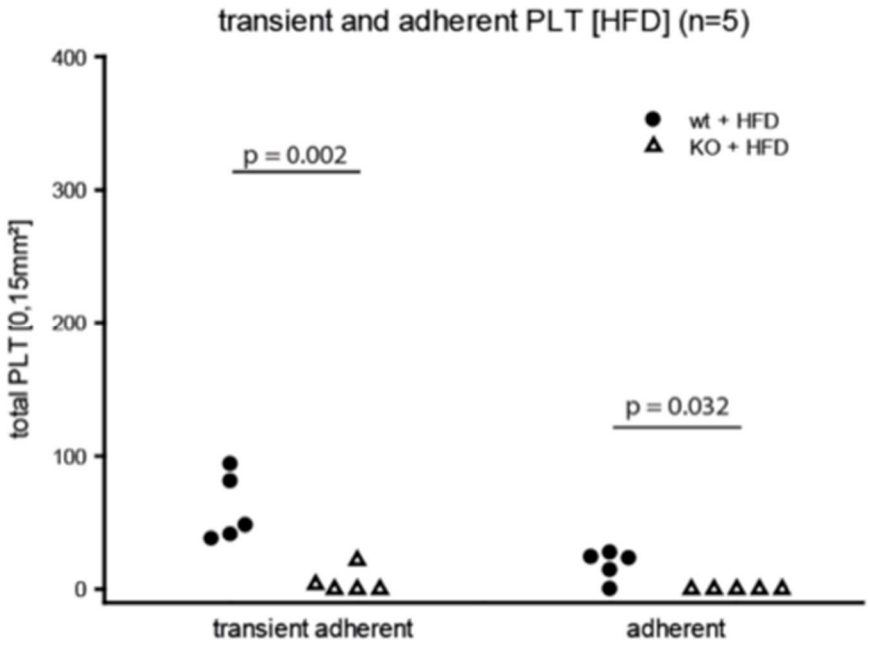

Figure 26: Number of transient adherent and adherent platelets wild type vs. KO fed a HFD

Platelet adhesion in visceral WAT vasculature was evaluated in wild type mice receiving high fat diet for 2 weeks versus Knockout animals that received high fat diet for 2 weeks. There was a significant decrease in the number of transient adherent and firm adherent platelets in Knockout animals that received a HFD for 2 weeks compared to wild type animals that received HFD for 2 weeks (p-value 0.002 and 0.03).

A significant increase in platelet and leukocyte recruitment was found in the setting of high fat diet versus control chow. Importantly, WBC adhesion was impaired in α_{IIb}-deficient mice compared to wild type siblings after consuming high fat diet.

Together, platelet-assisted leukocyte adhesion to microvasculature of adipose tissue seems to play a pivotal role in lean mice and high fat diet fed animals.

3. Fat pad and body weight measurement

As a consecutive step experiments were designed to analyze the effect of blocked platelet adhesion and consecutive impairment in leukocyte recruitment to adipose tissue phenotype. Therefore, body weight and carcass weight of sex-matched 16-17 week old α_{IIb}-deficient mice and their wild type controls as well as weight of the subcutaneous, visceral, retroperitoneal and brown fat depots were measured. Serum leptin concentrations and adipocyte size were measured.

The GPIIb deficient mice showed a crucial increase in the subcutaneous, visceral as well as the retroperitoneal fat pad compared to the wild type animals. The brown fat pad showed no increase as typically not relevantly expanding in the setting of obesity. No difference in carcass weight was detected, which excluded growth of the musculo-skeletal system as the source of weight gain. This initial work was also performed by PhD-student T. Konrad and served as the reference point for my following experiments.

The experiments were done using 10-16 week old, sex-matched GPIIb deficient mice and their wild type counterparts. Again, body weight and the white fat pads as well as the carcass weight were evaluated. The macroscopic view revealed significant differences in the white fat pad development already (Data determined by Echtler et al.). The fat pad of the α_{IIb}-deficient mice was considerably larger than of the wild type counterparts (Fig. 27).

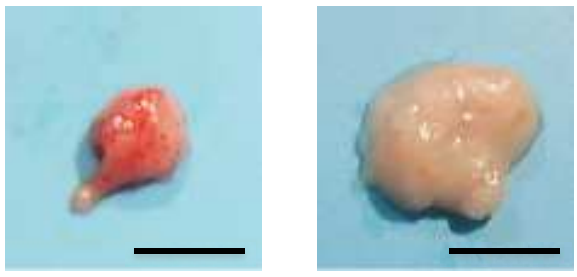

Figure 27: Comparison Fat pad appearance between GPIIb wild type and Knockout

The fat pad collected from a GPIIb wild type mouse (left side) was substantial smaller than the one taken from a GPIIb deficient mouse (right side) (Scale = 2 mm)

3.1. GPIIb deficient and wild type mice

T. Konrad analyzed whether there are differences in the body weight between GPIIb deficient mice and their wild type counterparts and was able to show a weight increase in GPIIb deficient animals compared to wild type controls.

He also measured serum leptin levels between GPIIb deficient and wild type animals, showing higher serum leptin levels in α_{IIb}-deficient mice compared to wild type animals.

T. Konrad also analyzed the adipocyte size and showed an increase of adipocyte size in GPIIb deficient mice compare to wild type mice. Further metabolic screenings revealed no differences in food consumption, energy expenditure or physical activity in α_{IIb}-deficient mice versus controls. This excluded that the observed differences in the WAT depend on alterations of energy intake/uptake, kinesic behavior or metabolism.

A set of experiments were performed to assess in more detail whether the observed effects was really a platelet-mediated process. As described α_{IIb}-Expression is restricted to the hematopoietic lineage (*73*). Early bone-marrow resident hematopoietic progenitors and megakaryocytes, as well as platelets and some mast cells are known to express α_{IIb}. Using whole mount embryo staining techniques Emambokus et al. could not detect any further tissue α_{IIb}-expression.

3.2. GPIIb deficient and wild type bone marrow chimera mice

Bone marrow chimera of α_{IIb}-deficient and wild type mice were created to restrict the GPIIb ablation to the hematopoietic system for a further verification that platelets are crucial for the regulation of WAT inflammation. Therefore 8-week-old female C57Bl/6J mice were sublethally irradiated and received either α_{IIb}-deficient or wild type bone marrow cells of female donor mice. 16 weeks after the transplantation the body weight and fat pad weight was measured.

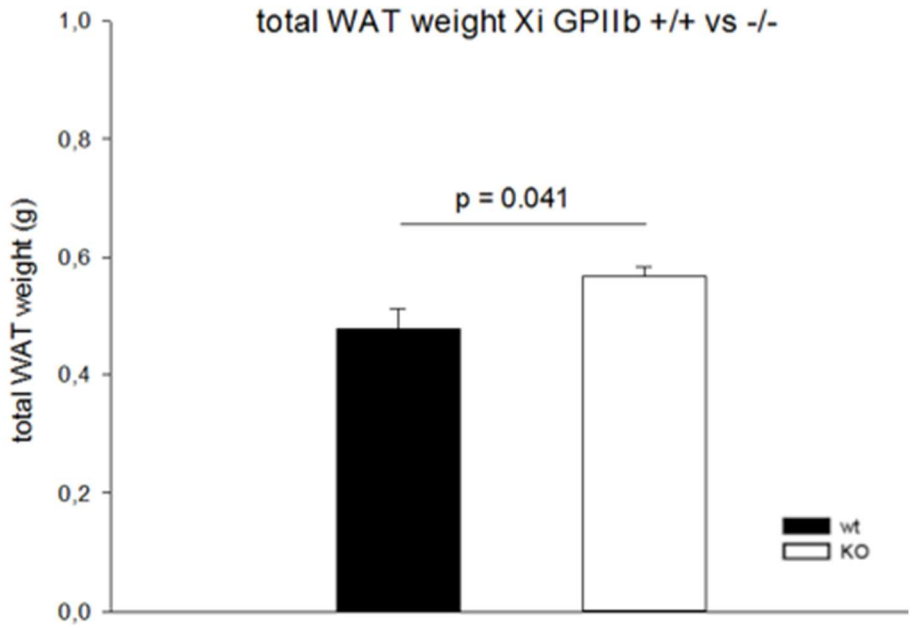

Figure 28: Total WAT quantification between GPIIb deficient and wild type chimera mice

Total WAT weight was evaluated in C57Bl/6J mice after receiving wild type or α_{IIb}-deficient bone marrow cells. There was a significant increase in the total WAT weight evaluated in C57Bl/6J mice after that α_{IIb}-deficient bone marrow cells compared to evaluated in C57Bl/6J mice that received wild type bone marrow cells (p-value 0.04).

A measurement of the total WAT amount revealed an increase in the GPIIb deficient chimera mouse group (p-value 0.04, n = 6, 0.477 ± 0.034 vs. 0.567 ± 0.0153) compared to the wild type chimera group (Fig. 28).

A closer look at the single fat pads of bone marrow chimera mice revealed an increase in the visceral fat (p-value 0.12, n = 6, 0.26 ± 0.03 vs. 0.31 ± 0.01) as well as in the abdominal fat pad (p-value 0.005, n = 6, 0.08 ± 0.01 vs. 0.12 ± 0.01).

The subcutaneous fat pad did not increase in GPIIb deficient mice (p-value 0.66, n = 6, 0.14 ± 0.01 vs. 0.135 ± 0.01) as being directly exposed to the irradiation, which badly influences the fat pad formation (Fig. 29).

The brown fat in the GPIIb deficient mice showed no weight gain (p-value 0.66, n = 6, 0.10 ± 0.01 vs. 0.11 ± 0.01), as brown adipose tissue is mainly responsible for energy production and not energy storage.

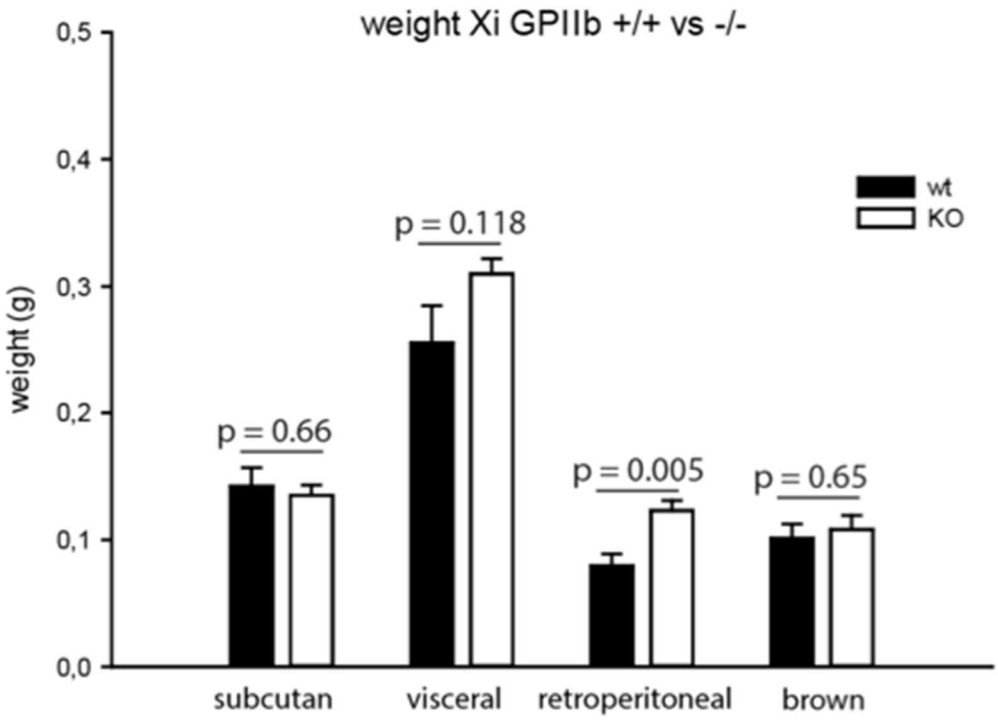

Figure 29: WAT depots of GPIIb deficient and wild type chimera mice in detail

WAT and BAT depot weight was evaluated in C57Bl/6J mice after receiving wild type or α_{IIb}-deficient bone marrow cells. There was an increase in the visceral and abdominal WAT weight in C57Bl/6J mice after receiving α_{IIb}-deficient bone marrow cells compared C57Bl/6J mice that received wild type bone marrow cells (p-value 0.12 and 0.005). No differences were detected in the subcutaneous WAT and the brown fat pad weight in C57Bl/6J mice after receiving α_{IIb}-deficient bone marrow cells compared to C57Bl/6J mice that received wild type bone marrow cells (p-value 0.66 and 0.65)

The generation and evaluation of GPIIb bone marrow chimera mice substantiated the notion, that platelets, which abundantly surface-express $\alpha_{IIb}\beta_3$-integrin integrin, mediate the observed regulatory processes of WAT expansion.

4. Analysis of fat pad vascularization

Our group also tested whether an alteration of WAT expansion could also be observed in other transgenic mice with impaired platelet function. For this reason, the fat depots of NFE2-deficient mice on a mixed C57BL/6 x SV129 background were analyzed. The NFE2 mice show a disturbed megakaryopoiesis and homozygous animals reveal virtually no circulating blood platelets with a smaller number of remaining functional platelets (*142*). As a result, the animals show frequent bleeding events and anemia.

Since novel vessel formation or growth of pre-existing vessels might play a role in adipose tissue expansion, we analyzed whether alterations in fat pad circulation occurred in α_{IIb}-deficient mice versus control.

For this reason, vessels were stained using a CD144-antibody; the subcutaneous fat depots were collected and subjected to multiphoton microscopy. The vessel structure was visualized 3-dimensionally and the vessel density was determined (Fig. 30).

Evaluation of the vessel structure in the subcutaneous fat pads of GPIIb deficient mice and their wild type counterparts revealed no difference between the two groups (p-value = 0.892, t-test, n = 4, wt mean = 1.93 ± 0.21, KO mean = 1.87 ± 0.67) (Fig. 31), implicating that differences of cell interactions within the various phenotypes are mainly due to the impaired GPIIb Integrin functions and not due to vascular variations and the related changes in cell counts.

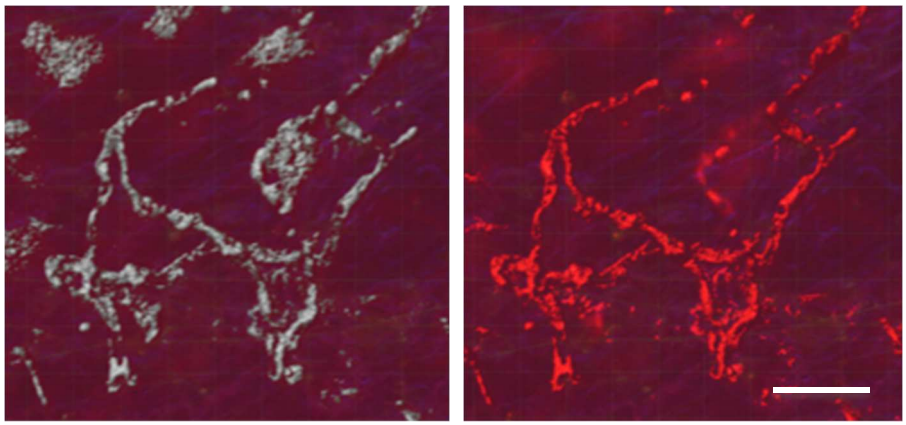

Figure 30: Three-dimensional visualization of CD144 stained subcutaneous fat pad vasculature

Representative freeze images of two photon microscopy of subcutaneous fat pad vasculature. No differences between GPIIb deficient mice and their wild type counterparts were detected (scale = 25 µm).

From the first part of the thesis it can be concluded that chronic platelet adhesion occurs in adipose tissue vasculature even at early stages of adipogenesis. This platelet adhesion enables leukocyte recruitment to WAT depots in the process of fat depot expansion.

Local adhesion of platelets is impaired in α_{IIb}-deficient mice; this was paralleled by a decrease in leukocyte adhesion and an increase in WAT enlargement. Latter was reflected by the expansion of WAT depots (subcutaneous, visceral and retroperitoneal) as well as body weight. The carcass weight remained unaltered in knockout animals showing that the increase in weight was not due growth of the musculo-skeletal system.

As a following step of the project the underlying factors of the observed effects were further analyzed. Chemokine mRNA-expression analysis in subcutaneous fat depots of α_{IIb}-deficient and control animals were evaluated. No difference in the expression of Chemokine ligand 1 (CXCL1), which is one of the first factors to be released in the neutrophil signal transduction cascade on the site of inflammation, was found (p-value 0.13, n = 4, 0.97 vs. 0.73) between wild type and Knockout animals.

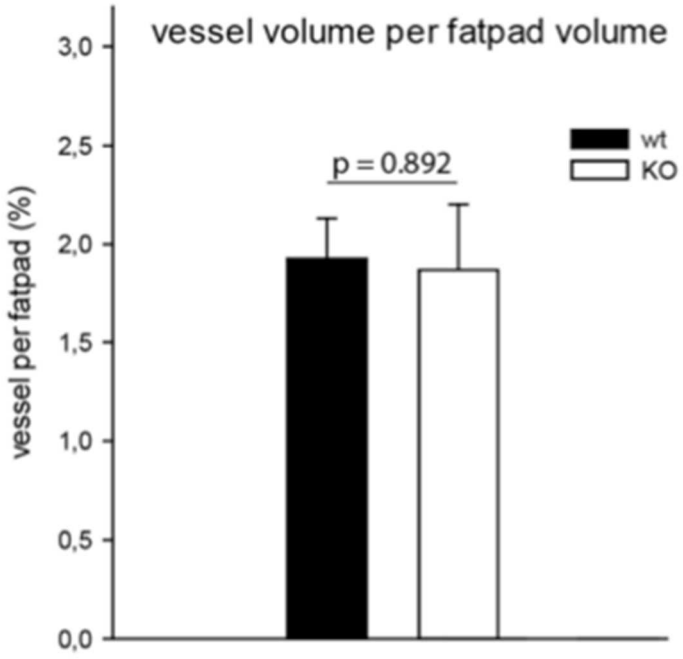

Figure 31: Quantification of vessel per fat pad volume in subcutaneous fat pad

Vessel volume per fat pad volume in subcutaneous WAT was evaluated in wild type mice versus GPIIb Knockout animals using two-photon microscopy. No differences were detected in the percentage of vessel per fat pad between wild type and Knockout animals (p-value 0.89).

There were also no differences in the expression of Chemokine ligand 5 (CXCL5) (p-value 0.58, n = 4, 0.46 vs. 1.62) and Chemokine ligand 2 (CXCL2) (p-value 0.87, n = 4, 1.04 vs. 1.00), that also play a crucial role in the inflammatory leukocyte signal transduction cascade, between wild type and GPIIb deficient mice. The levels of the inflammatory marker Interleukin 6 (IL-6) was also comparable between the two groups (p-value 0.26, n = 4, 1.52 vs. 0.53).

Despite the detected increase in WAT expansion in α_{IIb}-deficient mice, Tumor necrosis factor α (TNF-α) mRNA-expression was significantly reduced in subcutaneous WAT of α_{IIb}-deficient animals compared to their wild type counterparts (p-value 0.04, n = 4, 0.64 vs. 0.42). There were reports of TNF- α deficient animals that showed enlarged WAT depots after receiving high fat diet (*210*).

Therefore, it was further tested whether platelets and leukocyte recruitment could affect TNFα expression of adipocytes and adipocyte biology.

5. *In vitro* culture of adipocytes

The different behavior of platelets and leukocytes after adherence to the dysfunctional endothelium of the adipose tissue vasculature consists of their influence on adipocyte biology. While leukocytes could directly interact with adipocytes after transmigration into the adipose tissue and thus change the TNF-α expression levels of these cells, platelets could influence adipocytes only via paracrine effects. Platelets probably might release pro-inflammatory substances while interacting with the dysfunctional endothelium of adipose tissue.

When presumed that platelets after becoming adherent to the dysfunctional endothelium of the adipose tissue vasculature would release multiple, partly pro-inflammatory substances could in this way influence adipocytes only in a paracrine manner. Leukocytes, in contrast could - apart from paracrine effects mediated by adherent platelets - additionally directly interact with adipocytes after transmigration into the adipose tissue and by this way change TNF-α expression in adipocytes.

For this reason murine 3T3-L1 preadipocytes were purchased from ZenBio, Inc. (USA). These cells derived from mouse 3T3 cells and are well established for the research on adipose tissue and show a fibroblast like morphology with the ability to differentiate into an adipose like phenotype over a period of 14 days (Fig. 32).

Preadipocytes were delivered and seeded at passage number 8 and splitted until passage number 10, the cells grew in density and developed a fibroblast-like structure (Fig. 32 A). After a strict differentiation phase of three days the preadipocytes started to enrich with lipids (Fig. 32 B). This process took about 14 additional days with further enrichment of triglyceride lipids, forming larger lipid droplets (Fig. 32 C) and resulted in mature adipocytes with one large lipid vacuole (Fig. 32 D).

Experiments were done during the differentiation phase as well as with mature adipocytes after the developmental process took place.

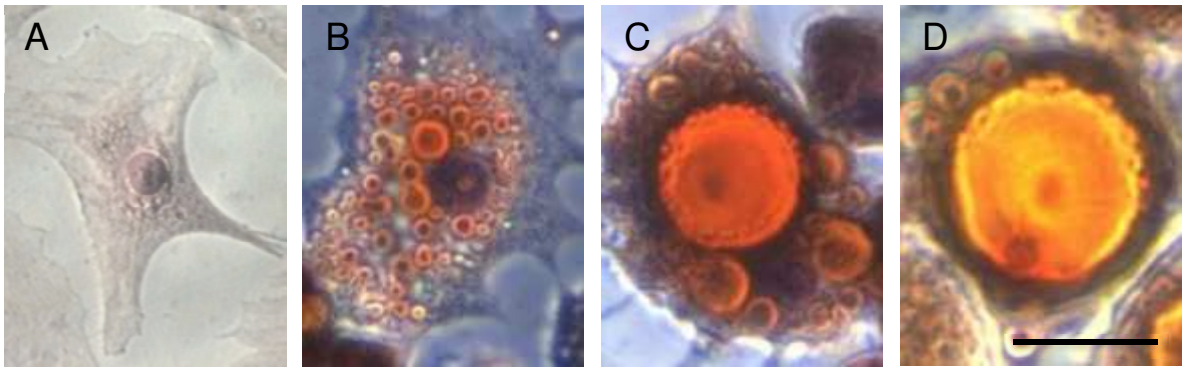

Figure 32: Preadipocyte to adipocyte development

The cells were stained using Sudan III for a better visualization. The development/maturation process took about four weeks from the preadipocyte to the mature adipocyte (Scale = 20µm).

5.1. TNF-α ELISA after adipocyte treatment

Murine mature adipocytes were co-incubated with different substances after the developmental processes were finished to evaluate whether these pro-inflammatory substances released by platelets and leukocytes could influence the TNF-α expression in adipocytes. The adipocytes were co-incubated with ADP-activated platelet supernatant, activated platelets, isolated murine polymorphonuclear leukocytes (PMA activated or unstimulated) or controls for 3 or 6 hours, washed and adipocyte TNF-α protein expression was assessed 18 hours thereafter.

While no TNF-α expression was detectable in controls (ADP, PMA, Tyrodes), a robust TNF-α expression was found in adipocytes treated with activated PMNs (mean = 133.24 ± 8.21, n = 3) and unstimulated PMNs (mean = 139.97 ± 9.62, n = 3). Treatment with platelet supernatant had no effect on TNF-α production in murine adipocytes (Fig. 33). Also co-incubation with activated platelets had no effect on the TNF-α expression. However, the combination of activated platelets with polymorphonuclear leukocytes, as well as the combination of inactivated platelets with PMNs caused TNF-α expression.

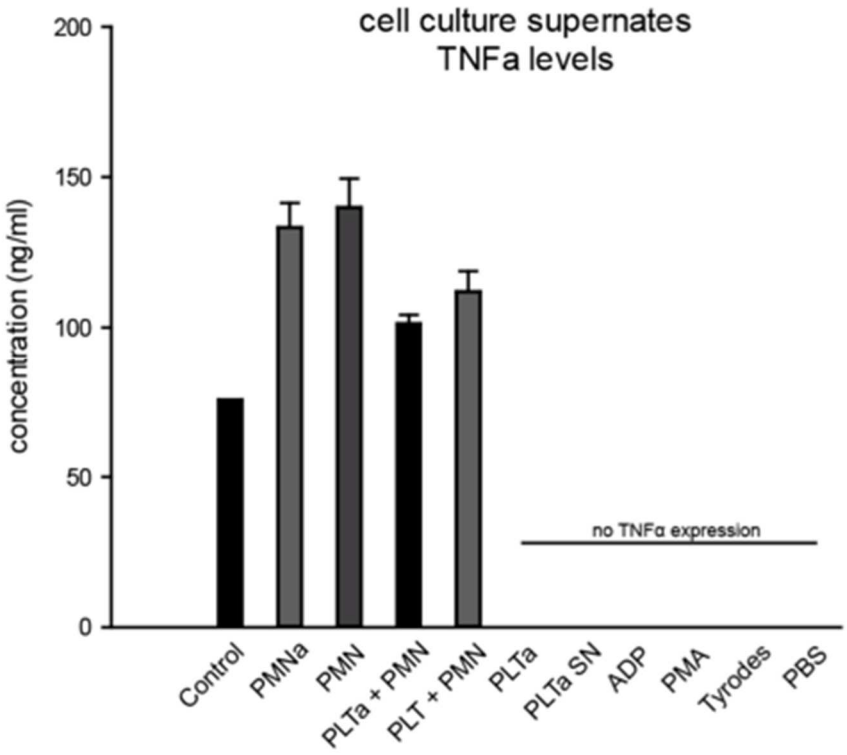

Figure 33: Cell culture supernates TNF-α levels after stimulation

Treatment of mature adipocytes for 3h after development phase revealed TNF-α expression in the groups treated with PMNa, PMN, PLTa+PMN and PLT+PMN.

5.2. Adipocyte proliferation evaluation

After getting a first impression on the TNF-α expression levels of mature adipocytes, cells were treated with TNF-α and other substances already during their differentiation phase as well as during the maturation phase to evaluate their proliferation behavior.

Cells were treated a total of three times each 24 hours. The first treatment was during day two and day three of the differentiation phase, the second treatment at day 8 of the maturation phase and the third treatment on day 14 of maturation phase.

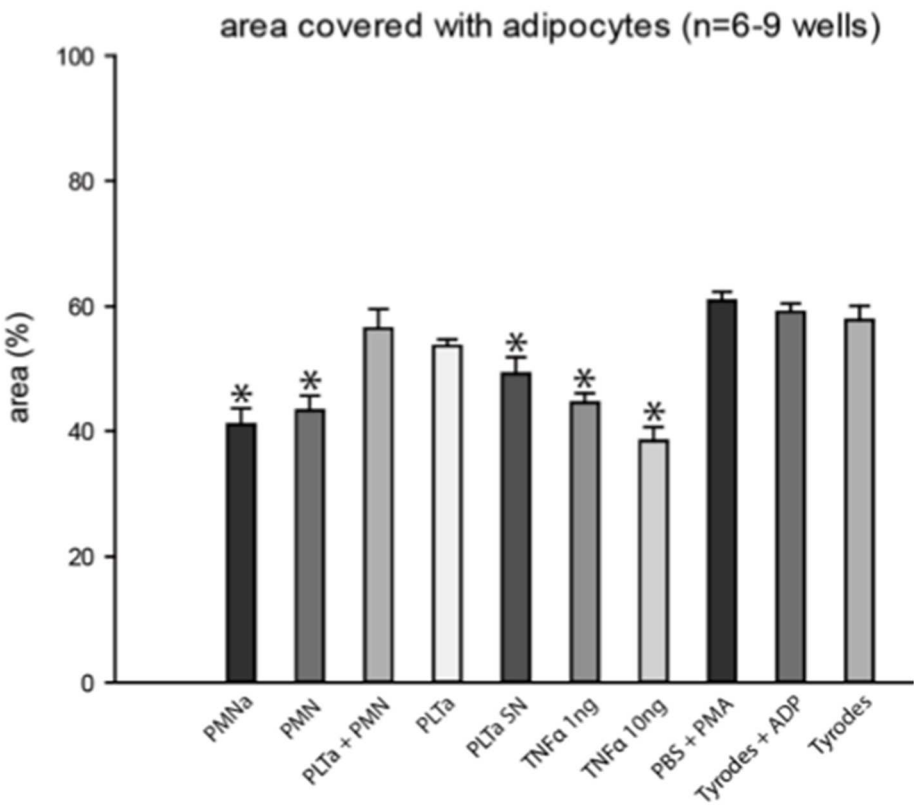

Figure 34: Area covered with adipocytes

A significant reduction of area covered with adipocytes was detected in the groups treated with PMNa, PMN, PLTa SN and TNF-α compared to cells treated with tyrodes buffer. No differences were detected in the groups treated with PLTa+PMN, PLTa, PBS+PMS and Tyrpdes+ADP compared to cells treated with tyrodes buffer (* = significance vs. Tyrodes group).

The proliferation was measured as the percentage of covered area per well using a phase contrast microscope. For a better differentiation the cells were first stained using Sudan III, however using ImageJ for evaluation made staining unnecessary as the experiments were repeated.

There was a decrease in the adipocyte covered area in the PMNa group compared to the control group treated with Tyrodes buffer (p-value 0.001, n = 2 biological replicates, 6 technical replicates, 41.03 ± 2.58 vs. 57.83 ± 2.25), in the group treated with PMN (p-value 0.002, n = 2 biological replicates, 6 technical replicates, 43.29 ± 2.52), in the group treated with PLTa SN (p-value 0.03, n = 2 biological replicates, 6 technical replicates, 49.27 ± 2.63), as well as in the group treated with TNF-α 1ng (p-value 0.001, n = 2 biological replicates, 6 technical replicates, 44.49 ± 1.67) and the

group treated with TNF-α 10ng (p-value 0.001, n = 2 biological replicates, 6 technical replicates, 38.43 ± 2.21). There was a decreasing tendency in the group treated with PLTa (p-value 0.18, n = 2 biological replicates, 6 technical replicates, 53.19 ± 1.05). The groups treated with PLTa + PMN (p-value 0.73, n = 2 biological replicates, 6 technical replicates, 56.46 ± 3.1), PBS + PMA (p-value 0.28, n = 2 biological replicates, 6 technical replicates, 60.88 ± 1.44) and Tyrodes + ADP (p-value 0.65, n = 2 biological replicates, 6 technical replicates, 59.09 ± 1.38) did not differ from the Tyrodes treated control group (Fig. 34).

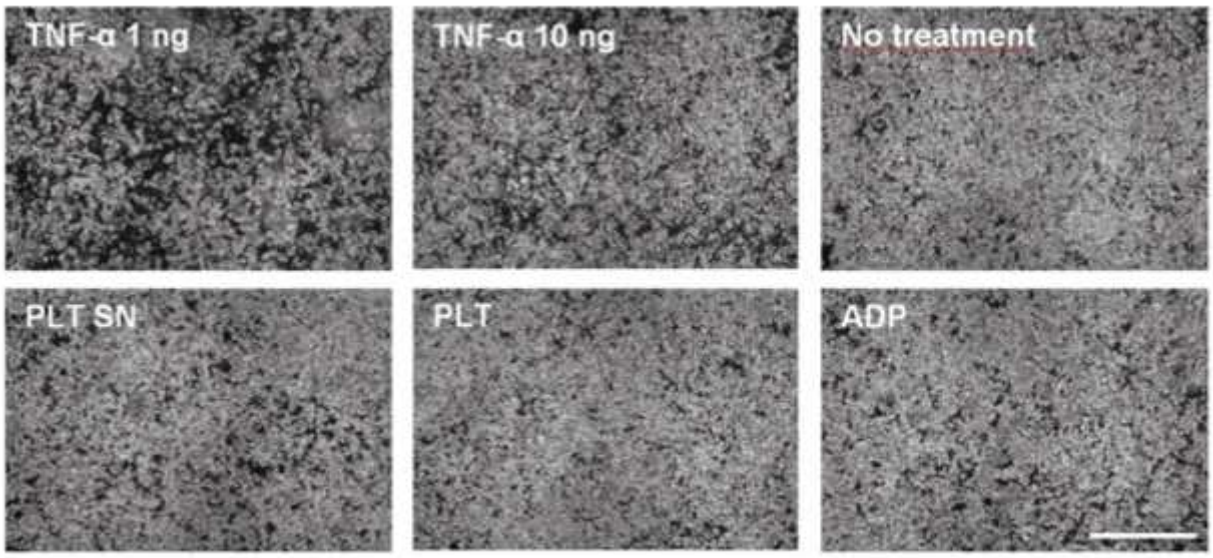

Figure 35: Microscopic images of adipocyte covered wells

Representative images of microscopy of adipocytes *in vitro* after stimulation with different substances (scale = 300 µm).

Different treatments of adipocytes resulted in a proliferation change. This was detectable already by eye as seen in Figure 35. The groups treated with TNF-α showed obvious changes in the area covered with adipocytes. These significant changes occurred also in the groups with leukocytes (PMNa and PMN) as well as the platelet supernatant group.

6. TNF-α blockade via Infliximab

For further evidence, that reduced TNF-α production in a lean mouse model culminated in an expansion of white adipose tissue, TNF-α was blocked *in vivo* and the fat deposition weight was evaluated as described before.

Therefore, Infliximab (Remicade®), a chimeric monoclonal antibody directed against TNF-α ligand and membrane-bound TNF-α or a vehicle (NaCl, 0.9%) was given intraperitoneally once a week over 6 weeks to adult C57BL/6 mice. The mice were weighed directly before the treatment. After the treatment period mice as well as their fat pads were weighed again. TNF-α serum levels were assessed using ELISA to evaluate a successful TNF-α blockade (Fig. 36).

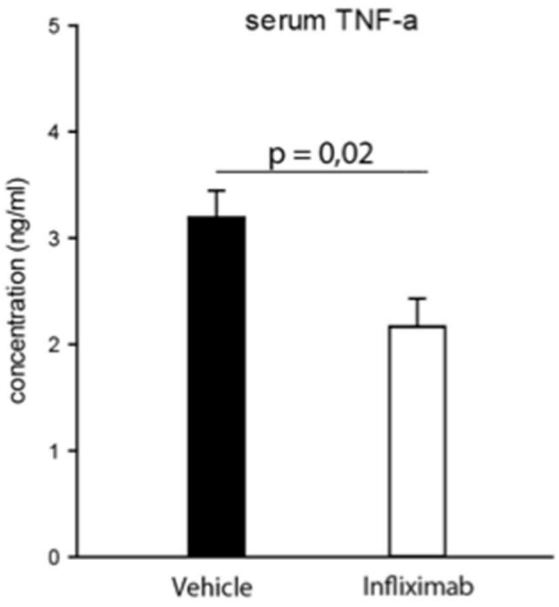

Figure 36: Measurement of serum TNF-α levels using ELISA

Serum TNF-α levels were evaluated in wild type mice receiving a vehicle for 6 weeks and mice receiving Infliximab for 6 weeks. Serum TNF-α levels were significantly decreased in mice treated with Infliximab compared to vehicle treated mice (p-value 0.02).

After 6 weeks of treatment clearly reduced TNF-α serum levels in animals treated with Infliximab (starting age 60-70 days) were found compared to vehicle control (p-value = 0.02, n = 5-6, 3.19 ± 0.26 vs. 2.17 ± 0.26).

Infliximab treatment provoked an increased body weight gain compared to vehicle controls (p-value = 0,01, n = 6, 1.63 ± 0.28 vs. 2.88 ± 0.32) (Fig. 37).

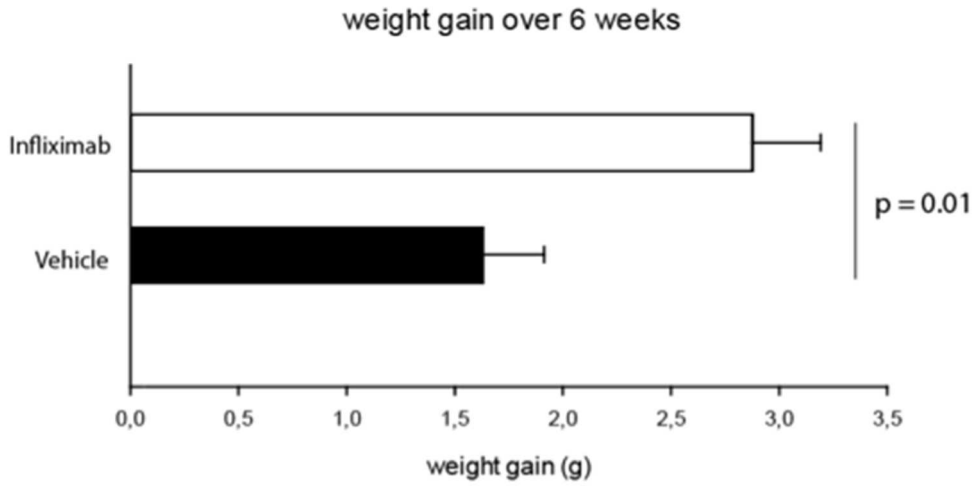

Figure 37: Total weight gain after Measurement of serum TNF-α levels using ELISA

Weight gain was evaluated in wild type mice receiving a vehicle for 6 weeks and mice receiving Infliximab for 6 weeks. Weight gain was significantly increased in mice treated with Infliximab compared to vehicle treated mice (p-value 0.01).

Already after 6 weeks of treatment, the animals that received Infliximab showed a clear and prominent increase in weight gain. This highlights the crucial role of TNF-α in the development of WAT and the inflammatory characteristics during adipogenesis.

To get an even more detailed impression of the weight gain in mice treated with Infliximab, the mice were anesthetized after the 6-week treatment and the fat pads were measured as described before.

All analyzed WAT depositions showed clear enlargement in Infliximab® treated animals, compared to vehicle treated groups, although results did not reach significance after 6 weeks of treatment (Fig. 38) (WAT total weight p-value 0.37, n = 9, Infliximab mean = 0.74 ± 0.09, vehicle mean = 0.63 ± 0.06, subcutan fat pad p-value 0.33, n = 9, Infliximab mean = 0.24 ± 0.02, vehicle mean = 0.22 ± 0.02, visceral fat pad p-value 0.48, n = 9, Infliximab mean = 0.38 ± 0.07, vehicle mean = 0.33 ± 0.04, abdominal fat pad p-value = 0.17, n = 9, Infliximab mean = 0.10 ± 0.01, vehicle mean = 0.08 ± 0.01).

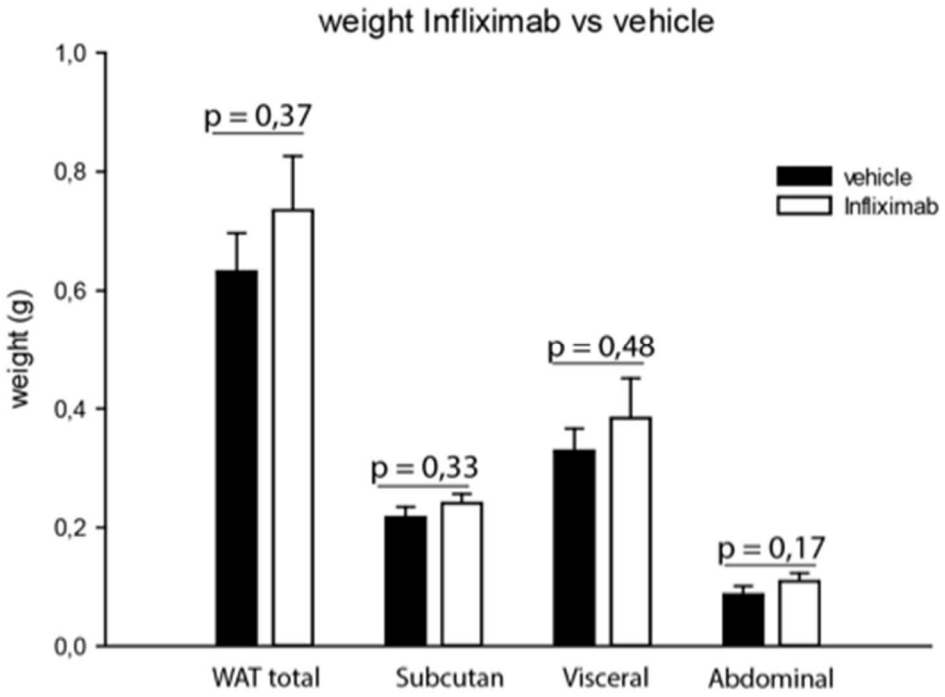

Figure 38: White fat pad measurement after Infliximab and vehicle treatment

WAT total weight and WAT weight was evaluated in wild type mice receiving a vehicle for 6 weeks and mice receiving Infliximab for 6 weeks. No differences were detected in the visceral fat pad between animals treated with Infliximab and animals treated with the vehicle (p-value 0.48). There was a decrease in subcutaneous and abdominal fat pad weight in animals treated with Infliximab compared to vehicle treated animals (p-value 0.33 and 0.17).

Interestingly, there was a clear increase in subcutaneous as well as abdominal fat pads of animals treated with Infliximab. Although the treatment lasted only 6 weeks it leads to this results, highlighting the important role of TNF-α in the development of WAT again.

To summarize, chronic platelet and leukocyte adhesion to vasculature of white adipose tissue was detected already at early stages of WAT expansion. Using immunohistochemical analysis and *in vivo* microscopy impairment of platelet adhesion by a lack of α_{IIb}-β3 integrin was detected, that consecutively culminates in diminished leukocyte recruitment to WAT depots in lean and HFD-fed mice, resulting in an increased WAT expansion.

In vitro analysis of adipocytes revealed that leukocytes not only delivered TNF-α to WAT but also were able to provoke upregulation of TNF-α expression in adipocytes. Co-incubation of adipocytes with leukocytes or TNF-α inhibited adipocyte growth. In line, subcutaneous fat depots of α_{IIb}-deficient animals revealed reduction of recruited leukocyte numbers in the WAT, reduced TNF-α expression and expanded white adipose depots. Consequently, blocking TNF-α *in vivo* with Infliximab provoked weight gain in a lean mouse model.

In this way, a novel axis in adipose tissue homeostasis was revealed with platelet-assisted leukocyte recruitment that provoked upregulation of TNF-α expression and in this way -at least in part- control fat pad expansion.

VI. DISCUSSION

1. Experimental procedure

1.1. Choice of mouse strain

The mouse was chosen as a research animal because of its easy to manipulate genetics on one side, as well as its short reproduction time on the other side including a large number of descendants. That is why there are many genetical knockout strains available for addressing various immunological questions.

Working in an animal model is necessary to address the role of platelets and neutrophils in the pathogenesis of obesity not only in an *in vitro* model, but also with *in vivo* experiments. The animal model allows for analysis of platelet-leukocyte interactions as well as observation of animal behavior and physiology under certain conditions like a different feeding regime but it makes it also possible to compare the pathophysiology of different genotypes.

The GPIIb Knockout strain was chosen, because it facilitates the analysis of potentially platelet driven and GPIIb mediated effects and the platelet dependent interactions with leukocytes in the pathogenesis of obesity. Due to the crucial role of the GPIIb ($\alpha_{IIb}\beta_3$) integrin in the platelet adhesion and fibrinogen-mediated activation process, a knockout of this integrin enables a highly appropriate animal model for studying platelet dependent effects (*38, 219*). Besides fibrinogen-mediated activation and aggregation processes (*102, 108*) the GPIIb/IIIa complex is highly important for platelet adhesion to the intact endothelium (*203, 244*) as well as signal transduction after binding (*168, 197*). The GPIIb receptor also mediates the adhesion of platelets on the dysfunctional endothelium (*240, 244*) and triggers secretion of various pro-inflammatory cytokines via outside-in-signaling (*90, 220-222, 224*).

2. Discussion of results

2.1. Platelet and leukocyte adhesion in visceral fat

In vivo microscopy of visceral adipose tissue revealed, that firm platelet adhesion to the vasculature of WAT already occurred during the initiation of obesity in the subcutaneous fat pad of GPIIb wild type mice. The data suggest, that the observed chronic platelet adhesion consecutively facilitates recruitment and infiltration of leukocytes into adipose tissue. This again culminates in a restriction of adipose tissue expansion.

With attenuation of platelet adhesion in GPIIb deficient mice as well as lack of platelets in NFE2 Knockout mice enhanced WAT expansion compared to the wild type counterparts can be observed.

An activation of endothelial cells is also described as endothelial dysfunction, representing an early pathophysiological feature in many acute and chronic inflammatory processes. Platelets also act as a major player in the initiation of the atherogenic process by adhering to the vascular endothelium before the development of manifest atherosclerotic lesions (*158*). The integrin GPIIb/IIIa on platelets mediates platelet aggregation and triggers platelet adhesion to the exposed extracellular matrices as well as dysfunctional endothelial cells contributing for instance to the pathogenesis of cerebral Ischemia/Reperfusion injury (*161*). Platelets also act as a major player in the initiation of the atherogenic process by adhering to the vascular endothelium before the development of manifest atherosclerotic lesions (*158*) and the progression of deep vein thrombosis (DVT). They have been shown to promote leukocyte recruitment (*158*) and stimulation of neutrophil dependent coagulation, here revealing a functional crosstalk between platelets and neutrophils (*253*).

Also in adipose tissue endothelial activation has been shown to be a common feature of chronic inflammatory processes (*262, 268*).

Upon activation the endothelial cells shift towards an increase in pro-adhesive properties by upregulation of P-Selectin (*149*) and other endothelial cell adhesion molecules like E-selectin, ICAM-1 and VCAM-1 (*55*). This reveals a reduction in/

downregulation of endothelial nitric oxide synthetase (*61*) as well as upregulation of surface deposition of adhesion molecules like von Willebrand factor (*141*) allowing for even more adhesion of circulating blood cells.

Platelet adhesion represents a typical response to endothelial activation with strong effects on subsequent inflammatory processes. For this reason, it was analyzed to what extent platelets interact with activated endothelium of adipose tissue vasculature. To do so, *in vivo* microscopy was performed in wild type versus $\alpha_{IIb}\beta_{3}$-deficient transgenic mice.

Endothelial activation occurs in many forms of pathogenensis with chronic inflammation like Rheumatoid Arthritis (*10*), Systemic Lupus Erythematosus (*266*) or Psoriasis (*29*). Also in obesity endothelial activation seems to occur (*183*). Endothelial activation leads to platelet adhesion in atherosclerosis/I/R-injury/ DVT (*158-161, 253*). In these examples of vascular inflammation platelet adhesions supports WBC recruitment and in this way further aggrevates inflammatory processes (*253*). *In vivo* microscopy here shows platelet adhesion in visceral fatpads. Neutrophil accumulation seems to enhance, however significance is not reached in lean anmals, it has to be mentioned, that subtle effects might be lost due to the small time window within the intravital microscopic analysis. However, an enhanced accumulation of leukocytes was found in adipose tissue seven weeks later by performing flow cytometric and immunohistological analysis compared to the wild type animals.

The depots of adipose tissue occur in multiple visceral and subcutaneous fat pads of the body. There is strong clinical evidence indicating adipose distribution is important since central obesity is typically associated with metabolic and vascular complications (*82*). Especially the visceral fat pad is not only a simple fat-storage side but rather has to be understood as an endocrine organ with high inflammatory potential (*53*).

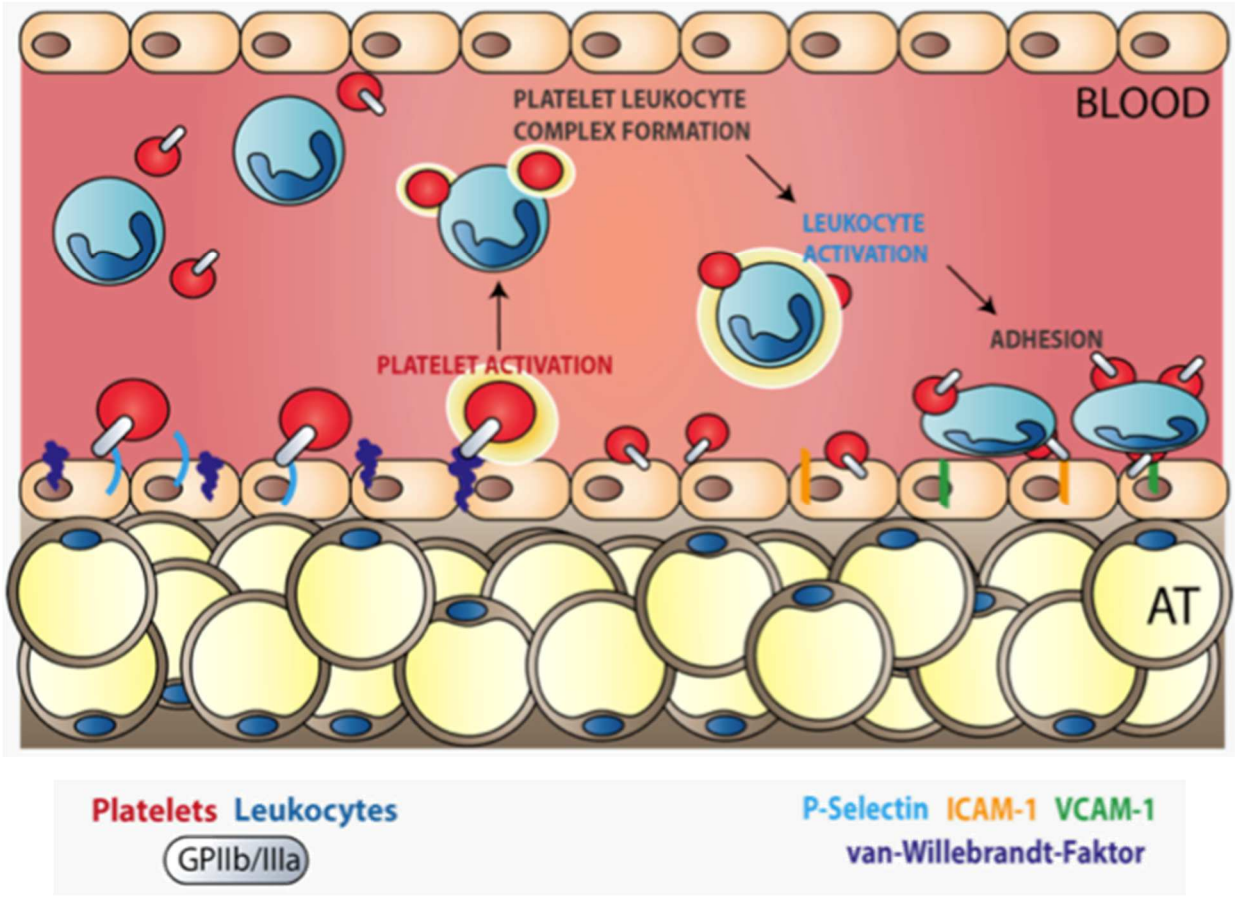

Figure 39: Model of leukocyte and platelet interation on adipose microvasculature endothelium

The scheme gives an overview of how the interaction of leukocytes (blue) and platelets (red) on the micovasculature endothelium take place. The cell components can be distinguished by color.

The adhesion of platelets on endothelial rolling leukocytes is the initial step of a multistep process. This process leads to an extravasation of white blood cells to sites of inflammation. The first part of the thesis suggests that this model is also true for the vasculature of adipose tissue (Fig. 39).

The platelets may also interact with the endothelium in the absence of perceptible/visible morphological damage. They probably may stick to an apparently intact endothelium that is inflamed and influenced by stimuli from site of adipose tissue. A mechanism by which adipose tissue inflammation promotes the vascular dysfunction is unclear, however endothelial dysfunction has already been described in obese children (*15, 247*).

Recruitment of leukocytes to vascular injury after interaction with activated platelets is a rapid response that is initially mediated by release of endothelial components like von Willebrand factor and P-Selectin.

P-Selectin mediates platelet adhesion but also initiates the process of leukocyte rolling (*250*). Activated platelets at the site of vascular damage play a pivotal role in leukocyte accumulation, also for example in growing thrombi (*253*) and may therefore also be from high importance in the recruitment and migration of leukocytes through the vessel wall.

After van Willebrand factor mediated activation platelets form complexes with leukocytes via PSGL-1 (*139*). These platelet-leukocyte complexes promote activation of leukocytes. Furthermore these complexes also produce chemokines, that might facilitate the recruitment of leukocytes into adipose tissue after deposition to the vessel wall (*255*).

2.2. Effect of High Fat Diet on platelet and leukocyte adhesion

Experiments illustrate how an impaired platelet adhesion in αIIbβ3 (GPIIb) or complete lack of platelets (NFE2) culminates in significant WAT expansion. This was shown in early studies of our group performed in GPIIb and NFE2 deficient mice. It is known that chronic inflammatory processes in obesity are enhanced when high fat diet is administered. Talukdar et al found a significant increase of neutrophil infiltration adipose tissue in mice, that were held on a HFD for two weeks. Putting the animals on a high fat diet also provoked high-grade inflammatory response (*238*). In conforming fashion increase in platelet and WBC adhesion was shown in lean versus HFD controls.

Free Fatty Acids (FFA) must cross the capillary endothelial cells to be available for adipocytes. After consuming a high fat diet or even a high fat meal, excessive FFA formation might trigger acute inflammatory events in the adipose tissue. These inflammatory events are likely to result in exposure of vWF (*148, 252*) and fast displacement of P-Selectin to the endothelial cell-surface (*162*). An upregulation of endothelial cell adhesion molecules was also demonstrated in healthy patients following intake of high fat meals (*225*).

Actions of the microcirculation caused by high fat diet might more importantly trigger a GPIIb dependent firm platelet adhesion after interaction with vWF, resulting in platelet interaction with leukocytes and moreover trafficking of leukocytes into adipose tissue.

Most intriguing outcome of the high fat diet experiments was the impaired WBC adhesion in αIIbβ3-deficient mice compared to wild type siblings due to a reduced GPIIb dependent firm platelet adhesion and furthermore a reduced platelet and leukocyte interaction.

It has to be mentioned that the experimental setup was able to replicate and confirm the hypothesis of Talukdar et al., showing an increase in the number of migrating neutrophils into the adipose tissue after high fat diet already in Wild type mice.

It was not only feasible in our experimental setup to show a significant increase in the number of rolling leukocytes even after two weeks of HFD, but also an obvious trend indicating an increase in the number of adherent leukocytes, performed in wild type animals.

The number of rolling WBC increased slightly in the HFD Knockout group, indicating not only a role of P-Selectin binding to Leukocytes via PSGL-1 (*129, 170, 185*) but also a prominent role of platelet interaction with leukocytes that facilitates the migration of leukocytes into adipose tissue. Less platelet adhesion to the endothelium due to the GPIIb deficiency led to less interaction of platelets with leukocytes and therefore less leukocyte migration to adipose tissue.

Data is consistent to what you have already seen in immunohstochemical analysis with reduced WBC accumulation in GPIIb deficent mice compared to the Wildtype group.

Taken together, the sheer numbers of rolling and adherent WBC were smaller in Knockout animals than in their wild type counterparts due to the αIIbβ3-deficient genotype along with platelets incapable of adhering to the endothelium via vWF and consequently unable to assist leukocytes migrating into the adipose tissue.

However, HFD raised these numbers in both genotypes by confronting leukocytes with a quite more dysfunctional endothelium through to diet-induced release of FFA linked with displacement of endothelial vWF and P-Selectin.

This allowed us detecting the most intriguing outcome of this HFD experiment. Although the difference in rolling leukocytes between wild type and Knockout animals both fed a HFD might not differ that much from each other by presenting just a slight increase in the wild type group, difference between the adherent leukocytes is quite remarkable. There is an explicit decrease in the number of adherent leukocytes in αIIbβ3-deficient animals compared to wild type mice both fed a HFD.

This effect can again be attributed to the HFD induced higher count of rolling and adhering leukocytes, illustrating the very likely platelet specific role of leukocyte assistance in migrating into adipose tissue after platelet interaction with leukocytes. The distinctness of this effect would not have been possible to demonstrate in a lean animal model to this extent.

Additionally, comparison of transient adherent and firm adherent platelets in a HFD setting remains identically to the previously described lean experimental setting, proving that the high caloric diet had no impact on the platelet behavior but obviously changed leukocyte dynamics significantly.

2.3. Fat pad and body weight measurement

2.3.1. Transgenic GPIIb deficient and wild type mice

In a next step it was tested whether the observed decrease in WBC adhesion had functional effects on adipose tissue phenotype. To do so body weight was measured in transgenic GPIIb wild type and Knockout mice.

Evaluation of body weight and fat pad analysis already revealed significant fat pad expansion in GPIIb-deficient mice compared to wild type controls (Konrad et al., unpublished data). Dong et al. found that Mice deficient in ICAM-1 became spontaneously obese in old age (*69*), which also supports our findings of a connection between impaired cell adhesion to the adipose tissue endothelium and increase in body weight. In contrast, Yang et al. found, that P-selectin deficiency protects against an increase of body weight after high-fat diet (*271*), affirming a crucial role of GPIIb integrin mediated platelet adhesion resulting in platelet-leukocyte interaction and leukocyte migration into adipose tissue, as examined in this thesis.

The body weight was again measured in transgenic GPIIb wild type and Knockout mice to further evaluate the link between platelet-leukocyte interaction on the dysfunctional endothelium in adipose tissue and the potentially related WAT expansion

The visceral fat pad is the most crucial representative for meta-inflammatory processes, meaning inflammatory responses like cytokine production (*104*), activation and recruitment of circulating leukocytes (*260*) and the remodeling of adipose tissue (*110*). Therefore, it was directly and most likely influenced by leukocyte-platelet mediated migration of leukocytes into the adipose tissue. The retroperitoneal and the subcutaneous fat pad showed also expansion in the experimental setup as well, however not in the extent of the visceral fat.

The brown fat pad was not affected by weight gain, as is main function presents heat production by non-shivering thermogenesis. It does not store energy in form of fat. However, in some cases it was hard to distinguish between BAT and WAT as the brown fat was somehow covered by a thin layer of white fat pad.

The animals showed no differences in carcass weight, this ruled out that weight gain occurred only due to enhanced musculoskeletal growth.

Serum leptin levels revealed a significant increase in $\alpha_{IIb}ß_3$ deficient animals. Typically correlating with the BMI (*56*), leptin levels are also reported to correlate with a number of endocrine substances such as insulin and thyroid hormones (*115*). The primary function of leptin is to appear as an anti-obesity hormone by suppressing the hungry feeling in the hypothalamus (*172*). Being expressed primarily by adipocytes, the correlation of fat pad weight and serum leptin levels detected in this work seems completely comprehensible.

The associated increase of adipocyte size in $\alpha_{IIb}ß_3$ deficient animals also supports position of literature. Obesity is defined as enlargement of adipose tissue to store surplus energy intake. Two possible mechanisms are the increase in cell number (Hyperplasia) as well as the increase in cell size (Hypertrophy). While hyperplastic growth appears only at early stages of adipose development (*21*), hypertrophic growth is more common, meeting the need for additional fat storage capacity (*114*).

Being crucially influenced by the lack of platelet-leukocyte mediated migration of leukocytes into the adipose tissue, $\alpha_{IIb}ß_3$ deficient animals develop larger adipocytes due to hypertrophic growth. Leukocyte migration seems somehow to control and mitigate energy intake of adipocytes. Absence of this trigger compels adipocytes to cope with their high-energy rate by hypertrophic events.

To validate in this first part of the project that the observed effects are in fact platelet driven effects, mRNA analysis was performed in a large selection of adult tissues to assess whether probably so far unidentified $\alpha_{IIb}ß_3$-expression occurred in adult mouse tissues. As already mentioned, $\alpha_{IIb}ß_3$ is also expressed in bone-marrow resident hematopoietic progenitors and megakaryocytes (*78*), as well as in some mast cells (*189*).

No expression was detected in most tested organs. Slight mRNA-levels in liver and kidney were found probably most due to platelet contamination. However, mRNA analysis affirmed the theory that platelet resident $\alpha_{IIb}ß_3$ as being solely accountable for the platelet-leukocyte mediated adipose tissue development.

2.3.2. GPIIb deficient and wild type bone marrow chimera mice

For further test whether it was a platelet specific process that influenced WAT expansion in Knockout mice, bone marrow chimera mice were created to distinguish the contribution of hematopoietic cells versus non-hemapoietic cells (*270*). After sublethally irradioation, 8-weeks old C57Bl/6J wildtype animals either received $\alpha_{IIb}\beta_3$ or wildtype bone marrow cells of sex matched donor mice. Body weight and fat pad weight were assessed 16 weeks after transplantation.

The total WAT amount showed an increase in the GPIIb deficient chimera group compared to their wild type counterparts.

Once more, $\alpha_{IIb}\beta_3$-deficient bone-marrow chimera revealed a significant increase in WAT expansion, implying transplantability of the GPIIb integrin mediated effect. This further substantiates the notion, that $\alpha_{IIb}\beta_3$-integrin expressing platelets mediate the observed regulatory processes in WAT expansion.

Brown fat pad as well as the carcass weight of Knockout and wild type chimeric mice were from equal measure in both genotypes. This again confirmed the previous findings in transgenic mice. Besides the fact that the brown fat pad is not influenced when it comes to weight gain due to its exclusive non-shivering thermogenesis behavior it also demonstrates once more, that the weight gain measured in GPIIb deficient animals was due to expansion of WAT and excluded a growth of the musculo-skeletal system as weight gain source.

2.4. Analysis of fat pad vascularization

Vascularization of the fat pads was analyzed using multiphoton microscopy to identify the potential role of de novo vessel formation or growth of pre-existing vessels within the expansion of adipose tissue.

Work of our group showed GPIbα-mediated platelet-leukocyte interactions to directly support innate immune cell recruitment and further promote arteriogenesis in a mouse model of hindlimb ischemia (*44*).

Hence, multiphoton microscopic analysis was used to investigate whether differences in cellular interactions on the dysfunctional adipose tissue endothelium as well as alterations of WAT expansion rates were only due to significant differences in novel vessel formation or vessel growth within these genotypes.

Arteriogenesis, usually linked to an increase in blood pressure, is also related to an upregulation of inflammatory cytokines and cell adhesion receptors. After increase of shear stress, monocyte chemo-attractant protein-1 (MCP-1) is highly expressed on the surface of vessel walls. This accompanies also with increased levels of TNF-α and matrix metalloproteinase (MMP). MMP remodel the space around the vessel, providing space for expansion (*248*). Also nitric oxide (NO) is reported to be a major factor in vessel diameter enlargement in response to increased blood flow (*245*).

However, no difference in vessel density between the groups was found, thus eliminating the hypothesis, that the observed effects described in the previous chapters were ascribed to changes and differences in vessel formation between the genotypes.

2.5. *In vitro* culture of adipocytes

2.5.1. TNF-α ELISA after adipocyte treatment

To further investigate underlying determinants of the observed effects, chemokine mRNA-expression in subcutaneous fat depots of wild type and GPIIb Knockout animals was performed revealing significantly reduced expression of TNF-α (mRNA) in $\alpha_{IIb}\beta_3$-deficient animals. In line, enlarged WAT depots were reported in TNF-α deficient animals after receiving HFD (*210*). For this reason, impact of platelet and leukocyte recruitment on TNF-α expression as well as adipocyte biology and proliferation was tested.

One of the most important questions remaining still incompletely addressed is the nature of the original TNF-α expression trigger in adipose tissue.

While obesity in rodents and humans is associated with an increase in apoptotic and necrotic adipocytes (*237*), it is also well known, that WAT expansion is associated with increased adipocyte death due to the limited capacity of adipocyte expansion.

Proper immune function is closely linked to nutritional status, prompting the possibility that also the type of dietary components, like specific fats, may play a role in the regulation of adipocyte inflammation (*126*).

Experiments described here showed no TNF-α expression after stimulation with ADP alone. Though ADP is an important factor for glucose utilization (*205*), respectively nutritional status, its influence on adipocyte cytokine expression might not be that important when administered alone.

PMA, representing a di-ester of phorbol and a potent tumor promoter, triggers the activation of Protein Kinase C (PKC). Although PKC is widely expressed in adipocytes as well as preadipocytes, stimulation via PMA does not effect TNF-α expression. It is more likely that PKC involved signaling pathways get activated via TNF-receptor 1 (TNFR1) after stimulation with TNF-α. Stimulation with Tyrodes, serving as negative control, revealed absolutely transparent results by not influencing the expression of TNF-α at all.

TNF-α expression was detectable after adipocytes were treated with stimulated PMNs as well as unstimulated PMNs. Looking at the results it is striking, that the amount of expressed TNF-α is nearly identical in the PMNa and PMN group. A possible explanation for this observation could be a potential activation even of unstimulated PMNs due to time and temperature limitations. Therefore, results of PMNa and PMN were on similar levels.

It seems that the pure presence of leukocytes in our setup influence the expression of TNF-α and that it makes no difference whether the leukocytes were previously activated or not.

In obese patients, their grade of adiposity highly correlates with increased numbers of adipose tissue neutrophils, expressing neutrophil elastase (*269*) and significantly more hyperoxides than compared to lean individuals (*34*). Neutrophil elastase is closely linked to expression of cytokines, like TNF-α, as revealed from previous studies (*9*).

Hyperoxides are involved in apoptosis of cells and therefore in the activation of macrophages, leading to a pro-inflammatory state in obesity. Hereby, neutrophils contribute to adipose tissue inflammation in the early stages of obesity and are likely linked to cytokines, like TNF-α.

This was also confirmed by treating the cells with a combination of platelets and leukocytes. While treatment with platelets alone had no effect on the expression of TNF-α, combination with leukocytes restored the previous described effect of expression. It made no difference, whether the platelets were activated or not in our setup. However, the both combinations with platelets revealed slightly lower levels of TNF-α serum levels compared to PMNa and PMN single groups. This could be partially due to diminished reactivity of neutrophils after complex forming with platelets and an accompanied altered effect on adipocyte TNF-α expression behavior. But importantly, the pure presence of neutrophils (and probably their secreted compounds) was the limiting factor in the TNF-α ELISA setting.

Furthermore, it has to be mentioned that *in vivo* cytokine action results from a complex interplay between networks of pro- and anti-inflammatory cytokines (*258*). It is therefore likely that a coordinate regulation of anti-inflammatory cytokines such as IL-10 may play a role in both TNF-α expression and action *in vivo*, difficult to transfer into an *in vitro* setting.

2.5.2. Adipocyte proliferation evaluation

The experiments done previously were targeted at the expression profiles of mature adipocytes after stimulation with various substances. However, during the progress of adipogenesis, the differentiation phase from preadipocytes to adipocytes *in vitro* as well as the approximately 14-day long maturation phase is a critical step in the development of adipose tissue (*236*). For this reason, it was a consistent step to treat the premature adipocytes in a comparable way like previously described and the proliferation behavior was checked.

The experiments showed, that the proliferation/maturation of adipocytes decreased after they were treated with activated leukocytes. The same was true for the co-incubation with inactivated leukocytes. Previous studies revealed a potential role of leukocytes in the regulation of adipogenesis via Interleukin-17 (IL-17), also after stimulation with PMA as described in chapter II 4.6.3 (*85, 151*).

The group treated with the supernatant of activated platelets showed a decrease in proliferation behavior as well. Activated platelets, mainly releasing soluble CD40, may contribute to adipogenesis. In humans a close link between soluble CD40 Ligand (sCD40L) and BMI was found (*246*). This sCD40L is most likely to interact with CD40 found on adipocytes and stromal adipose fraction. After being activated, CD40 induces adipose cytokine secretion (*199*) and a dose dependent expression of inflammatory cytokines IL-6 and IL-8 (*167*), major regulators of adipose tissue metabolism.

The group treated solely with activated platelets showed no effect on adipocyte proliferation. This may be due to the fact that leukocytes are able to interact with adipocytes directly after transmigration. Platelets are quite unlikely to be interacting with adipocytes, rather than interacting via paracrine effects. This paracrine effects can be detected in the platelet supernatant group but they lack in the setting described here and therefore have no influence on the proliferation behavior of adipocytes *in vitro*.

The most prominent decrease of adipocyte proliferation was found in the groups treated with TNF-α. Being significantly reduced on mRNA levels in the fat pad of GPIIb deficient mice and on the other hand overexpressed after stimulation with diverse substances, TNF-α probably links cytokine expression in adipose tissue with adipocyte development and proliferation. The tumor necrosis factor receptors (TNFR) may not have catalytic activity itself; instead they can transmit signals by recruiting intracellular proteins (adapter-proteins). These adapter-proteins can interact with domains of cytoplasmic sections of the receptors to activate specific downstream signals.

Several adapter complexes are linked to the death domain of tumor necrosis factor receptor 1 (TNFR1-DD) that has been closely linked to mediate many effects on

adipocyte biology (*41, 60*). TNFR1-DD is responsible for the cytotoxic signals induced by TNF-α, for example TNF-α induced cell death in adipocytes (*201*).

TNFR1-DD is also linked to the activation of nuclear factor-kappa B (NFκB), activated by TNF-α, mediating metabolic dysregulation (*113*) and controlling cell proliferation (*123, 216*). Moreover, inhibition of NFκB has shown to lead to an increase in human adipogenesis (*71*).

Interestingly, groups treated with a combination of activated platelets and leukocytes did not significantly chance the proliferation behavior of adipocytes. This setup was used to further investigate a potential role of platelet and leukocyte interaction in the development of obesity. However, the previous experiments focused on an interaction to facilitate migration of leukocytes to the adipose tissue. Since migration was not examined directly in this proliferation assays, it may be, that although leukocytes and activated platelets formed complexes, these complexes did not further affect the proliferation behavior of adipocytes *in vitro*.

Co-incubation of tyrodes and ADP did not influence adipocyte differentiation or proliferation, as mentioned in literature (*191*) and it is also reflected in the here described experiments. Stimulation with tyrodes alone revealed absolutely transparent results by not influencing the proliferation behavior of adipocytes. Also stimulation with PMA mainly triggering activation of Protein Kinase C in adipocytes did not affect the proliferation behavior as described in literature (*81*), comprehensible also in the experiments performed here.

2.6. TNF-α blockage via Infliximab

To further dissect a potential link of reduced TNF-α production in a lean mouse model culminating in expansion of WAT, TNF-α was blocked *in vivo* and the fat pad weight was evaluated as described above. Infliximab (Remicade®) is a chimeric monoclonal antibody directed against soluble and membrane-bound TNF-α and has shown to have considerable anti-inflammatory effects even in a mouse model by successfully blocking TNF-α effects (*64*).

In this project, reactivity of Infliximab was confirmed by ELISA, showing significantly reduced serum TNF-α levels in animals that were treated with Infliximab once per week, over a period of 6 weeks.

Infliximab provokes a significant weight gain in all of the treated animals. The weight gain was triggered by significant increased fat pad weight. All analyzed WAT depots showed enlargement, although not in a significant manner.

These findings once more support the theory of a platelet dependent leukocyte migration to WAT in the pathogenesis of adipose tissue inflammation. In addition to the direct effect of Infliximab blocking TNF-α activity in WAT resulting in increased fat pad formation, there is also connection at another level:

Already inhibition of ICAM-1; impairing leukocyte binding, adhesion and furthermore leukocyte transmigration into the tissue; leads to a significant WAT expansion in mice (*69, 257*). Same findings were also confirmed in mice with deficiency of the integrin αMβ2 (Mac-1), ICAM-1 counter receptor expressed on leukocytes (*69*). Increased WAT expansion was also found in TNF-α deficient animals after receiving HFD (*210*).

Also in humans, treatment with Infliximab causes significant weight gain, for example in the treatment of Crohn's disease (*130*) or Psoriasis (*239*).

Taken together, the results described here support a role of TNF-α in adipose tissue biology. In similar fashion to TNF-α deficient animals, which have been reported to show significantly higher weight gain after HFD than wild type animals (*210*), direct blockade of TNF-α also leads to an increase of WAT formation, even after a treatment of 6 weeks. It is absolutely likely that TNF-α expression in adipose tissue leads to activation of NFκB, influencing adipocyte proliferation and adipogenesis.

3. Summary

In conclusion a previously unknown role of platelets in the pathogenesis of obesity and homeostasis of body weight was identified by this work. Platelets chronically adhere to vessels of the inflamed adipose tissue and in this manner support leukocytes migrating into adipose tissue to regulate chronic inflammatory processes

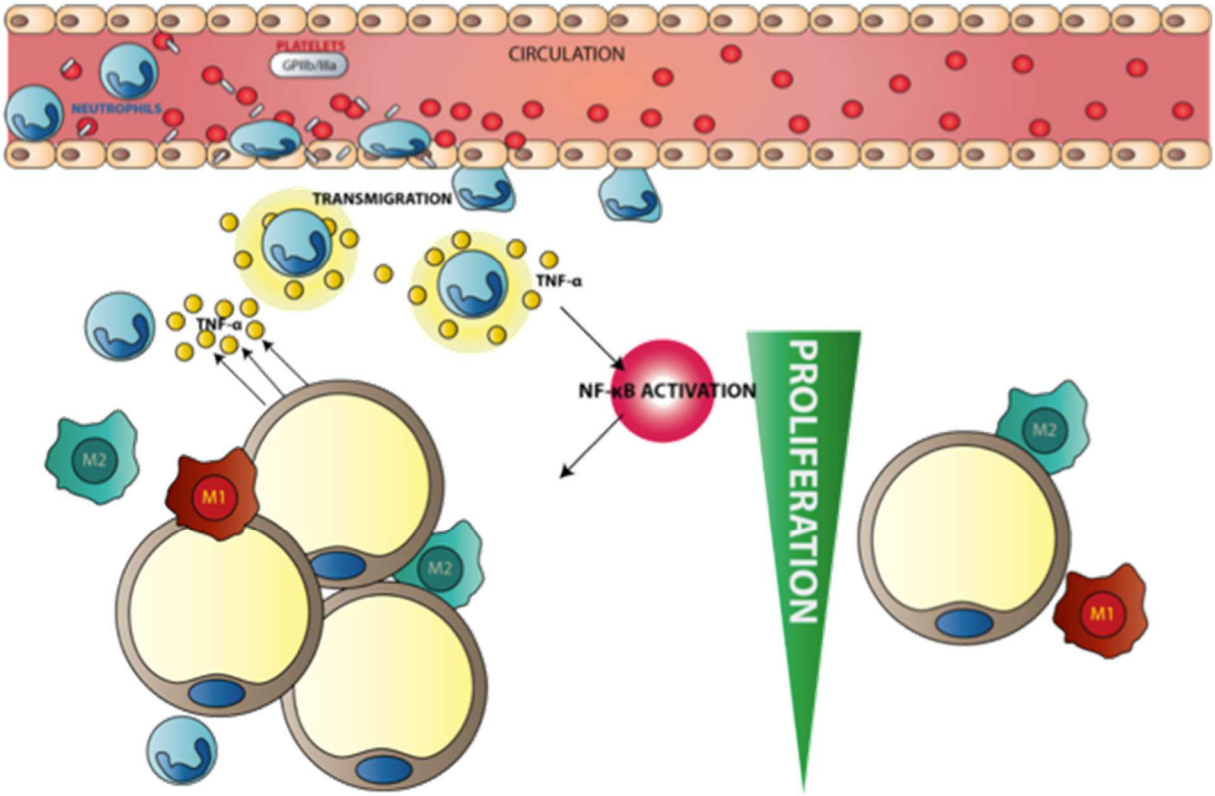

in the pathogenesis of obesity. The data supports the concept that impairment of immune cell accumulation in WAT allows for an increase in body fat and obesity.

Figure 40: Model on adipocyte proliferation in GPIIb wild type animals

In the presence of functional GPIIb integrin (grey) platelets (red) support leukocytes (neutrophils, blue)

migrating into the adipose tissue and in this way regulate adipocyte proliferation via TNF-α (yellow).

Platelet $\alpha_{IIb}\beta_3$ integrin mediates binding to the endothelial receptor ICAM-1 via adhesive bridging proteins like vWF. Adherent platelets facilitate leukocyte accumulation, partially by formation of platelet-leukocytes complexes. In addition, leukocytes get activated after interaction with platelets and migrate into the adipose tissue via intracellular adhesion molecules. Within the adipose tissue activated leukocytes seem to trigger the expression of TNF-α and might provoke release of further, so far unidentified pro-inflammatory cytokines, which transmit signals by recruiting intracellular adapter-proteins. These adapter-proteins might enable downstream signals, closely linked to the activation of NFκB. NFκB could probably control metabolic dysregulation, leading to inhibition of cell proliferation and a potential decrease of adipogenesis (Fig. 40).

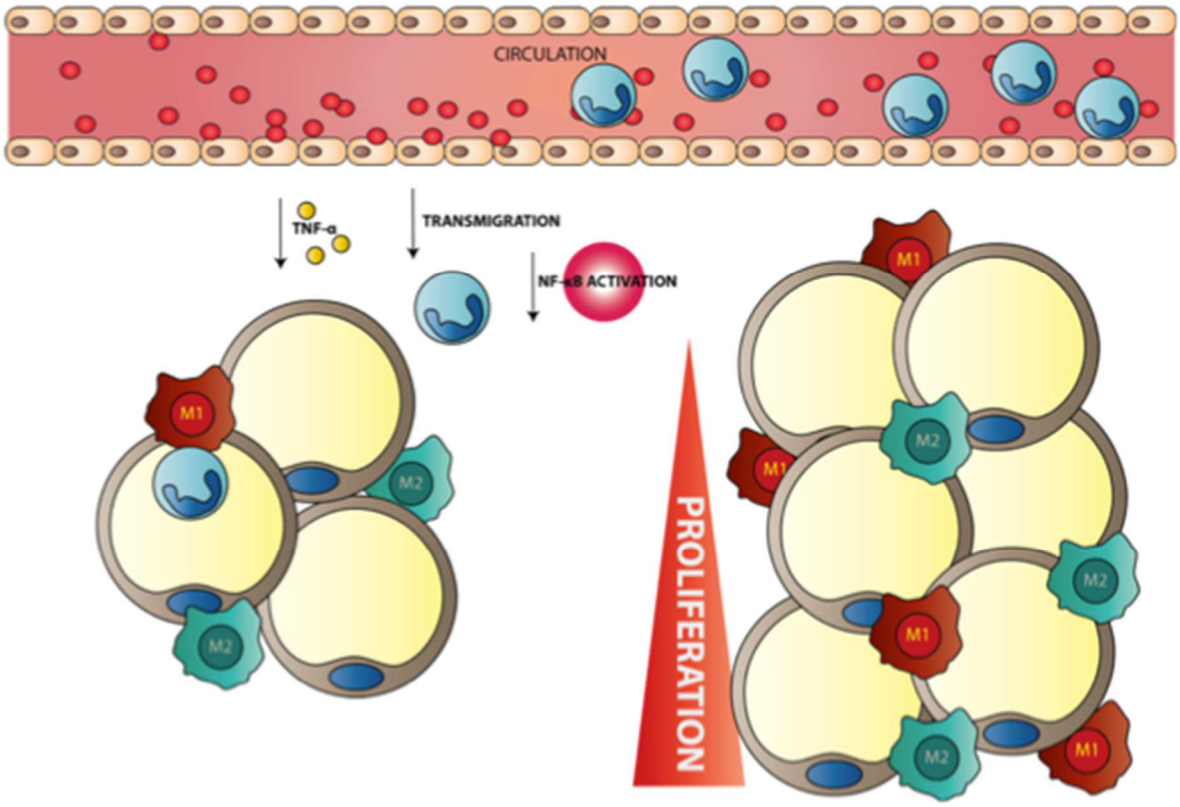

Figure 41: Model on adipocyte proliferation in GPIIb Knockout animals

In the absence of functional GPIIb integrin (grey) platelets (red) cannot support leukocytes (neutrophils, blue) migrating into the adipose tissue. In this way adipocyte proliferation is not influenced via TNF-α (yellow).

With deficient $\alpha_{IIb}\beta_3$ integrin on platelets they cannot bind to the endothelium, at the same time interaction with leukocytes via platelet-leukocyte complexes is impaired. Less platelet adhesion to the endothelium in GPIIb deficient mice was confirmed by intravital microscopy. In addition, platelet interaction with leukocytes is down regulated, resulting in less migration of leukocytes into the adipose tissue, as confirmed by Immunohistological experiments. Moreover, expression of TNF-α and other pro-inflammatory cytokines is reduced as seen in mRNA analysis and *in vitro* assays. Activation and effect of NFκB might be reduced, leading to uncontrolled adipocyte proliferation and the increase of WAT formation (Fig. 41), as detected in the weight development of GPIIb-deficient animals compared to wild type mice. The same effect was also repeated after inhibiting the TNF-α expression in BL/6 mice using Infliximab, resulting in an increased weight gain even after 6-week treatment compared to vehicle treated mice.

To this date a role of so far unidentified platelet-mediated effects on obesity may not be completely ruled out. It is from high priority to further examine exact platelet and leukocyte mechanisms during adipose tissue inflammation for a better understanding of normal body weight maintenance.

Chronic inflammatory processes were identified in WAT during onset and promotion of obesity, with endothelial activation and transmigration of leukocytes after interaction with platelets during the initiation of weight gain. It can be concluded, that platelets regulate inflammatory processes of the adipose tissue, as shown in chronic platelet adhesion to adipose tissue vasculature, which seems to promote white blood cell recruitment to adipose tissue.

Transgenic mice with malfunction in platelet adhesion showed decreased white blood cell accumulation in the WAT, resulting in significantly increased body fat mass. There is an essential role of platelets and leukocytes in chronic inflammatory

processes during initiation and development of obesity.

VII. TABLE OF FIGURES

Figure 1: Human platelet spreading 3

Figure 2: Hematopoiesis 7

Figure 3: The neutrophil adhesion cascade 10

Figure 4: Integrin structure. 12

Figure 5: Pathway for activation of $\alpha_{IIb}\beta_3$. 14

Figure 6: Excitation and emission spectrum of Alexa Fluor ® 488 33

Figure 7: Surgical preparation of the visceral fat pad 35

Figure 8: Schematic overview of the chimera creation process 38

Figure 9: Structural formula of Rhodamine B 40

Figure 10: Optical path of the epifluorescence microscope 41

Figure 11. Structural formula of Sudan III 46

Figure 12: Production of the standard series 57

Figure 13: Jablonski diagram for one-photon (a) and two-photon (b) excitation 60

Figure 14: Number of transient and firm adherent platelets 66

Figure 15: Rhodamine B labeled platelets in GPIIb wild type and Knockout mice ... 67

Figure 16: Number of rolling and adherent leukocytes 68

Figure 17: Alexa Fluor ® 488 labeled leukocytes in GPIIb wild type and Knockout mice 68

Figure 18: CD45+ cell count in WAT of wild type and GPIIb deficient mice 69

Figure 19: Number of rolling and adherent leukocytes normal chow vs. HFD 70

Figure 20: Number of rolling and adherent leukocytes normal chow vs. HFD 71

Figure 21: Alexa Fluor ® 488 labeled leukocytes in GPIIb wild type and Knockout mice after high fat diet for 2 weeks 72

Figure 22: Number of transient adherent and firm adherent platelets normal chow vs. HFD 73

Figure 23: Rhodamine B labeled platelets in GPIIb wild type and Knockout mice after high fat diet for 2 weeks 73

Figure 24: Number of transient adherent and firm adherent platelets normal chow vs. HFD 74

Figure 25: Number of rolling and adherent leukocytes wild type vs. KO fed a HFD . 75

Figure 26: Number of transient adherent and adherent platelets wild type vs. KO fed a HFD 76

Figure 27: Comparison Fat pad appearance between GPIIb wild type and Knockout 77

Figure 28: Total WAT quantification between GPIIb deficient and wild type chimera mice 79

Figure 29: WAT depots of GPIIb deficient and wild type chimera mice in detail..... 80

Figure 30: Three-dimensional visualization of CD144 stained subcutaneous fat pad vasculature 82

Figure 31: Quantification of vessel per fat pad volume in subcutaneous fat pad..... 83

Figure 32: Preadipocyte to adipocyte development 85

Figure 33: Cell culture supernates TNF-α levels after stimulation 86

Figure 34: Area covered with adipocytes 87

Figure 35: Microscopic images of adipocyte covered wells 88

Figure 36: Measurement of serum TNF-α levels using ELISA 89

Figure 37: Total weight gain after Measurement of serum TNF-α levels using ELISA 90

Figure 38: White fat pad measurement after Infliximab and vehicle treatment..... 91

Figure 39: Model of leukocyte and platelet interation on adipose microvasculature endothelium 96

Figure 40: Model on adipocyte proliferation in GPIIb wild type animals 109

Figure 41: Model on adipocyte proliferation in GPIIb Knockout animals 111

VIII. ABBREVIATION LIST

3D:	three-dimensional
A:	Arteria (lat.)
AA:	Amino acid
Aa:	Arteriae (lat.)
Ab:	Antibody
Abbr:	Abbreviation
ADP:	Adenosindiphsophat
ApoE:	Apolipoprotein E
ATP:	Adenosintriphosphat
BAT:	Brown adipose tissue
BM:	Basal membrane
Bm:	Bone marrow
BSA:	Bovine serum albumin
°C:	Degree Celsius
CCL2:	Chemokine (C-C motif) ligand 2
CD:	Cluster of Differentiation
Cm:	Centimeter
CNS:	Central nervous system
Co:	Company
CXCL:	CXC chemokine ligand
CXCR:	CXC chemokine receptor
DAMPs:	Damage associated molecular patterns
DNA:	Desoxyribonucleinacid
E.g.:	Exempli gratia
eGFP:	Enhanced green fluorescent protein
F1:	Filial generation 1

F2:	Filial generation 2
FACS:	Fluorescence activated cell-sorting system
FCS:	Fetal calve serum
f.i.:	For instance
Fig:	Figure
g:	Gramm
GP:	Glycoprotein
GFP:	Green fluorescent protein
h:	Hour
ICAM-1:	Intracellular adhesion molecule-1
ICAM-2:	Intracellular adhesion molecule-2
IL-1b:	Interleukin 1 beta
IL-4:	Interleukin 4
IL-6:	Interleukin 6
IL-8:	Interleukin 8
IL-10:	Interleukin 10
IL-11:	Interleukin 11
IL-13:	Interleukin 13
IL-17:	Interleukin 17
i.p.:	Intraperitoneal
i.v.:	Intravenous
IVC:	Individually ventilated cages
kg:	Kilogram
kDa:	Kilo Dalton
KO:	knockout
LDL:	Low density lipoprotein
LPS:	Lipopolysaccharide
M.:	Musculus (lat.)

m:	Meter
Mac-1:	Macrophages-1 antigen
min:	Minutes
µg:	Microgram
µl:	Microliter
µM:	Micromolar
µm:	Micrometer
MMP:	Matrix metalloproteases
ml:	Milliliter
mm:	Millimeter
mM:	Millimolar
ms:	Millisecond
nm:	Nanometer
n:	Number
NaCl:	Natrium chloride
NE:	Neutrophil elastase
NET:	Neutrophil extracellular traps
NKC:	Natural killer cell
PBS:	Phosphate Buffered Saline
PCR:	Polymerase chain reaction
PECAM:	Platelet endothelial cell adhesion molecule
PFA:	Paraformaldehyde
pH:	numeric scale to specify acidity of basicity of an aqueous solution
Plt:	Platelet
PMN:	Polymorphonuclear neutrophil
PRP:	Platelet rich plasma
PSGL-1:	P-selectin glycoprotein ligand 1

rcf:	Relative centrifugal force
resp.:	Respectively
RNA:	Ribonucleic acid
rpm:	Rounds per minute
RT:	Room temperature
s.:	Second
s.c.:	Subcutan
SD:	Standard deviation
SEM:	Standard error of the mean
Tab:	Table
TNF-α:	Tumor necrosis factor α
V:	Vena (lat.)
VCAM-1:	Vascular cell adhesion molecule-1
VE-cadherine:	Vascular endothelial-cadherin
vs:	Versus
vWF:	Von Willebrand Factor
WAT:	White adipose tissue
wt:	wild type

IX. ACKNOWLEDGEMENT

First of all, I would like to thank my supervisor Prof. Dr. med. Steffen Massberg for giving me the opportunity to work on this intriguing project. I want to thank him for his doctoral supervision, enthusiasm, encouragement and support during the entire period of my PhD study.

I also want to thank my thesis advisory committee, Prof. Dr. rer. nat. Kirsten Lauber and Prof. Dr. med. Markus Sperandio for inspiring meetings and discussions and their courteous help and support.

Being highlighted in particular is my supervisor Dr. med. vet. Katrin Echtler. I'm very grateful for her invaluable supervision and steady support throughout my entire PhD project. I learned a lot from her in many respects. Her practical teaching and guidance, as well as many constructive advices, facilitated the work of this thesis. I truly value the experience of working with her.

I want to acknowledge the SFB914 and the IRTG for outstanding professional training within a perfectly structured PhD-program. A big thank you goes to Dr. rer. nat. Verena Kochan for her guidance through organizational steps as well as supportive talks.

I especially want to thank Michael Lorenz for helpful ideas and encompassing support at any time.

Particular thanks also to my group members, Dr. med. vet. Meike Miller, Dr. med. vet. Vanessa Philippi, Dr. med. vet. Johanna Busse, Gerhild Rosenberger and Dr. med. vet. Susanne Sauer for your support, advices and the great atmosphere.

I also want to extent the thanks to all members of our group, especially Dr. med. vet. Annekathrin Eckart, Dr. med. vet. Irene Schubert, Dr. med. vet. Nicole Urtz, Dr. rer. nat. Anca Tirniceriu and Dr. med. vet. Sue Chandraratne, providing an excellent working atmosphere. It was a pleasure to work with you!

Furthermore, I would like to thank Sebastian Helmer, Anna Titova and Anne-Maria Suhr for excellent technical assistance. A special thanks to Nicole Blount and Beate Jantz for responsible and reliable animal care.

A very special thanks goes to my family, I'm grateful to my parents for their unlimited support throughout my life, making my study and doctorate possible. I also want to thank my two sisters for our unique and particular connection.

I want to extent the special thanks to my partner, Holger, for his never ending support, patience and encouragement. Thank you for your leveraging and inspiring art and for being the essential part of my life.

.

X. LITERATURE

1. Aggarwal, B. B., Gupta, S. C., Kim, J. H., Historical perspectives on tumor necrosis factor and its superfamily: 25 years later, a golden journey. *Blood* **119**, 651-665 (2012).
2. Allingham, M. J., van Buul, J. D., Burridge, K., ICAM-1-mediated, Src- and Pyk2-dependent vascular endothelial cadherin tyrosine phosphorylation is required for leukocyte transendothelial migration. *Journal of immunology (Baltimore, Md. : 1950)* **179**, 4053-4064 (2007).
3. Andre, P., Prasad, K. S., Denis, C. V., He, M., Papalia, J. M., Hynes, R. O., Phillips, D. R., Wagner, D. D., CD40L stabilizes arterial thrombi by a beta3 integrin--dependent mechanism. *Nature medicine* **8**, 247-252 (2002).
4. Asch, A. S., Leung, L. L., Polley, M. J., Nachman, R. L., Platelet membrane topography: colocalization of thrombospondin and fibrinogen with the glycoprotein IIb-IIIa complex. *Blood* **66**, 926-934 (1985).
5. Baune, B. T., Wiede, F., Braun, A., Golledge, J., Arolt, V., Koerner, H., Cognitive dysfunction in mice deficient for TNF- and its receptors. *American journal of medical genetics. Part B, Neuropsychiatric genetics : the official publication of the International Society of Psychiatric Genetics* **147b**, 1056-1064 (2008).
6. Beattie, E. C., Stellwagen, D., Morishita, W., Bresnahan, J. C., Ha, B. K., Von Zastrow, M., Beattie, M. S., Malenka, R. C., Control of synaptic strength by glial TNFalpha. *Science (New York, N.Y.)* **295**, 2282-2285 (2002).
7. Beer, P. M., Wong, S. J., Schartman, J. P., Kulas, K. E., Hartman, C. L., Giganti, M., Falk, N. S., Infliximab stability after reconstitution, dilution, and storage under refrigeration. *Retina (Philadelphia, Pa.)* **30**, 81-84 (2010).
8. Behnke, O., The morphology of blood platelet membrane systems. *Series haematologica (1968)* **3**, 3-16 (1970).
9. Benabid, R., Wartelle, J., Malleret, L., Guyot, N., Gangloff, S., Lebargy, F., Belaaouaj, A., Neutrophil elastase modulates cytokine expression: contribution to host defense against Pseudomonas aeruginosa-induced pneumonia. *The Journal of biological chemistry* **287**, 34883-34894 (2012).
10. Bergholm, R., Leirisalo-Repo, M., Vehkavaara, S., Makimattila, S., Taskinen, M. R., Yki-Jarvinen, H., Impaired responsiveness to NO in newly diagnosed patients with rheumatoid arthritis. *Arteriosclerosis, thrombosis, and vascular biology* **22**, 1637-1641 (2002).
11. Berndt, M. C., Gregory, C., Chong, B. H., Zola, H., Castaldi, P. A., Additional glycoprotein defects in Bernard-Soulier's syndrome: confirmation of genetic basis by parental analysis. *Blood* **62**, 800-807 (1983).
12. Beste, C., Baune, B. T., Falkenstein, M., Konrad, C., Variations in the TNF-alpha gene (TNF-alpha -308G-->A) affect attention and action selection mechanisms in a dissociated fashion. *Journal of neurophysiology* **104**, 2523-2531 (2010).
13. Beutler, B., Cerami, A., Tumor necrosis, cachexia, shock, and inflammation: a common mediator. *Annual review of biochemistry* **57**, 505-518 (1988).
14. Bevilacqua, M. P., Stengelin, S., Gimbrone, M. A., Jr., Seed, B., Endothelial leukocyte adhesion molecule 1: an inducible receptor for neutrophils related to complement regulatory proteins and lectins. *Science (New York, N.Y.)* **243**, 1160-1165 (1989).
15. Bhattacharjee, R., Alotaibi, W. H., Kheirandish-Gozal, L., Capdevila, O. S., Gozal, D., Endothelial dysfunction in obese non-hypertensive children without evidence of sleep disordered breathing. *BMC pediatrics* **10**, 8 (2010).
16. Bianchi, M. E., DAMPs, PAMPs and alarmins: all we need to know about danger.

Journal of leukocyte biology **81**, 1-5 (2007).
17. Biolegend. (2016), pp. Fluorescence Spectra Analyzer.
18. Birbrair, A., Zhang, T., Wang, Z. M., Messi, M. L., Enikolopov, G. N., Mintz, A., Delbono, O., Role of pericytes in skeletal muscle regeneration and fat accumulation. *Stem cells and development* **22**, 2298-2314 (2013).
19. Bizzozero, J., Ueber einen neuen Formbestandtheil des Blutes und dessen Rolle bei der Thrombose und der Blutgerinnung. *Archiv für pathologische Anatomie und Physiologie und für klinische Medicin* **90**, 261-332.
20. Bledzka, K., Smyth, S. S., Plow, E. F., Integrin alphaIIbbeta3: from discovery to efficacious therapeutic target. *Circulation research* **112**, 1189-1200 (2013).
21. Boden, G., Chen, X., Mozzoli, M., Ryan, I., Effect of fasting on serum leptin in normal human subjects. *The Journal of clinical endocrinology and metabolism* **81**, 3419-3423 (1996).
22. Bombeli, T., Schwartz, B. R., Harlan, J. M., Adhesion of activated platelets to endothelial cells: evidence for a GPIIbIIIa-dependent bridging mechanism and novel roles for endothelial intercellular adhesion molecule 1 (ICAM-1), alphavbeta3 integrin, and GPIbalpha. *The Journal of experimental medicine* **187**, 329-339 (1998).
23. Borish, L., Rosenbaum, R., Albury, L., Clark, S., Activation of neutrophils by recombinant interleukin 6. *Cellular immunology* **121**, 280-289 (1989).
24. Bouma, G., Doffinger, R., Patel, S. Y., Peskett, E., Sinclair, J. C., Barcenas-Morales, G., Cerron-Gutierrez, L., Kumararatne, D. S., Davies, E. G., Thrasher, A. J., Burns, S. O., Impaired neutrophil migration and phagocytosis in IRAK-4 deficiency. *British journal of haematology* **147**, 153-156 (2009).
25. Bout, D., Joseph, M., Pontet, M., Vorng, H., Deslee, D., Capron, A., Rat resistance to schistosomiasis: platelet-mediated cytotoxicity induced by C-reactive protein. *Science (New York, N.Y.)* **231**, 153-156 (1986).
26. Bouvard, D., Brakebusch, C., Gustafsson, E., Aszodi, A., Bengtsson, T., Berna, A., Fassler, R., Functional consequences of integrin gene mutations in mice. *Circulation research* **89**, 211-223 (2001).
27. Boyle, J. J., Macrophage activation in atherosclerosis: pathogenesis and pharmacology of plaque rupture. *Current vascular pharmacology* **3**, 63-68 (2005).
28. Brekke, O. H., Sandlie, I., Therapeutic antibodies for human diseases at the dawn of the twenty-first century. *Nature reviews. Drug discovery* **2**, 52-62 (2003).
29. Brezinski, E. A., Follansbee, M. R., Armstrong, E. J., Armstrong, A. W., Endothelial dysfunction and the effects of TNF inhibitors on the endothelium in psoriasis and psoriatic arthritis: a systematic review. *Current pharmaceutical design* **20**, 513-528 (2014).
30. Brill, A., Fuchs, T. A., Chauhan, A. K., Yang, J. J., De Meyer, S. F., Kollnberger, M., Wakefield, T. W., Lammle, B., Massberg, S., Wagner, D. D., von Willebrand factor-mediated platelet adhesion is critical for deep vein thrombosis in mouse models. *Blood* **117**, 1400-1407 (2011).
31. Brinkmann, V., Reichard, U., Goosmann, C., Fauler, B., Uhlemann, Y., Weiss, D. S., Weinrauch, Y., Zychlinsky, A., Neutrophil extracellular traps kill bacteria. *Science (New York, N.Y.)* **303**, 1532-1535 (2004).
32. Brocker, C., Thompson, D., Matsumoto, A., Nebert, D. W., Vasiliou, V., Evolutionary divergence and functions of the human interleukin (IL) gene family. *Human genomics* **5**, 30-55 (2010).
33. Brooks, P., Clark, R., Cheresh, D., Requirement of vascular integrin alpha v beta 3 for angiogenesis. *Science (New York, N.Y.)* **264**, 569-571 (1994).
34. Brotfain, E., Hadad, N., Shapira, Y., Avinoah, E., Zlotnik, A., Raichel, L., Levy, R., Neutrophil functions in morbidly obese subjects. *Clinical and experimental immunology* **181**, 156-163 (2015).
35. Bruun, J. M., Lihn, A. S., Madan, A. K., Pedersen, S. B., Schiott, K. M., Fain, J. N., Richelsen, B., Higher production of IL-8 in visceral vs. subcutaneous adipose tissue. Implication of nonadipose cells in adipose tissue. *American journal of physiology.*

Endocrinology and metabolism **286**, E8-13 (2004).
36. Bryckaert, M., Rosa, J. P., Denis, C. V., Lenting, P. J., Of von Willebrand factor and platelets. *Cellular and molecular life sciences : CMLS* **72**, 307-326 (2015).
37. Byzova, T. V., Rabbani, R., D'Souza, S. E., Plow, E. F., Role of integrin alpha(v)beta3 in vascular biology. *Thrombosis and haemostasis* **80**, 726-734 (1998).
38. Calvete, J. J., On the structure and function of platelet integrin alpha IIb beta 3, the fibrinogen receptor. *Proceedings of the Society for Experimental Biology and Medicine. Society for Experimental Biology and Medicine (New York, N.Y.)* **208**, 346-360 (1995).
39. Cannon, B., Hedin, A., Nedergaard, J., Exclusive occurrence of thermogenin antigen in brown adipose tissue. *FEBS letters* **150**, 129-132 (1982).
40. Carbone, F., Vuilleumier, N., Bertolotto, M., Burger, F., Galan, K., Roversi, G., Tamborino, C., Casetta, I., Seraceni, S., Trentini, A., Dallegri, F., da Silva, A. R., Pende, A., Artom, N., Mach, F., Coen, M., Fainardi, E., Montecucco, F., Treatment with recombinant tissue plasminogen activator (r-TPA) induces neutrophil degranulation in vitro via defined pathways. *Vascular pharmacology* **64**, 16-27 (2015).
41. Cawthorn, W. P., Heyd, F., Hegyi, K., Sethi, J. K., Tumour necrosis factor-alpha inhibits adipogenesis via a beta-catenin/TCF4(TCF7L2)-dependent pathway. *Cell death and differentiation* **14**, 1361-1373 (2007).
42. Cawthorn, W. P., Sethi, J. K., TNF-alpha and adipocyte biology. *FEBS letters* **582**, 117-131 (2008).
43. Cerletti, C., Tamburrelli, C., Izzi, B., Gianfagna, F., de Gaetano, G., Platelet-leukocyte interactions in thrombosis. *Thrombosis research* **129**, 263-266 (2012).
44. Chandraratne, S., von Bruehl, M. L., Pagel, J. I., Stark, K., Kleinert, E., Konrad, I., Farschtschi, S., Coletti, R., Gartner, F., Chillo, O., Legate, K. R., Lorenz, M., Rutkowski, S., Caballero-Martinez, A., Starke, R., Tirniceriu, A., Pauleikhoff, L., Fischer, S., Assmann, G., Mueller-Hoecker, J., Ware, J., Nieswandt, B., Schaper, W., Schulz, C., Deindl, E., Massberg, S., Critical role of platelet glycoprotein ibalpha in arterial remodeling. *Arteriosclerosis, thrombosis, and vascular biology* **35**, 589-597 (2015).
45. Chen, C. S., Thiagarajan, P., Schwartz, S. M., Harlan, J. M., Heimark, R. L., The platelet glycoprotein IIb/IIIa-like protein in human endothelial cells promotes adhesion but not initial attachment to extracellular matrix. *The Journal of cell biology* **105**, 1885-1892 (1987).
46. Chiu, J. J., Usami, S., Chien, S., Vascular endothelial responses to altered shear stress: pathologic implications for atherosclerosis. *Annals of medicine* **41**, 19-28 (2009).
47. Chosay, J. G., Fisher, M. A., Farhood, A., Ready, K. A., Dunn, C. J., Jaeschke, H., Role of PECAM-1 (CD31) in neutrophil transmigration in murine models of liver and peritoneal inflammation. *The American journal of physiology* **274**, G776-782 (1998).
48. Choy, E. H., Panayi, G. S., Cytokine pathways and joint inflammation in rheumatoid arthritis. *The New England journal of medicine* **344**, 907-916 (2001).
49. Cinti, S., The adipose organ. *Prostaglandins, leukotrienes, and essential fatty acids* **73**, 9-15 (2005).
50. Claytor, R. B., Li, J. M., Furman, M. I., Garnette, C. S., Rohrer, M. J., Barnard, M. R., Krueger, L. A., Frelinger, A. L., 3rd, Michelson, A. D., Laser scanning cytometry: a novel method for the detection of platelet--endothelial cell adhesion. *Cytometry* **43**, 308-313 (2001).
51. Clemetson, J. M., Polgar, J., Magnenat, E., Wells, T. N., Clemetson, K. J., The platelet collagen receptor glycoprotein VI is a member of the immunoglobulin superfamily closely related to FcalphaR and the natural killer receptors. *The Journal of biological chemistry* **274**, 29019-29024 (1999).
52. Clemetson, K. J., McGregor, J. L., James, E., Dechavanne, M., Luscher, E. F., Characterization of the platelet membrane glycoprotein abnormalities in Bernard-

Soulier syndrome and comparison with normal by surface-labeling techniques and high-resolution two-dimensional gel electrophoresis. *The Journal of clinical investigation* **70**, 304-311 (1982).
53. Coelho, M., Oliveira, T., Fernandes, R., Biochemistry of adipose tissue: an endocrine organ. *Archives of Medical Science : AMS* **9**, 191-200 (2013).
54. Coller, B. S., Folts, J. D., Smith, S. R., Scudder, L. E., Jordan, R., Abolition of in vivo platelet thrombus formation in primates with monoclonal antibodies to the platelet GPIIb/IIIa receptor. Correlation with bleeding time, platelet aggregation, and blockade of GPIIb/IIIa receptors. *Circulation* **80**, 1766-1774 (1989).
55. Collins, T., Read, M. A., Neish, A. S., Whitley, M. Z., Thanos, D., Maniatis, T., Transcriptional regulation of endothelial cell adhesion molecules: NF-kappa B and cytokine-inducible enhancers. *FASEB journal : official publication of the Federation of American Societies for Experimental Biology* **9**, 899-909 (1995).
56. Considine, R. V., Sinha, M. K., Heiman, M. L., Kriauciunas, A., Stephens, T. W., Nyce, M. R., Ohannesian, J. P., Marco, C. C., McKee, L. J., Bauer, T. L., et al., Serum immunoreactive-leptin concentrations in normal-weight and obese humans. *The New England journal of medicine* **334**, 292-295 (1996).
57. Cooper, G., in *The Cell: A Molecular Approach*. (Sunderland (MA): Sinauer Associates, 2000).
58. Cornelius, P., MacDougald, O. A., Lane, M. D., Regulation of adipocyte development. *Annual review of nutrition* **14**, 99-129 (1994).
59. Coughlin, S. R., Protease-activated receptors in hemostasis, thrombosis and vascular biology. *Journal of thrombosis and haemostasis : JTH* **3**, 1800-1814 (2005).
60. Csehi, S. B., Mathieu, S., Seifert, U., Lange, A., Zweyer, M., Wernig, A., Adam, D., Tumor necrosis factor (TNF) interferes with insulin signaling through the p55 TNF receptor death domain. *Biochemical and biophysical research communications* **329**, 397-405 (2005).
61. Davenpeck, K. L., Gauthier, T. W., Lefer, A. M., Inhibition of endothelial-derived nitric oxide promotes P-selectin expression and actions in the rat microcirculation. *Gastroenterology* **107**, 1050-1058 (1994).
62. Denk, W., Strickler, J. H., Webb, W. W., Two-photon laser scanning fluorescence microscopy. *Science (New York, N.Y.)* **248**, 73-76 (1990).
63. Deuel, T. F., Senior, R. M., Chang, D., Griffin, G. L., Heinrikson, R. L., Kaiser, E. T., Platelet factor 4 is chemotactic for neutrophils and monocytes. *Proceedings of the National Academy of Sciences of the United States of America* **78**, 4584-4587 (1981).
64. Deveci, F., Muz, M. H., Ilhan, N., Kirkil, G., Turgut, T., Akpolat, N., Evaluation of the anti-inflammatory effect of infliximab in a mouse model of acute asthma. *Respirology (Carlton, Vic.)* **13**, 488-497 (2008).
65. Diacovo, T. G., Roth, S. J., Buccola, J. M., Bainton, D. F., Springer, T. A., Neutrophil rolling, arrest, and transmigration across activated, surface-adherent platelets via sequential action of P-selectin and the beta 2-integrin CD11b/CD18. *Blood* **88**, 146-157 (1996).
66. Dillon, S. B., Verghese, M. W., Snyderman, R., Signal transduction in cells following binding of chemoattractants to membrane receptors. *Virchows Archiv. B, Cell pathology including molecular pathology* **55**, 65-80 (1988).
67. Dinarello, C. A., Biologic basis for interleukin-1 in disease. *Blood* **87**, 2095-2147 (1996).
68. Dole, V. S., Bergmeier, W., Mitchell, H. A., Eichenberger, S. C., Wagner, D. D., Activated platelets induce Weibel-Palade-body secretion and leukocyte rolling in vivo: role of P-selectin. *Blood* **106**, 2334-2339 (2005).
69. Dong, Z. M., Gutierrez-Ramos, J. C., Coxon, A., Mayadas, T. N., Wagner, D. D., A new class of obesity genes encodes leukocyte adhesion receptors. *Proceedings of the National Academy of Sciences of the United States of America* **94**, 7526-7530 (1997).

70. Dore, M., Korthuis, R. J., Granger, D. N., Entman, M. L., Smith, C. W., P-selectin mediates spontaneous leukocyte rolling in vivo. *Blood* **82**, 1308-1316 (1993).
71. Dorronsoro, A., Lang, V., Jakobsson, E., Ferrin, I., Salcedo, J. M., Fernandez-Rueda, J., Fechter, K., Rodriguez, M. S., Trigueros, C., Identification of the NF-kappaB inhibitor A20 as a key regulator for human adipogenesis. *Cell death & disease* **4**, e972 (2013).
72. Dubinsky, M. C., Fleshner, P. P., Treatment of Crohn's Disease of Inflammatory, Stenotic, and Fistulizing Phenotypes. *Current treatment options in gastroenterology* **6**, 183-200 (2003).
73. Emambokus, N. R., Frampton, J., The glycoprotein IIb molecule is expressed on early murine hematopoietic progenitors and regulates their numbers in sites of hematopoiesis. *Immunity* **19**, 33-45 (2003).
74. Emsley, J., Knight, C. G., Farndale, R. W., Barnes, M. J., Liddington, R. C., Structural basis of collagen recognition by integrin alpha2beta1. *Cell* **101**, 47-56 (2000).
75. Evangelista, V., Manarini, S., Sideri, R., Rotondo, S., Martelli, N., Piccoli, A., Totani, L., Piccardoni, P., Vestweber, D., de Gaetano, G., Cerletti, C., Platelet/polymorphonuclear leukocyte interaction: P-selectin triggers protein-tyrosine phosphorylation-dependent CD11b/CD18 adhesion: role of PSGL-1 as a signaling molecule. *Blood* **93**, 876-885 (1999).
76. Fain, J. N., Release of inflammatory mediators by human adipose tissue is enhanced in obesity and primarily by the nonfat cells: a review. *Mediators of inflammation* **2010**, 513948 (2010).
77. Fain, J. N., Madan, A. K., Hiler, M. L., Cheema, P., Bahouth, S. W., Comparison of the release of adipokines by adipose tissue, adipose tissue matrix, and adipocytes from visceral and subcutaneous abdominal adipose tissues of obese humans. *Endocrinology* **145**, 2273-2282 (2004).
78. Faraday, N., Rade, J. J., Johns, D. C., Khetawat, G., Noga, S. J., DiPersio, J. F., Jin, Y., Nichol, J. L., Haug, J. S., Bray, P. F., Ex vivo cultured megakaryocytes express functional glycoprotein IIb-IIIa receptors and are capable of adenovirus-mediated transgene expression. *Blood* **94**, 4084-4092 (1999).
79. Feghali, C. A., Wright, T. M., Cytokines in acute and chronic inflammation. *Frontiers in bioscience : a journal and virtual library* **2**, d12-26 (1997).
80. Feldmann, M., Maini, R. N., Lasker Clinical Medical Research Award. TNF defined as a therapeutic target for rheumatoid arthritis and other autoimmune diseases. *Nature medicine* **9**, 1245-1250 (2003).
81. Fleming, I., MacKenzie, S. J., Vernon, R. G., Anderson, N. G., Houslay, M. D., Kilgour, E., Protein kinase C isoforms play differential roles in the regulation of adipocyte differentiation. *Biochemical Journal* **333**, 719-727 (1998).
82. Fox, C. S., Massaro, J. M., Hoffmann, U., Pou, K. M., Maurovich-Horvat, P., Liu, C. Y., Vasan, R. S., Murabito, J. M., Meigs, J. B., Cupples, L. A., D'Agostino, R. B., Sr., O'Donnell, C. J., Abdominal visceral and subcutaneous adipose tissue compartments: association with metabolic risk factors in the Framingham Heart Study. *Circulation* **116**, 39-48 (2007).
83. Frenette, P. S., Johnson, R. C., Hynes, R. O., Wagner, D. D., Platelets roll on stimulated endothelium in vivo: an interaction mediated by endothelial P-selectin. *Proceedings of the National Academy of Sciences of the United States of America* **92**, 7450-7454 (1995).
84. Friedl, P., Weigelin, B., Interstitial leukocyte migration and immune function. *Nature immunology* **9**, 960-969 (2008).
85. Gaffen, S. L., Kramer, J. M., Yu, J. J., Shen, F., The IL-17 cytokine family. *Vitamins and hormones* **74**, 255-282 (2006).
86. Gawaz, M., *Physiology, Pathophysiology, Membrane Receptors, Antiplatelet Drugs, Coronary Heart Disease, Stroke, Peripheral Arterial Disease*. (Stuttgart Thieme, 2001), pp. 190.
87. Gawaz, M., Ruf, A., Pogatsa-Murray, G., Dickfeld, T., Rudiger, S., Taubitz, W.,

Fischer, J., Muller, I., Meier, D., Patscheke, H., Schomig, A., Incomplete inhibition of platelet aggregation and glycoprotein IIb-IIIa receptor blockade by abciximab: importance of internal pool of glycoprotein IIb-IIIa receptors. *Thrombosis and haemostasis* **83**, 915-922 (2000).

88. Geng, J. G., Bevilacqua, M. P., Moore, K. L., McIntyre, T. M., Prescott, S. M., Kim, J. M., Bliss, G. A., Zimmerman, G. A., McEver, R. P., Rapid neutrophil adhesion to activated endothelium mediated by GMP-140. *Nature* **343**, 757-760 (1990).
89. Giambelluca, M. S., Bertheau-Mailhot, G., Laflamme, C., Rollet-Labelle, E., Servant, M. J., Pouliot, M., TNF-alpha expression in neutrophils and its regulation by glycogen synthase kinase-3: a potentiating role for lithium. *FASEB journal : official publication of the Federation of American Societies for Experimental Biology* **28**, 3679-3690 (2014).
90. Ginsberg, M. H., Partridge, A., Shattil, S. J., Integrin regulation. *Current opinion in cell biology* **17**, 509-516 (2005).
91. Glanzmann, E., in *J Kinderkr.* (1918), vol. 88, pp. 113–141.
92. Green, H., Kehinde, O., An established preadipose cell line and its differentiation in culture. II. Factors affecting the adipose conversion. *Cell* **5**, 19-27 (1975).
93. Griffin, J. D., Spertini, O., Ernst, T. J., Belvin, M. P., Levine, H. B., Kanakura, Y., Tedder, T. F., Granulocyte-macrophage colony-stimulating factor and other cytokines regulate surface expression of the leukocyte adhesion molecule-1 on human neutrophils, monocytes, and their precursors. *Journal of immunology (Baltimore, Md. : 1950)* **145**, 576-584 (1990).
94. Gupta, A. K., Skinner, A. R., A review of the use of infliximab to manage cutaneous dermatoses. *Journal of cutaneous medicine and surgery* **8**, 77-89 (2004).
95. Hanson, S. R., Pareti, F. I., Ruggeri, Z. M., Marzec, U. M., Kunicki, T. J., Montgomery, R. R., Zimmerman, T. S., Harker, L. A., Effects of monoclonal antibodies against the platelet glycoprotein IIb/IIIa complex on thrombosis and hemostasis in the baboon. *The Journal of clinical investigation* **81**, 149-158 (1988).
96. Harker, L. A., Roskos, L. K., Marzec, U. M., Carter, R. A., Cherry, J. K., Sundell, B., Cheung, E. N., Terry, D., Sheridan, W., Effects of megakaryocyte growth and development factor on platelet production, platelet life span, and platelet function in healthy human volunteers. *Blood* **95**, 2514-2522 (2000).
97. Harrison, P., Cramer, E. M., Platelet alpha-granules. *Blood reviews* **7**, 52-62 (1993).
98. Hartl, D., Krauss-Etschmann, S., Koller, B., Hordijk, P. L., Kuijpers, T. W., Hoffmann, F., Hector, A., Eber, E., Marcos, V., Bittmann, I., Eickelberg, O., Griese, M., Roos, D., Infiltrated neutrophils acquire novel chemokine receptor expression and chemokine responsiveness in chronic inflammatory lung diseases. *Journal of immunology (Baltimore, Md. : 1950)* **181**, 8053-8067 (2008).
99. Haslett, C., Savill, J. S., Meagher, L., The neutrophil. *Current opinion in immunology* **2**, 10-18 (1989).
100. Hattori, R., Hamilton, K. K., Fugate, R. D., McEver, R. P., Sims, P. J., Stimulated secretion of endothelial von Willebrand factor is accompanied by rapid redistribution to the cell surface of the intracellular granule membrane protein GMP-140. *The Journal of biological chemistry* **264**, 7768-7771 (1989).
101. Hollopeter, G., Jantzen, H. M., Vincent, D., Li, G., England, L., Ramakrishnan, V., Yang, R. B., Nurden, P., Nurden, A., Julius, D., Conley, P. B., Identification of the platelet ADP receptor targeted by antithrombotic drugs. *Nature* **409**, 202-207 (2001).
102. Holmsen, H., Platelet metabolism and activation. *Seminars in hematology* **22**, 219-240 (1985).
103. Hordijk, P., Endothelial signaling in leukocyte transmigration. *Cell biochemistry and biophysics* **38**, 305-322 (2003).
104. Hotamisligil, G. S., Shargill, N. S., Spiegelman, B. M., Adipose expression of tumor necrosis factor-alpha: direct role in obesity-linked insulin resistance. *Science (New York, N.Y.)* **259**, 87-91 (1993).
105. Hovig, T., Blood Platelet Surface and Shape A Scanning Electron Microscopic Study.

Scandinavian Journal of Haematology **7**, 420-427 (1970).
106. Hunger, K., Mischke, P., Rieper, W., Raue, R., Kunde, K., Engel, A., in *Ullmann's Encyclopedia of Industrial Chemistry*. (Wiley-VCH Verlag GmbH & Co. KGaA, 2000).
107. Ibele, G. M., Kay, N. E., Johnson, G. J., Jacob, H. S., Human platelets exert cytotoxic effects on tumor cells. *Blood* **65**, 1252-1255 (1985).
108. Ikeda, Y., Handa, M., Kawano, K., Kamata, T., Murata, M., Araki, Y., Anbo, H., Kawai, Y., Watanabe, K., Itagaki, I., et al., The role of von Willebrand factor and fibrinogen in platelet aggregation under varying shear stress. *The Journal of clinical investigation* **87**, 1234-1240 (1991).
109. Italiano, J. E., Jr., Shivdasani, R. A., Megakaryocytes and beyond: the birth of platelets. *Journal of thrombosis and haemostasis : JTH* **1**, 1174-1182 (2003).
110. Itoh, M., Suganami, T., Hachiya, R., Ogawa, Y., Adipose tissue remodeling as homeostatic inflammation. *International journal of inflammation* **2011**, 720926 (2011).
111. Jackson, S. P., Nesbitt, W. S., Kulkarni, S., Signaling events underlying thrombus formation. *Journal of thrombosis and haemostasis : JTH* **1**, 1602-1612 (2003).
112. Jain, N. C., A scanning electron microscopic study of platelets of certain animal species. *Thrombosis et diathesis haemorrhagica* **33**, 501-507 (1975).
113. Jain, R. G., Phelps, K. D., Pekala, P. H., Tumor necrosis factor-alpha initiated signal transduction in 3T3-L1 adipocytes. *Journal of cellular physiology* **179**, 58-66 (1999).
114. Janeckova, R., [New findings on the role of leptins in regulation of the reproductive system in humans]. *Ceskoslovenska fysiologie / Ustredni ustav biologicky* **50**, 25-30 (2001).
115. Janeckova, R., The role of leptin in human physiology and pathophysiology. *Physiological research / Academia Scientiarum Bohemoslovaca* **50**, 443-459 (2001).
116. Janeway, C., Travers, P., Walport, M., *Immunobiology: The Immune System in Health and Disease. 5th edition*. (New York: Garland Science, 2001), vol. 5.
117. Jin, J. O., Yu, Q., Fucoidan delays apoptosis and induces pro-inflammatory cytokine production in human neutrophils. *International journal of biological macromolecules* **73**, 65-71 (2015).
118. Jirouskova, M., Shet, A. S., Johnson, G. J., A guide to murine platelet structure, function, assays, and genetic alterations. *Journal of thrombosis and haemostasis : JTH* **5**, 661-669 (2007).
119. Justement, L. B., Campbell, K. S., Chien, N. C., Cambier, J. C., Regulation of B cell antigen receptor signal transduction and phosphorylation by CD45. *Science (New York, N.Y.)* **252**, 1839-1842 (1991).
120. Jutila, M. A., Rott, L., Berg, E. L., Butcher, E. C., Function and regulation of the neutrophil MEL-14 antigen in vivo: comparison with LFA-1 and MAC-1. *Journal of immunology (Baltimore, Md. : 1950)* **143**, 3318-3324 (1989).
121. Kaiser, W., Garrett, C. G. B., Two-Photon Excitation in Ca F2 : Eu2+. *Physical Review Letters* **7**, 229-231 (1961).
122. Kanda, H., Tateya, S., Tamori, Y., Kotani, K., Hiasa, K., Kitazawa, R., Kitazawa, S., Miyachi, H., Maeda, S., Egashira, K., Kasuga, M., MCP-1 contributes to macrophage infiltration into adipose tissue, insulin resistance, and hepatic steatosis in obesity. *The Journal of clinical investigation* **116**, 1494-1505 (2006).
123. Karin, M., Ben-Neriah, Y., Phosphorylation meets ubiquitination: the control of NF-[kappa]B activity. *Annual review of immunology* **18**, 621-663 (2000).
124. Kaur, J., A comprehensive review on metabolic syndrome. *Cardiology research and practice* **2014**, 943162 (2014).
125. Kavanaugh, A. F., Ritchlin, C. T., Systematic review of treatments for psoriatic arthritis: an evidence based approach and basis for treatment guidelines. *The Journal of rheumatology* **33**, 1417-1421 (2006).
126. Kelley, D. S., Modulation of human immune and inflammatory responses by dietary fatty acids. *Nutrition (Burbank, Los Angeles County, Calif.)* **17**, 669-673 (2001).
127. Kershaw, E. E., Flier, J. S., Adipose tissue as an endocrine organ. *The Journal of clinical endocrinology and metabolism* **89**, 2548-2556 (2004).

128. Kim, M., Carman, C. V., Springer, T. A., Bidirectional transmembrane signaling by cytoplasmic domain separation in integrins. *Science (New York, N.Y.)* **301**, 1720-1725 (2003).
129. Kim, M. B., Sarelius, I. H., Role of shear forces and adhesion molecule distribution on P-selectin-mediated leukocyte rolling in postcapillary venules. *American journal of physiology. Heart and circulatory physiology* **287**, H2705-2711 (2004).
130. Kim, M. J., Lee, W. Y., Choi, K. E., Choe, Y. H., Effect of infliximab top-down therapy on weight gain in pediatric Crohns disease. *Indian pediatrics* **49**, 979-982 (2012).
131. Kim, Y. J., Hong, K. S., Chung, J. W., Kim, J. H., Hahm, K. B., Prevention of colitis-associated carcinogenesis with infliximab. *Cancer prevention research (Philadelphia, Pa.)* **3**, 1314-1333 (2010).
132. Kishimoto, T. K., Jutila, M. A., Berg, E. L., Butcher, E. C., Neutrophil Mac-1 and MEL-14 adhesion proteins inversely regulated by chemotactic factors. *Science (New York, N.Y.)* **245**, 1238-1241 (1989).
133. Kobayashi, S. D., Voyich, J. M., DeLeo, F. R., Regulation of the neutrophil-mediated inflammatory response to infection. *Microbes and infection / Institut Pasteur* **5**, 1337-1344 (2003).
134. Koppaka, S., Kehlenbrink, S., Carey, M., Li, W., Sanchez, E., Lee, D. E., Lee, H., Chen, J., Carrasco, E., Kishore, P., Zhang, K., Hawkins, M., Reduced adipose tissue macrophage content is associated with improved insulin sensitivity in thiazolidinedione-treated diabetic humans. *Diabetes* **62**, 1843-1854 (2013).
135. Krueger, J. M., The role of cytokines in sleep regulation. *Current pharmaceutical design* **14**, 3408-3416 (2008).
136. Kuijpers, M. J. E., Gilio, K., Reitsma, S., Nergiz-Unal, R., Prinzen, L., Heeneman, S., Lutgens, E., Van Zandvoort, M. A. M. J., Nieswandt, B., Oude Egbrink, M. G. A., Heemskerk, J. W. M., Complementary roles of platelets and coagulation in thrombus formation on plaques acutely ruptured by targeted ultrasound treatment: a novel intravital model. *Journal of Thrombosis and Haemostasis* **7**, 152-161 (2009).
137. Kulmala, S., Suomi, J., Current status of modern analytical luminescence methods. *Analytica Chimica Acta* **500**, 21-69 (2003).
138. Larochelle, A., Dunbar, C. E., Genetic manipulation of hematopoietic stem cells. *Seminars in hematology* **41**, 257-271 (2004).
139. Larsen, E., Celi, A., Gilbert, G. E., Furie, B. C., Erban, J. K., Bonfanti, R., Wagner, D. D., Furie, B., PADGEM protein: a receptor that mediates the interaction of activated platelets with neutrophils and monocytes. *Cell* **59**, 305-312 (1989).
140. Latz, E., Xiao, T. S., Stutz, A., Activation and regulation of the inflammasomes. *Nature reviews. Immunology* **13**, 397-411 (2013).
141. Lenting, P. J., Pegon, J. N., Groot, E., de Groot, P. G., Regulation of von Willebrand factor-platelet interactions. *Thrombosis and haemostasis* **104**, 449-455 (2010).
142. Levin, J., Peng, J. P., Baker, G. R., Villeval, J. L., Lecine, P., Burstein, S. A., Shivdasani, R. A., Pathophysiology of thrombocytopenia and anemia in mice lacking transcription factor NF-E2. *Blood* **94**, 3037-3047 (1999).
143. Lewinsohn, D. M., Bargatze, R. F., Butcher, E. C., Leukocyte-endothelial cell recognition: evidence of a common molecular mechanism shared by neutrophils, lymphocytes, and other leukocytes. *Journal of immunology (Baltimore, Md. : 1950)* **138**, 4313-4321 (1987).
144. Ley, K., Gaehtgens, P., Fennie, C., Singer, M. S., Lasky, L. A., Rosen, S. D., Lectin-like cell adhesion molecule 1 mediates leukocyte rolling in mesenteric venules in vivo. *Blood* **77**, 2553-2555 (1991).
145. Ley, K., Laudanna, C., Cybulsky, M. I., Nourshargh, S., Getting to the site of inflammation: the leukocyte adhesion cascade updated. *Nature reviews. Immunology* **7**, 678-689 (2007).
146. Li, J. M., Podolsky, R. S., Rohrer, M. J., Cutler, B. S., Massie, M. T., Barnard, M. R., Michelson, A. D., Adhesion of activated platelets to venous endothelial cells is mediated via GPIIb/IIIa. *The Journal of surgical research* **61**, 543-548 (1996).

147. Li, Z., Delaney, M. K., O'Brien, K. A., Du, X., Signaling during platelet adhesion and activation. *Arteriosclerosis, thrombosis, and vascular biology* **30**, 2341-2349 (2010).
148. Lip, G. Y., Blann, A., von Willebrand factor: a marker of endothelial dysfunction in vascular disorders? *Cardiovascular research* **34**, 255-265 (1997).
149. Lorant, D. E., Topham, M. K., Whatley, R. E., McEver, R. P., McIntyre, T. M., Prescott, S. M., Zimmerman, G. A., Inflammatory roles of P-selectin. *The Journal of clinical investigation* **92**, 559-570 (1993).
150. Lumeng, C. N., Bodzin, J. L., Saltiel, A. R., Obesity induces a phenotypic switch in adipose tissue macrophage polarization. *The Journal of clinical investigation* **117**, 175-184 (2007).
151. Lumeng, C. N., Maillard, I., Saltiel, A. R., T-ing up inflammation in fat. *Nature medicine* **15**, 846-847 (2009).
152. MacDougald, O. A., Burant, C. F., The rapidly expanding family of adipokines. *Cell metabolism* **6**, 159-161 (2007).
153. MacDougald, O. A., Lane, M. D., Transcriptional regulation of gene expression during adipocyte differentiation. *Annual review of biochemistry* **64**, 345-373 (1995).
154. Maffei, M., Halaas, J., Ravussin, E., Pratley, R. E., Lee, G. H., Zhang, Y., Fei, H., Kim, S., Lallone, R., Ranganathan, S., et al., Leptin levels in human and rodent: measurement of plasma leptin and ob RNA in obese and weight-reduced subjects. *Nature medicine* **1**, 1155-1161 (1995).
155. Mann, A., Thompson, A., Robbins, N., Blomkalns, A. L., Localization, identification, and excision of murine adipose depots. *Journal of visualized experiments : JoVE*, (2014).
156. Marcus, A. J., Pathways of oxygen utilization by stimulated platelets and leukocytes. *Seminars in hematology* **16**, 188-195 (1979).
157. Marguerie, G. A., Plow, E. F., The fibrinogen-dependent pathway of platelet aggregation. *Annals of the New York Academy of Sciences* **408**, 556-566 (1983).
158. Massberg, S., Brand, K., Gruner, S., Page, S., Muller, E., Muller, I., Bergmeier, W., Richter, T., Lorenz, M., Konrad, I., Nieswandt, B., Gawaz, M., A critical role of platelet adhesion in the initiation of atherosclerotic lesion formation. *The Journal of experimental medicine* **196**, 887-896 (2002).
159. Massberg, S., Enders, G., Leiderer, R., Eisenmenger, S., Vestweber, D., Krombach, F., Messmer, K., Platelet-endothelial cell interactions during ischemia/reperfusion: the role of P-selectin. *Blood* **92**, 507-515 (1998).
160. Massberg, S., Gawaz, M., Gruner, S., Schulte, V., Konrad, I., Zohlnhofer, D., Heinzmann, U., Nieswandt, B., A crucial role of glycoprotein VI for platelet recruitment to the injured arterial wall in vivo. *The Journal of experimental medicine* **197**, 41-49 (2003).
161. Massberg, S., Schurzinger, K., Lorenz, M., Konrad, I., Schulz, C., Plesnila, N., Kennerknecht, E., Rudelius, M., Sauer, S., Braun, S., Kremmer, E., Emambokus, N. R., Frampton, J., Gawaz, M., Platelet adhesion via glycoprotein IIb integrin is critical for atheroprogression and focal cerebral ischemia: an in vivo study in mice lacking glycoprotein IIb. *Circulation* **112**, 1180-1188 (2005).
162. Mathew, M., Tay, E., Cusi, K., Elevated plasma free fatty acids increase cardiovascular risk by inducing plasma biomarkers of endothelial activation, myeloperoxidase and PAI-1 in healthy subjects. *Cardiovascular diabetology* **9**, 9 (2010).
163. Matsumoto, T., Kano, K., Kondo, D., Fukuda, N., Iribe, Y., Tanaka, N., Matsubara, Y., Sakuma, T., Satomi, A., Otaki, M., Ryu, J., Mugishima, H., Mature adipocyte-derived dedifferentiated fat cells exhibit multilineage potential. *Journal of cellular physiology* **215**, 210-222 (2008).
164. Mauer, J., Chaurasia, B., Goldau, J., Vogt, M. C., Ruud, J., Nguyen, K. D., Theurich, S., Hausen, A. C., Schmitz, J., Bronneke, H. S., Estevez, E., Allen, T. L., Mesaros, A., Partridge, L., Febbraio, M. A., Chawla, A., Wunderlich, F. T., Bruning, J. C., Signaling by IL-6 promotes alternative activation of macrophages to limit

endotoxemia and obesity-associated resistance to insulin. *Nature immunology* **15**, 423-430 (2014).
165. May, A. E., Kalsch, T., Massberg, S., Herouy, Y., Schmidt, R., Gawaz, M., Engagement of glycoprotein IIb/IIIa (alpha(IIb)beta3) on platelets upregulates CD40L and triggers CD40L-dependent matrix degradation by endothelial cells. *Circulation* **106**, 2111-2117 (2002).
166. Memon, R. A., Feingold, K. R., Moser, A. H., Fuller, J., Grunfeld, C., Regulation of fatty acid transport protein and fatty acid translocase mRNA levels by endotoxin and cytokines. *The American journal of physiology* **274**, E210-217 (1998).
167. Missiou, A., Wolf, D., Platzer, I., Ernst, S., Walter, C., Rudolf, P., Zirlik, K., Kostlin, N., Willecke, F. K., Munkel, C., Schonbeck, U., Libby, P., Bode, C., Varo, N., Zirlik, A., CD40L induces inflammation and adipogenesis in adipose cells--a potential link between metabolic and cardiovascular disease. *Thrombosis and haemostasis* **103**, 788-796 (2010).
168. Miyamoto, S., Teramoto, H., Gutkind, J. S., Yamada, K. M., Integrins can collaborate with growth factors for phosphorylation of receptor tyrosine kinases and MAP kinase activation: roles of integrin aggregation and occupancy of receptors. *The Journal of cell biology* **135**, 1633-1642 (1996).
169. Mohri, H., Ohkubo, T., How vitronectin binds to activated glycoprotein IIb-IIIa complex and its function in platelet aggregation. *American journal of clinical pathology* **96**, 605-609 (1991).
170. Moore, K. L., Patel, K. D., Bruehl, R. E., Li, F., Johnson, D. A., Lichenstein, H. S., Cummings, R. D., Bainton, D. F., McEver, R. P., P-selectin glycoprotein ligand-1 mediates rolling of human neutrophils on P-selectin. *The Journal of cell biology* **128**, 661-671 (1995).
171. Moore, K. L., Stults, N. L., Diaz, S., Smith, D. F., Cummings, R. D., Varki, A., McEver, R. P., Identification of a specific glycoprotein ligand for P-selectin (CD62) on myeloid cells. *The Journal of cell biology* **118**, 445-456 (1992).
172. Morash, B., Li, A., Murphy, P. R., Wilkinson, M., Ur, E., Leptin gene expression in the brain and pituitary gland. *Endocrinology* **140**, 5995-5998 (1999).
173. Moser, B., Clark-Lewis, I., Zwahlen, R., Baggiolini, M., Neutrophil-activating properties of the melanoma growth-stimulatory activity. *The Journal of experimental medicine* **171**, 1797-1802 (1990).
174. Moser, M., Legate, K. R., Zent, R., Fassler, R., The tail of integrins, talin, and kindlins. *Science (New York, N.Y.)* **324**, 895-899 (2009).
175. Mühlpfordt, H. (2008), pp. Schematic of a fluorescence microscope.
176. Mulligan, M. S., Varani, J., Dame, M. K., Lane, C. L., Smith, C. W., Anderson, D. C., Ward, P. A., Role of endothelial-leukocyte adhesion molecule 1 (ELAM-1) in neutrophil-mediated lung injury in rats. *The Journal of clinical investigation* **88**, 1396-1406 (1991).
177. Nascimento, J., Rufino, S., Susana, T. (2010).
178. Nathan, D. G., Orkin, S. H., *Nathan and Oski's Hematology of Infancy and Childhood*. (2009), vol. 1, pp. 1841.
179. Nedelcev, T., Racko, D., Krupa, I., Preparation and characterization of a new derivative of Rhodamine B with an alkoxysilane moiety. *Dyes and Pigments* **76**, 550 - 556 (2008).
180. Nedwin, G. E., Naylor, S. L., Sakaguchi, A. Y., Smith, D., Jarrett-Nedwin, J., Pennica, D., Goeddel, D. V., Gray, P. W., Human lymphotoxin and tumor necrosis factor genes: structure, homology and chromosomal localization. *Nucleic acids research* **13**, 6361-6373 (1985).
181. Niemiec, M. J., De Samber, B., Garrevoet, J., Vergucht, E., Vekemans, B., De Rycke, R., Bjorn, E., Sandblad, L., Wellenreuther, G., Falkenberg, G., Cloetens, P., Vincze, L., Urban, C. F., Trace element landscape of resting and activated human neutrophils on the sub-micrometer level. *Metallomics : integrated biometal science* **7**, 996-1010 (2015).

182. Nieswandt, B., Varga-Szabo, D., Elvers, M., Integrins in platelet activation. *Journal of thrombosis and haemostasis : JTH* **7 Suppl 1**, 206-209 (2009).
183. Nishimura, S., Manabe, I., Nagasaki, M., Seo, K., Yamashita, H., Hosoya, Y., Ohsugi, M., Tobe, K., Kadowaki, T., Nagai, R., Sugiura, S., In vivo imaging in mice reveals local cell dynamics and inflammation in obese adipose tissue. *The Journal of clinical investigation* **118**, 710-721 (2008).
184. Nordenfelt, P., Quantitative assessment of neutrophil phagocytosis using flow cytometry. *Methods in molecular biology (Clifton, N.J.)* **1124**, 279-289 (2014).
185. Norman, K. E., Moore, K. L., McEver, R. P., Ley, K., Leukocyte rolling in vivo is mediated by P-selectin glycoprotein ligand-1. *Blood* **86**, 4417-4421 (1995).
186. Nurden, A. T., Platelets, inflammation and tissue regeneration. *Thrombosis and haemostasis* **105 Suppl 1**, S13-33 (2011).
187. Nurden, A. T., Platelet membrane glycoproteins: a historical review. *Seminars in thrombosis and hemostasis* **40**, 577-584 (2014).
188. Nurden, A. T., Caen, J. P., An abnormal platelet glycoprotein pattern in three cases of Glanzmann's thrombasthenia. *British journal of haematology* **28**, 253-260 (1974).
189. Oki, T., Kitaura, J., Eto, K., Lu, Y., Maeda-Yamamoto, M., Inagaki, N., Nagai, H., Yamanishi, Y., Nakajima, H., Kumagai, H., Kitamura, T., Integrin alphaIIbbeta3 induces the adhesion and activation of mast cells through interaction with fibrinogen. *Journal of immunology (Baltimore, Md. : 1950)* **176**, 52-60 (2006).
190. Olofsson, A. M., Arfors, K. E., Ramezani, L., Wolitzky, B. A., Butcher, E. C., von Andrian, U. H., E-selectin mediates leukocyte rolling in interleukin-1-treated rabbit mesentery venules. *Blood* **84**, 2749-2758 (1994).
191. Omatsu-Kanbe, M., Inoue, K., Fujii, Y., Yamamoto, T., Isono, T., Fujita, N., Matsuura, H., Effect of ATP on preadipocyte migration and adipocyte differentiation by activating P2Y receptors in 3T3-L1 cells. *Biochemical Journal* **393**, 171-180 (2006).
192. Panaro, M. A., Mitolo, V., Cellular responses to FMLP challenging: a mini-review. *Immunopharmacology and immunotoxicology* **21**, 397-419 (1999).
193. Pears, C. (2015).
194. Pellegrino, M., Minervini, B., Musto, P., Matera, R., Greco, A., Checchia de Ambrosio, C., Tumor necrosis factor-alpha and interleukin-1 beta. Two possible mediators of allergic inflammation. *Minerva pediatrica* **48**, 309-312 (1996).
195. Pelleymounter, M. A., Cullen, M. J., Baker, M. B., Hecht, R., Winters, D., Boone, T., Collins, F., Effects of the obese gene product on body weight regulation in ob/ob mice. *Science (New York, N.Y.)* **269**, 540-543 (1995).
196. Persson, T., Monsef, N., Andersson, P., Bjartell, A., Malm, J., Calafat, J., Egesten, A., Expression of the neutrophil-activating CXC chemokine ENA-78/CXCL5 by human eosinophils. *Clinical and experimental allergy : journal of the British Society for Allergy and Clinical Immunology* **33**, 531-537 (2003).
197. Perutelli, P., Mori, P. G., The human platelet membrane glycoprotein IIb/IIIa complex: a multi functional adhesion receptor. *Haematologica* **77**, 162-168 (1992).
198. Phillips, D. R., Fitzgerald, L. A., Charo, I. F., Parise, L. V., The platelet membrane glycoprotein IIb/IIIa complex. Structure, function, and relationship to adhesive protein receptors in nucleated cells. *Annals of the New York Academy of Sciences* **509**, 177-187 (1987).
199. Poggi, M., Jager, J., Paulmyer-Lacroix, O., Peiretti, F., Gremeaux, T., Verdier, M., Grino, M., Stepanian, A., Msika, S., Burcelin, R., de Prost, D., Tanti, J. F., Alessi, M. C., The inflammatory receptor CD40 is expressed on human adipocytes: contribution to crosstalk between lymphocytes and adipocytes. *Diabetologia* **52**, 1152-1163 (2009).
200. Polasek, J., Release of multivesicular bodies from platelets as observed in SEM. *Haematologia* **17**, 267-279 (1984).
201. Prins, J. B., Niesler, C. U., Winterford, C. M., Bright, N. A., Siddle, K., O'Rahilly, S., Walker, N. I., Cameron, D. P., Tumor necrosis factor-alpha induces apoptosis of human adipose cells. *Diabetes* **46**, 1939-1944 (1997).

202. Qin, J., Vinogradova, O., Plow, E. F., Integrin bidirectional signaling: a molecular view. *PLoS biology* **2**, e169 (2004).
203. Reininger, A. J., Korndorfer, M. A., Wurzinger, L. J., Adhesion of ADP-activated platelets to intact endothelium under stagnation point flow in vitro is mediated by the integrin alphaIIbeta3. *Thrombosis and haemostasis* **79**, 998-1003 (1998).
204. Riordan, N. H., Ichim, T. E., Min, W. P., Wang, H., Solano, F., Lara, F., Alfaro, M., Rodriguez, J. P., Harman, R. J., Patel, A. N., Murphy, M. P., Lee, R. R., Minev, B., Non-expanded adipose stromal vascular fraction cell therapy for multiple sclerosis. *Journal of translational medicine* **7**, 29 (2009).
205. Robertson, J. P., Faulkner, A., Vernon, R. G., Regulation of glycolysis and fatty acid synthesis from glucose in sheep adipose tissue. *Biochemical Journal* **206**, 577-586 (1982).
206. Rosen, E. D., MacDougald, O. A., Adipocyte differentiation from the inside out. *Nature reviews. Molecular cell biology* **7**, 885-896 (2006).
207. Ross, D. W., Ayscue, L. H., Watson, J., Bentley, S. A., Stability of hematologic parameters in healthy subjects. Intraindividual versus interindividual variation. *American journal of clinical pathology* **90**, 262-267 (1988).
208. Rowinsky, E. K., Signal events: Cell signal transduction and its inhibition in cancer. *The oncologist* **8 Suppl 3**, 5-17 (2003).
209. Rutgeerts, P., Sandborn, W. J., Feagan, B. G., Reinisch, W., Olson, A., Johanns, J., Travers, S., Rachmilewitz, D., Hanauer, S. B., Lichtenstein, G. R., de Villiers, W. J., Present, D., Sands, B. E., Colombel, J. F., Infliximab for induction and maintenance therapy for ulcerative colitis. *The New England journal of medicine* **353**, 2462-2476 (2005).
210. Salles, J., Tardif, N., Landrier, J. F., Mothe-Satney, I., Guillet, C., Boue-Vaysse, C., Combaret, L., Giraudet, C., Patrac, V., Bertrand-Michel, J., Denis, P., Chardigny, J. M., Boirie, Y., Walrand, S., TNFalpha gene knockout differentially affects lipid deposition in liver and skeletal muscle of high-fat-diet mice. *The Journal of nutritional biochemistry* **23**, 1685-1693 (2012).
211. Sandborn, W. J., Feagan, B. G., Stoinov, S., Honiball, P. J., Rutgeerts, P., Mason, D., Bloomfield, R., Schreiber, S., Certolizumab pegol for the treatment of Crohn's disease. *The New England journal of medicine* **357**, 228-238 (2007).
212. Sarjeant, K., Stephens, J. M., Adipogenesis. *Cold Spring Harbor perspectives in biology* **4**, a008417 (2012).
213. Savage, B., Almus-Jacobs, F., Ruggeri, Z. M., Specific synergy of multiple substrate-receptor interactions in platelet thrombus formation under flow. *Cell* **94**, 657-666 (1998).
214. Savill, J., Apoptosis in resolution of inflammation. *Journal of leukocyte biology* **61**, 375-380 (1997).
215. Scherer, P. E., Williams, S., Fogliano, M., Baldini, G., Lodish, H. F., A novel serum protein similar to C1q, produced exclusively in adipocytes. *The Journal of biological chemistry* **270**, 26746-26749 (1995).
216. Sen, R., Baltimore, D., Inducibility of kappa immunoglobulin enhancer-binding protein Nf-kappa B by a posttranslational mechanism. *Cell* **47**, 921-928 (1986).
217. Sepuru, K. M., Poluri, K. M., Rajarathnam, K., Solution structure of CXCL5--a novel chemokine and adipokine implicated in inflammation and obesity. *PloS one* **9**, e93228 (2014).
218. Sfikakis, P. P., Behcet's disease: a new target for anti-tumour necrosis factor treatment. *Annals of the rheumatic diseases* **61 Suppl 2**, ii51-53 (2002).
219. Shattil, S. J., Signaling through platelet integrin alpha IIb beta 3: inside-out, outside-in, and sideways. *Thrombosis and haemostasis* **82**, 318-325 (1999).
220. Shattil, S. J., Integrins and Src: dynamic duo of adhesion signaling. *Trends in cell biology* **15**, 399-403 (2005).
221. Shattil, S. J., Ginsberg, M. H., Perspectives series: cell adhesion in vascular biology. Integrin signaling in vascular biology. *The Journal of clinical investigation* **100**, 1-5

(1997).
222. Shattil, S. J., Kashiwagi, H., Pampori, N., Integrin signaling: the platelet paradigm. *Blood* **91**, 2645-2657 (1998).
223. Shattil, S. J., Kim, C., Ginsberg, M. H., The final steps of integrin activation: the end game. *Nature reviews. Molecular cell biology* **11**, 288-300 (2010).
224. Shattil, S. J., Newman, P. J., Integrins: dynamic scaffolds for adhesion and signaling in platelets. *Blood* **104**, 1606-1615 (2004).
225. Shimabukuro, M., Chinen, I., Higa, N., Takasu, N., Yamakawa, K., Ueda, S., Effects of dietary composition on postprandial endothelial function and adiponectin concentrations in healthy humans: a crossover controlled study. *The American journal of clinical nutrition* **86**, 923-928 (2007).
226. Sigma-Aldrich. (Sigma-Aldrich), vol. 2016, pp. Datasheet.
227. Sigma-Aldrich. (Sigma-Aldrich), pp. Datasheet.
228. Siiteri, P. K., Adipose tissue as a source of hormones. *The American journal of clinical nutrition* **45**, 277-282 (1987).
229. Smart, S. J., Casale, T. B., TNF-alpha-induced transendothelial neutrophil migration is IL-8 dependent. *The American journal of physiology* **266**, L238-245 (1994).
230. Smith, R. A., Baglioni, C., The active form of tumor necrosis factor is a trimer. *The Journal of biological chemistry* **262**, 6951-6954 (1987).
231. Smith, R. J., Sam, L. M., Justen, J. M., Bundy, G. L., Bala, G. A., Bleasdale, J. E., Receptor-coupled signal transduction in human polymorphonuclear neutrophils: effects of a novel inhibitor of phospholipase C-dependent processes on cell responsiveness. *The Journal of pharmacology and experimental therapeutics* **253**, 688-697 (1990).
232. Smyth, S. S., McEver, R. P., Weyrich, A. S., Morrell, C. N., Hoffman, M. R., Arepally, G. M., French, P. A., Dauerman, H. L., Becker, R. C., Platelet functions beyond hemostasis. *Journal of thrombosis and haemostasis : JTH* **7**, 1759-1766 (2009).
233. So, P. T., Dong, C. Y., Masters, B. R., Berland, K. M., Two-photon excitation fluorescence microscopy. *Annual review of biomedical engineering* **2**, 399-429 (2000).
234. Stahl, A., A current review of fatty acid transport proteins (SLC27). *Pflugers Archiv : European journal of physiology* **447**, 722-727 (2004).
235. Starr, M. E., Evers, B. M., Saito, H., Age-associated increase in cytokine production during systemic inflammation: adipose tissue as a major source of IL-6. *The journals of gerontology. Series A, Biological sciences and medical sciences* **64**, 723-730 (2009).
236. Stephens, J. M., The fat controller: adipocyte development. *PLoS biology* **10**, e1001436 (2012).
237. Strissel, K. J., Stancheva, Z., Miyoshi, H., Perfield, J. W., 2nd, DeFuria, J., Jick, Z., Greenberg, A. S., Obin, M. S., Adipocyte death, adipose tissue remodeling, and obesity complications. *Diabetes* **56**, 2910-2918 (2007).
238. Talukdar, S., Oh da, Y., Bandyopadhyay, G., Li, D., Xu, J., McNelis, J., Lu, M., Li, P., Yan, Q., Zhu, Y., Ofrecio, J., Lin, M., Brenner, M. B., Olefsky, J. M., Neutrophils mediate insulin resistance in mice fed a high-fat diet through secreted elastase. *Nature medicine* **18**, 1407-1412 (2012).
239. Tan, E., Baker, C., Foley, P., Weight gain and tumour necrosis factor-alpha inhibitors in patients with psoriasis. *The Australasian journal of dermatology* **54**, 259-263 (2013).
240. Tanahashi, N., Fukuuchi, Y., Tomita, M., Tomita, Y., Inoue, K., Satoh, H., Abe, T., Adhesion of adenosine diphosphate-activated platelets to human brain microvascular endothelial cells under flow in vitro is mediated via GPIIb/IIIa. *Neuroscience letters* **301**, 33-36 (2001).
241. Tang, T., Zhang, J., Yin, J., Staszkiewicz, J., Gawronska-Kozak, B., Jung, D. Y., Ko, H. J., Ong, H., Kim, J. K., Mynatt, R., Martin, R. J., Keenan, M., Gao, Z., Ye, J., Uncoupling of inflammation and insulin resistance by NF-kappaB in transgenic mice

through elevated energy expenditure. *The Journal of biological chemistry* **285**, 4637-4644 (2010).
242. Tecchio, C., Cassatella, M. A., Neutrophil-derived cytokines involved in physiological and pathological angiogenesis. *Chemical immunology and allergy* **99**, 123-137 (2014).
243. Thon, J. N., Italiano, J. E., Platelets: production, morphology and ultrastructure. *Handbook of experimental pharmacology*, 3-22 (2012).
244. Tomita, Y., Tanahashi, N., Tomita, M., Itoh, Y., Yokoyama, M., Takeda, H., Schiszler, I., Fukuuchi, Y., Role of platelet glycoprotein IIb/IIIa in ADP-activated platelet adhesion to aortic endothelial cells in vitro: observation with video-enhanced contrast microscopy. *Clinical hemorheology and microcirculation* **24**, 1-9 (2001).
245. Tronc, F., Wassef, M., Esposito, B., Henrion, D., Glagov, S., Tedgui, A., Role of NO in flow-induced remodeling of the rabbit common carotid artery. *Arteriosclerosis, thrombosis, and vascular biology* **16**, 1256-1262 (1996).
246. Unek, I. T., Bayraktar, F., Solmaz, D., Ellidokuz, H., Yuksel, F., Sisman, A. R., Yesil, S., Enhanced levels of soluble CD40 ligand and C-reactive protein in a total of 312 patients with metabolic syndrome. *Metabolism: clinical and experimental* **59**, 305-313 (2010).
247. Valle Jimenez, M., Estepa, R. M., Camacho, R. M., Estrada, R. C., Luna, F. G., Guitarte, F. B., Endothelial dysfunction is related to insulin resistance and inflammatory biomarker levels in obese prepubertal children. *European journal of endocrinology / European Federation of Endocrine Societies* **156**, 497-502 (2007).
248. Van Royen, N., Piek, J. J., Schaper, W., Bode, C., Buschmann, I., Arteriogenesis: mechanisms and modulation of collateral artery development. *Journal of nuclear cardiology : official publication of the American Society of Nuclear Cardiology* **8**, 687-693 (2001).
249. Vestweber, D., Ligand-specificity of the selectins. *Journal of cellular biochemistry* **61**, 585-591 (1996).
250. Vestweber, D., Blanks, J. E., Mechanisms that regulate the function of the selectins and their ligands. *Physiological reviews* **79**, 181-213 (1999).
251. Vickers, J. D., Binding of polymerizing fibrin to integrin alpha(IIb)beta(3) on chymotrypsin-treated rabbit platelets decreases phosphatidylinositol 4,5-bisphosphate and increases cytoskeletal actin. *Platelets* **10**, 228-237 (1999).
252. Vischer, U. M., von Willebrand factor, endothelial dysfunction, and cardiovascular disease. *Journal of thrombosis and haemostasis : JTH* **4**, 1186-1193 (2006).
253. von Bruhl, M. L., Stark, K., Steinhart, A., Chandraratne, S., Konrad, I., Lorenz, M., Khandoga, A., Tirniceriu, A., Coletti, R., Kollnberger, M., Byrne, R. A., Laitinen, I., Walch, A., Brill, A., Pfeiler, S., Manukyan, D., Braun, S., Lange, P., Riegger, J., Ware, J., Eckart, A., Haidari, S., Rudelius, M., Schulz, C., Echtler, K., Brinkmann, V., Schwaiger, M., Preissner, K. T., Wagner, D. D., Mackman, N., Engelmann, B., Massberg, S., Monocytes, neutrophils, and platelets cooperate to initiate and propagate venous thrombosis in mice in vivo. *The Journal of experimental medicine* **209**, 819-835 (2012).
254. Wagner, C. L., Mascelli, M. A., Neblock, D. S., Weisman, H. F., Coller, B. S., Jordan, R. E., Analysis of GPIIb/IIIa receptor number by quantification of 7E3 binding to human platelets. *Blood* **88**, 907-914 (1996).
255. Wagner, D. D., Frenette, P. S., The vessel wall and its interactions. *Blood* **111**, 5271-5281 (2008).
256. Wajant, H., Pfizenmaier, K., Scheurich, P., Tumor necrosis factor signaling. *Cell death and differentiation* **10**, 45-65 (2003).
257. Wang, H. W., Babic, A. M., Mitchell, H. A., Liu, K., Wagner, D. D., Elevated soluble ICAM-1 levels induce immune deficiency and increase adiposity in mice. *FASEB journal : official publication of the Federation of American Societies for Experimental Biology* **19**, 1018-1020 (2005).
258. Wang, Y., Wang, H., Hegde, V., Dubuisson, O., Gao, Z., Dhurandhar, N. V., Ye, J.,

Interplay of pro- and anti-inflammatory cytokines to determine lipid accretion in adipocytes. *International journal of obesity (2005)* **37**, 1490-1498 (2013).
259. Watchmaker, P. B., Lahl, K., Lee, M., Baumjohann, D., Morton, J., Kim, S. J., Zeng, R., Dent, A., Ansel, K. M., Diamond, B., Hadeiba, H., Butcher, E. C., Comparative transcriptional and functional profiling defines conserved programs of intestinal DC differentiation in humans and mice. *Nature immunology* **15**, 98-108 (2014).
260. Weisberg, S. P., McCann, D., Desai, M., Rosenbaum, M., Leibel, R. L., Ferrante, A. W., Jr., Obesity is associated with macrophage accumulation in adipose tissue. *The Journal of clinical investigation* **112**, 1796-1808 (2003).
261. Weiss, A., Irving, B. A., Tan, L. K., Koretzky, G. A., Signal transduction by the T cell antigen receptor. *Seminars in immunology* **3**, 313-324 (1991).
262. Weyer, C., Yudkin, J. S., Stehouwer, C. D., Schalkwijk, C. G., Pratley, R. E., Tataranni, P. A., Humoral markers of inflammation and endothelial dysfunction in relation to adiposity and in vivo insulin action in Pima Indians. *Atherosclerosis* **161**, 233-242 (2002).
263. Whiteheart, S. W., Platelet granules: surprise packages. *Blood* **118**, 1190-1191 (2011).
264. WHO. (2015).
265. Woodfin, A., Voisin, M. B., Beyrau, M., Colom, B., Caille, D., Diapouli, F. M., Nash, G. B., Chavakis, T., Albelda, S. M., Rainger, G. E., Meda, P., Imhof, B. A., Nourshargh, S., The junctional adhesion molecule JAM-C regulates polarized transendothelial migration of neutrophils in vivo. *Nature immunology* **12**, 761-769 (2011).
266. Wright, S. A., O'Prey, F. M., Rea, D. J., Plumb, R. D., Gamble, A. J., Leahey, W. J., Devine, A. B., McGivern, R. C., Johnston, D. G., Finch, M. B., Bell, A. L., McVeigh, G. E., Microcirculatory hemodynamics and endothelial dysfunction in systemic lupus erythematosus. *Arteriosclerosis, thrombosis, and vascular biology* **26**, 2281-2287 (2006).
267. Wu, D., Molofsky, A. B., Liang, H. E., Ricardo-Gonzalez, R. R., Jouihan, H. A., Bando, J. K., Chawla, A., Locksley, R. M., Eosinophils sustain adipose alternatively activated macrophages associated with glucose homeostasis. *Science (New York, N.Y.)* **332**, 243-247 (2011).
268. Xu, H., Barnes, G. T., Yang, Q., Tan, G., Yang, D., Chou, C. J., Sole, J., Nichols, A., Ross, J. S., Tartaglia, L. A., Chen, H., Chronic inflammation in fat plays a crucial role in the development of obesity-related insulin resistance. *The Journal of clinical investigation* **112**, 1821-1830 (2003).
269. Xu, X., Su, S., Wang, X., Barnes, V., De Miguel, C., Ownby, D., Pollock, J., Snieder, H., Chen, W., Wang, X., Obesity is associated with more activated neutrophils in African American male youth. *International journal of obesity (2005)* **39**, 26-32 (2015).
270. Yang, D., Postnikov, Y. V., Li, Y., Tewary, P., de la Rosa, G., Wei, F., Klinman, D., Gioannini, T., Weiss, J. P., Furusawa, T., Bustin, M., Oppenheim, J. J., High-mobility group nucleosome-binding protein 1 acts as an alarmin and is critical for lipopolysaccharide-induced immune responses. *The Journal of experimental medicine* **209**, 157-171 (2012).
271. Yang, J.-W., Day, Y.-J., Hung, L.-M., P-selectin deficiency protects against high-fat diet-induced obesity and insulin resistance (641.1). *The FASEB Journal* **28**, (2014).
272. Ye, J., Gao, Z., Yin, J., He, Q., Hypoxia is a potential risk factor for chronic inflammation and adiponectin reduction in adipose tissue of ob/ob and dietary obese mice. *American journal of physiology. Endocrinology and metabolism* **293**, E1118-1128 (2007).
273. Yeo, E. L., Sheppard, J. A., Feuerstein, I. A., Role of P-selectin and leukocyte activation in polymorphonuclear cell adhesion to surface adherent activated platelets under physiologic shear conditions (an injury vessel wall model). *Blood* **83**, 2498-2507 (1994).

274. Zhang, Y., Proenca, R., Maffei, M., Barone, M., Leopold, L., Friedman, J. M., Positional cloning of the mouse obese gene and its human homologue. *Nature* **372**, 425-432 (1994).
275. Zhu, J., Yamane, H., Paul, W. E., Differentiation of effector CD4 T cell populations (*). *Annual review of immunology* **28**, 445-489 (2010).
276. Zucker-Franklin, D., Greaves, M. F., Grossi, C. E., Marmont, A. M., *"Neutrophils". Atlas of Blood Cells: Function and Pathology 1* (Philadelphia: Lea & Ferbiger, ed. 2, 1988).
277. Zucker-Franklin, D., Grusky, G., The actin and myosin filaments of human and bovine blood platelets. *The Journal of clinical investigation* **51**, 419-430 (1972).

XI. APPENDIX

Affidavit

Herbert, Henrik H.

Surname, first name

Fürstenrieder Str. 60

Street

80686, Munich

Zip code, town

Germany

Country

I hereby declare, that the submitted thesis entitled

Platelets in the pathogenesis of obesity

is my own work. I have only used the sources indicated and have not made unauthorized use of services of a third party. Where the work of others has been quoted or reproduced, the source is always given.

I further declare that the submitted thesis or parts thereof have not been presented as part of an examination degree to any other university.

_____ _____

Ort, Datum Unterschrift, Doktorand